

Ingeborg Pay

Changes in driving stresses and horizontal
surface velocity on Hellstugubreen,
Jotunheimen, Norway.

An investigation of inter-decadal fluctuations.

Abstract

The study of dynamics is crucial to the understanding of how a glacier responds to fluctuations in climate. The driving forces behind glacier flow are determined by ice thickness and surface slope. A multi-dataset approach was used to determine these factors for Hellstugubreen, a small (3.38 km² in 2009) valley glacier located on the west-east water divide in the Jotunheimen region of south-western Norway, between 1941 and 2009. Maps for the glacier exist from the 1940s onwards and it has long records of frontal changes, velocity and mass balance data. The most recent DEM was created from LiDAR data, while the DEMs for the older maps were generated from the contour lines. Volume changes and surface slope were computed by subtracting the DEMs. Between 1941 and 2009, Hellstugubreen lost 58% of its mass (the equivalent of a 20 m water layer) and saw its extent reduced by 20%. Losses have been constant, with the exception of a slight advance and volume gain in the 1990s. Hellstugubreen behaved according to its location on the west-east profile in the region, and its volume and frontal have fluctuated in line with other glaciers in the area. It was found that both local and global (NAO) climate influence the ice mass. The compared stakes for the different datasets show an increase in the angle of the surface slope, but no spatial pattern could be established in these changes. Changes in ice thickness were determined by combining the DEMs with interpolated data obtained during an echo sounding survey in 2011. Thus, driving stresses could be computed for selected stakes. With great fluctuations in both ice thickness and slope, driving stresses have changed considerably, from -50% to 45% between 1941 and 2009. During the same period, Hellstugubreen's average annual surface velocity increased by 15%, from 8.14 m yr⁻¹ in 1941 to 9.53 m yr⁻¹ in 2009. However, the differences in average daily velocity are too small to be statistically significant. The steepening of the surface could have countered the effects from the ice loss, at least partly. However, the velocity changes are not in correspondence with the magnitude of volume changes, pointing to other factors influencing the surface flow. An investigation of vertical velocity, longitudinal stress and the glacier's hydrological system would greatly benefit future research. Both a study of the glacier bed and the application of existing climatic models would allow for the assessment of impact of possible climate change.

Acknowledgements

I have a great many people to thank for helping me complete this dissertation. First of all, my supervisor at NTNU, Geir Vatne for keeping me focused on the bigger picture and for repeatedly reminding me that it was “just a master’s dissertation”. Secondly, my second supervisor, Liss M. Andreassen at the glacier section of *NVE*, who took me on board (and to the mountains) and patiently instructed me in field methodology. She is the greatest source of information on glaciers in Norway and especially Jotunheimen. She has also guided me through the immense archives of data.

A special thank you goes to Bjarne Kjølmoen at *NVE* for processing the raw dGP. Other people at *NVE* should be mentioned as well, for making this very intimidated master student feel welcome at the offices in Oslo and at the IGS Nordic Branch meetings: Hallgeir Elvehøy, Rune Engeset, Miriam Jackson, Kjetil Melvold and Solveig Windsvold.

I am greatly indebted to Jan Ketil Rød and Wenche Larsen, for help with GIS-software, as well as Mark Allan, Ágúst Þor Gunnlaugsson and Andrew Newton for last minute ArcMap help. Mark and Andrew have also gotten hold of a great many papers that were unavailable to me behind a pay wall. Andy: thank you for proofreading the final draft. I also want to extend heartfelt gratitude to staff and co-students at UNIS, Svalbard, for being an inspiration and for constantly reminding me why I do what I do.

Thank you to the father of my girls without whose support I would not have been able to spend time away from home. And thank you to Ellinor and Eydis, for being there when I got home and being forgiving of my absence. They have waited many months for their mummy to finish school, and deserve the promised outings more than anyone.

So many people have helped me retain my sanity, at least partly, over the past few years, and I should mention Ivar Pande Braathen: he helped me in the field on several occasions, but also provided a place to sleep and food after late evenings spent at uni. Dorota Medrzycka can’t be praised enough for her eternal encouragement and, quite often, a deserved kick up the bum. D, you are an inspiration, and you have a good kick.

Finally, my greatest thanks should go to Thomas Shaw. He joined me in the field, proofread, helped with Excel and ArcMap, came with criticism and ideas, took the time to help me while drowning in his own work and told me on several occasions to get a grip and just get to work. But most of all: thank you for always being there, even if you are a bad quality Skype conversation away.

Tusen takk,



Trondheim, May 2014

Table of Contents

List of Figures	ix
List of Tables.....	xi
Abbreviations	xiii
1. Introduction	1
2. Study site	5
3. Background	9
3.1. Driving stresses and volume changes	9
3.1.1. Driving stresses	9
3.1.2. Volume changes	12
3.2. Glacier flow	15
3.2.1. Measurements of glacier velocity	17
3.2.2. Temporal and spatial variations in glacier flow	17
3.3. Previous work on Hellstugubreen.....	22
3.3.1. Volume	22
3.3.2. Extent and terminus.....	24
3.3.3. Velocity	25
4. Datasets	29
4.1. Maps	30
4.2. Volume changes and slope	31
4.3. Frontal changes and extent	33
4.4. Speed records.....	34
4.5. Mass balance data.....	36
5. Methodology	39
5.1. Field methods: glaciological method.....	39
5.1.1. Determining the stake network	39
5.1.2. Stake coordinates.....	41

5.1.3.	Glacier front	43
5.2.	Data analysis procedure.....	44
5.2.1.	Glacier outline	46
5.2.2.	Elevation and volume changes	47
5.2.3.	Frontal changes	48
5.2.4.	Velocity data	49
5.2.5.	Driving stresses	49
6.	Results	51
6.1.	Driving stresses.....	51
6.1.1.	Surface elevations and volume changes	51
6.1.2.	Slope.....	56
6.1.3.	Driving stresses	57
6.2.	Velocity	58
6.2.1.	Annual velocity	58
6.2.2.	Summer and winter velocities	67
6.3.	Extent and frontal changes	71
7.	Discussion	77
7.1.	Volume, terminus and extent.....	77
7.2.	Slope	84
7.3.	Velocity	84
7.4.	Driving stresses and velocity	87
7.5.	Other factors	87
8.	Limitations and suggestions for future work.....	89
9.	Conclusions	91
	References	93

List of Figures

Figure 2.1.	Study site. Jotunheimen, Norway.....	5
Figure 2.2.	Relative area change per glacier from 1966-1993 to 2003.....	6
Figure 2.3.	View from the south across Vestre Memurubreen and Hellstugubreen.....	7
Figure 2.4.	View from the north across Hellstugubreen and Vestre Memurubreen.....	7
Figure 2.5.	Hellstugubreen, Jotunheimen.....	8
Figure 3.1.	Gravitational forces composing the driving stress.....	9
Figure 3.2.	Diagram illustrating dependence of balance velocity on accumulation.....	16
Figure 3.3.	Surface elevation change between 1968 and 1980 in m	23
Figure 3.4.	Annual frontal fluctuations of the glaciers in Jotunheimen.....	25
Figure 3.5.	Map of Hellstugubreen with isotachs for 1942.....	26
Figure 3.6.	Winter precipitation and summer temperature for stations in the greater Jotunheimen region.....	27
Figure 4.1.	Example of the original KOL40 dataset.....	29
Figure 4.2.	Ice thickness derived from radar soundings.....	32
Figure 4.3.	Frontal retreat on Hellstugubreen between 1901 and 1948.....	33
Figure 4.4.	Measurements on Hellstugubreen.....	35
Figure 4.5.	Map showing vectors representing the movement of stakes as measured by R. Pytte for 1962–1963.....	36
Figure 5.1.	Stake map for the NVE10 fieldwork.....	40
Figure 5.2.	Recording handheld GPS data while the Rover is positioned as close to the stake as possible.....	42
Figure 5.3.	Measuring of antenna height above the snow surface.....	42
Figure 5.4.	The boulder used to position the dGPS base station.....	43
Figure 5.5.	The dGPS base in place.....	43
Figure 5.6.	Overlaying stake maps and glacier outlines for KOL40, PYT60 and NVE10.....	45
Figure 5.7.	Glacier outline used by NVE, the ice divide between Hellstugubreen and Vestre Memurubreen should be noted (NVE 2014).....	47

Figure 5.8.	Polygon showing the outline used for area and volume calculations on the tongue. Glacier outline and contours from 1941.....	48
Figure 6.1.	Surface elevation changes (m) on Hellstugubreen.....	52
Figure 6.2.	Interpolated ice thickness on Hellstugubreen as recorded by LiDAR survey in May 2011.....	53
Figure 6.3.	Hellstugubreen's hypsometry between 1941 and 2009.....	54
Figure 6.4.	Average daily velocities (in m d^{-1}) for the NVE10 stakes.....	59
Figure 6.5.	Average daily velocities (in m d^{-1}) for 2009–2013.....	59
Figure 6.6	Vector map showing the direction of movement from 2009 to 2013 for NVE10.....	60
Figure 6.7.	Average daily velocities (in m d^{-1}) for 1937–1946 calculated from KOL40.....	60
Figure 6.8.	Average daily velocities for each year (in m d^{-1}) for the KOL40 stakes.....	61
Figure 6.9.	Average daily velocities (in m d^{-1}) for 1961 – 1963, calculated from PYT60.....	62
Figure 6.10.	Average movement of stakes (m d^{-1}) since the last observation for the compared stakes of all datasets.....	65
Figure 6.11.	Average daily velocities for all three datasets.....	68
Figure 6.12.	Average daily winter and summer velocities and average daily summer velocities (in %) for the KOL40 stakes.....	69
Figure 6.13.	Hellstugubreen's area (km^2).....	70
Figure 6.14.	Evolution of Hellstugubreen's extent between 1941 and 2009.....	71
Figure 6.15.	Cumulative frontal changes (m) and total volume (km^2) on Hellstugubreen from 1901 until 2011.....	73
Figure 7.1.	Thinning and frontal retreat of Tverråbreen and Hellstugubreen.....	76
Figure 7.2.	Hellstugubreen's terminus with exposed debris in the forefield.....	77
Figure 7.3.	NAO index data from the CPC (NOAA 2012) combined with reconstructed data from before January 1950.....	79
Figure 7.4.	Mean summer (July) and winter (January) temperatures from 1920-1970 (Fokstua) and 1970-2014 (Fokstugu).....	81
Figure 7.5.	Annual and winter precipitation in south-western Norway.....	81

List of Tables

Table 4.1.	Maps used in this thesis.....	30
Table 4.2.	Observation dates for KOL40.....	34
Table 5.1.	Overview of the fieldwork gathering primary data.....	39
Table 5.2.	Selected stakes for comparison.....	46
Table 5.3.	Relative distance from front for selected stakes.....	46
Table 5.4.	DEMs constructed.....	47
Table 6.1.	Volume changes (m^3) for Hellstugubreen since 1941.....	53
Table 6.2.	Volume changes (m^3) for Hellstugubreen's tongue (up to ~1600 m.a.s.l) since 1941	54
Table 6.3.	Elevation (m a.s.l.) for given stake locations on Hellstugubreen.....	55
Table 6.4.	Elevation changes for the compared stakes from 1941 to 2009.....	55
Table 6.5.	Recorded (2011) and reconstructed ice thickness for the compared stakes from 1941 to 2009.....	56
Table 6.6.	Changes in slope ($^\circ$) for the compared stakes, from 1941 to 2009.....	57
Table 6.7.	Driving stresses (kPa) for the compared stakes from 1941 to 2009.....	57
Table 6.8.	Calculated velocities for the NVE10 stakes.....	59
Table 6.9.	Average daily velocities for Hellstugubreen for all three datasets.....	62
Table 6.10.	Average daily velocities for the periods 1937–1946 (KOL40), 1961–1963 (PYT60) and 1997–2013 (NVE10).....	63
Table 6.11	Average movement of stakes (m d^{-1}), rounded to the fourth decimal, since the last observation for the compared stakes of all datasets.....	64
Table 6.12.	Average daily summer velocities (m d^{-1}), rounded to the fourth decimal, for NVE10.....	66
Table 6.13.	Average daily winter velocities (m d^{-1}), rounded to the fourth decimal, for NVE10.....	66
Table 6.14.	Average summer and winter velocities (in m d^{-1}), rounded to the fourth decimal) for 2010 – 2013 for NVE10.....	66
Table 6.15.	Average summer and winter velocities (in m d^{-1}) for 1937 – 1946, rounded to the fourth decimal, calculated from KOL40.....	68
Table 6.16.	Average summer and winter velocities (in m d^{-1}) for 1937 – 1946, rounded to the fourth decimal, calculated from KOL40.....	69

Table 6.17.	Evolution of Hellstugubreen’s area coverage between 1941 and 2009.....	70
Table 6.18.	Comparison of area extent results from this research and those from <i>NVE</i> (2014).....	71
Table 6.19.	Absolute and cumulative frontal changes on Hellstugubreen from 1901 until 2011.....	72
Table 6.20.	Frontal retreat on Hellstugubreen.....	74
Table 7.1.	Example of measured fluxes for some glaciers.....	82
Table 7.2.	Calculated driving stresses and velocities of the compared stakes	85

Abbreviations

CPC	Climate Prediction Center (at NOAA)
KOL40	Dataset from the 1940s, fieldwork by A. Koller, processed by Liestøl (1962)
LiDAR	LIght Detection And Ranging
NVE10	Dataset from 2009 – 2013, data from <i>NVE</i>
NVE	Norges Vassdrags- og Energidirektorat (Norwegian Water Resources and Energy Directorate)
NOAA	National Oceanic and Atmospheric Administration
PYT60	Dataset from 1961 – 1963, from Pytte (1964)
SLP	Sea Level Pressure

For Ellinor and Eydis

Climb the mountains and get their good tidings. Nature's peace will flow into you as sunshine flows into trees. The winds will blow their own freshness into you, and the storms their energy, while cares will drop away from you like the leaves of Autumn.

John Muir

1. Introduction

Globally, people's lives are directly affected by changes in glacier discharge, as drinking water availability, agriculture and hydro-electricity production are dependent on glacial run-off. In addition, because glacier fluctuations (at least those not influenced by debris cover, calving or surge events) give an easily observable signal, they are considered to be excellent indicators of climate change (Benn and Evans 1998; Oerlemans et al. 1998; Hooke 2005). By investigating glacier mass balance (MB) and length fluctuations, links can be established with climatic variations, both on a greater regional level and locally (Nye 1960; Dyurgerov 2003; Bamber and Payne 2004; Dyurgerov and Meier 2005; Nesje and Matthews 2012). Regional climate is responsible for the amount and phase of precipitation, solar radiation and air temperature. Locally, the regional climatic conditions will be influenced by topography and by the glacier aspect and elevation. The local climate determines accumulation and ablation processes, which result in the glacier's net balance (Nesje and Matthews 2012).

Glaciers, ice caps and continental ice sheets cover about 10 percent of the Earth's surface and lock up over 33 million km³ of fresh water, three quarters of the world's fresh water resources (Benn and Evans 1998; Cuffey and Paterson 2010). Were all of these ice bodies to melt in altering climatic conditions, they would raise global sea level by ~70 m (Benn and Evans 1998). The total contribution to sea level rise from all ice-covered regions was estimated to be 1.48 ± 0.26 mm¹ in 2012 (Jacob et al. 2012), a number that agrees well with other independent studies (Willis et al. 2010). Meier (1984) estimated that glaciers have contributed to about 4 cm of global sea level rise over the last 100 years. Between 2003 and 2009, glacier mass wastage contributed 0.71 ± 0.08 mm of sea level equivalent yr⁻¹, accounting for $29 \pm 13\%$ of the observed sea-level rise (2.50 ± 0.54 mm yr⁻¹) for the same period (Gardner et al. 2013).

The large number of glacier MB and length variation records in Scandinavia reflects the importance of glaciers for this region. In Norway, 98% of electricity is produced by hydropower, with 15% of the run-off originating from glacierised basins, and MB monitoring has been included in the licensing terms for hydropower production in these areas. In the 1960s, the Glacier Office (*Brekontoret*) was established at the Norwegian Water Resources and Energy Directorate (NVE) under leadership of G. Østrem. Since then, NVE has performed MB and glacier length variation measurements on a yearly basis (Andreassen et al. 2005;

Andreassen and Winsvold 2012). Their report, *Glaciological investigations in Norway*, has been published annually or biannually since 1963 (Kjøllmoen et al. 2011). Hellstugubreen (also spelled Hellstugubreen in the literature) is an interesting study object for several reasons. Firstly, it has long records, with observations of its frontal position dating back to 1901, continuous MB measurements from 1962 and surface velocity records from both the 40s and 60s. Secondly, its position on the west-east precipitation gradient across the region makes Hellstugubreen a fitting study object, as the more continental glaciers experience different climatic conditions than those located closer to the coast (Matthews 2005; Støren et al. 2008). Thirdly, Hellstugubreen makes for a convenient study site, as it is easily accessible. A two-hour walk in summer or a short snow mobile ride in winter make for an easy approach. More importantly, Hellstugubreen has a moderate slope and is comparatively free from crevasses and it is therefore easy to move about on the glacier (Hoel and Werenskiold 1962).

Several problems in glaciology require an understanding of the dynamics of a glacier. Flow redistributes energy and affects temperature distribution, which in turn has an effect on the coupling with the glacier bed. Spatial variations in velocity will have an effect on the entrainment of debris and the character of moraines, and are therefore of interest to geomorphologists (Hooke 2005). More importantly for this research, glacier flow determines the response time to fluctuations in climate. MB and glacier flow work as feedback mechanisms: when the MB changes, the glacier's movement will respond, which in turn results in an altered hypsometry as the glacier will change its gradient in order to keep the system in balance. With the hypsometry and geometry of the glacier altered, MB will again fluctuate. Thus, the way a glacier distributes its mass determines the shape of the glacier and its response time to climatic changes (Oerlemans 1991; Hooke 2005).

Glacier surface velocity and retreat are two important parameters used to determine glacier dynamics (Saraswat et al. 2013) and will be the main focus of this investigation. *NVE* has been measuring MB on the Norwegian main land glaciers since the 1960s, and currently monitors MB on 15 glaciers (Kjøllmoen et al. 2011). In 2009, *NVE* resumed surface velocity measurements on Hellstugubreen, the results of which will be used in this research.

This research aims to answer three main questions with regards to Hellstugubreen's dynamics. Firstly, how has the ice mass volume changed since the 1940s? GIS software will be used to compute ice thickness and volume changes that have occurred over the past 70 years. As surface slope influences glacier dynamics, changes in slope will be considered as

well. Secondly, are fluctuations in the driving forces (such as ice thickness and surface slope) of the glacier reflected in changes in its surface velocity? Present day (2009 – 2013) surface velocities will be calculated and compared to velocities recorded in the 40s and 60s. Field data will be compared to records from the 40s and 60s in order to establish if there have been any changes at all, and if so, if there is a noticeable trend in the evolution of Hellstugubreen's dynamics. Thirdly, as frontal changes are an important indicator for the dynamics of the glacier system, it will be considered if fluctuations at the glacier's terminus reflect changes in glacier dynamics and flow. Frontal changes are a simple and observable measure of glacial degradation. As Hellstugubreen has retreated noticeably, it is expected that both its volume and flow have changed considerably since the 1940s.

2. Study site

Jotunheimen, northern Europe's highest mountain range, is located in central southern Norway (Figure 2.1). The region has an alpine topography and contains around 300 cirque and valley glaciers and small ice caps (Hoel and Werenskiold 1962; Østrem et al. 1988; Andreassen et al. 2008). Many mountains rise above 2000 m a.s.l., the loftiest of which is Galdhøpiggen, 2469 m a.s.l. At the margins of the region, the valley floors descend to below 1000 m a.s.l. (Matthews 2005). Jotunheimen's boundaries can be given as between 61° 20' N and between 7°40' and 9° E. Based on these coordinates, the area measures 55 km from north to south and 70 km east to west, and the area can be estimated at approximately 2500 km² (Hoel and Werenskiold 1962).

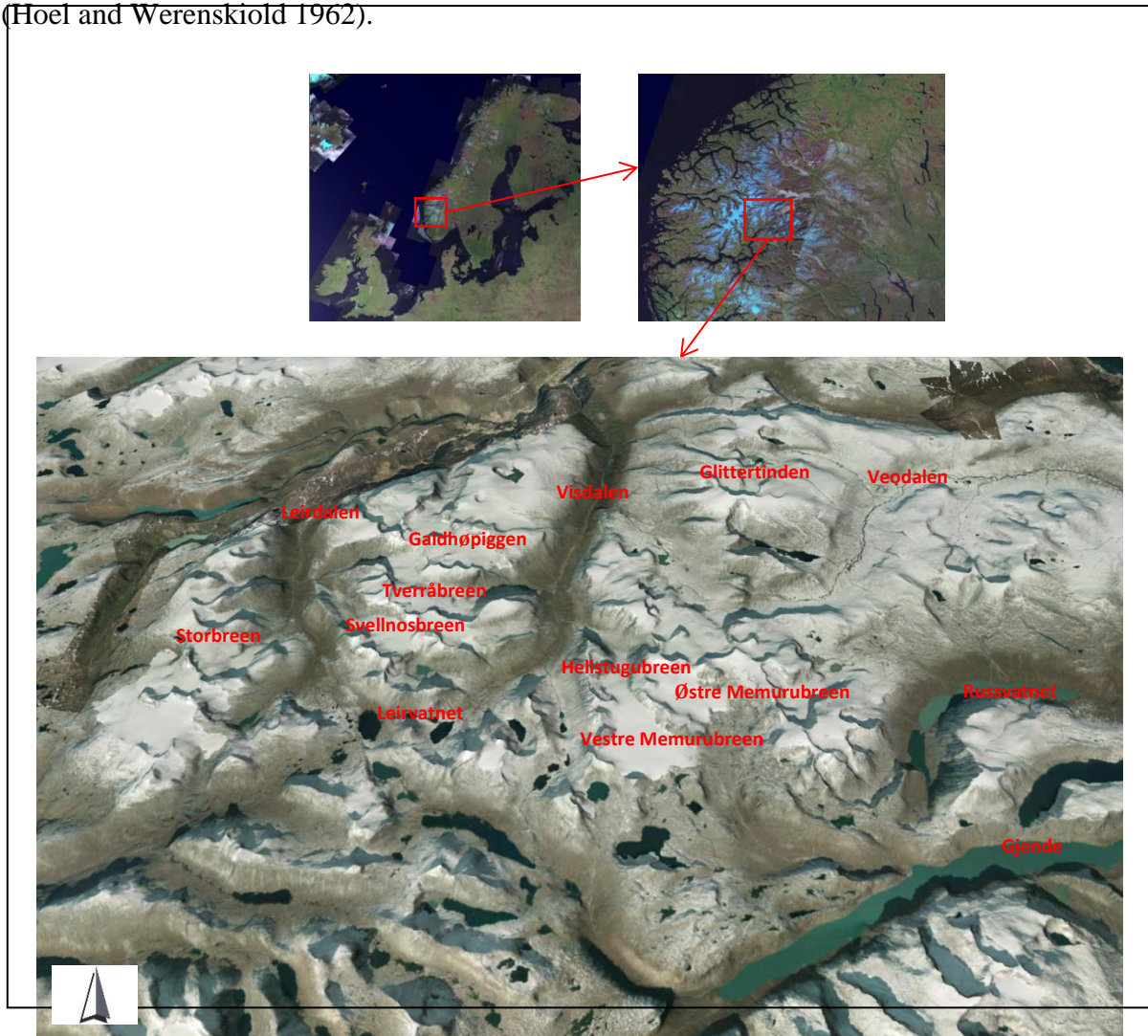


Figure 2.1. Study site. Jotunheimen, Norway. Main landmarks have been marked on the 3D image (Images: www.norgei3d.no).

Located 150 km from the west coast, and with prevailing west-southwesterly wind direction, the climate of Jotunheimen is transitional between maritime western Norway and the more continental conditions found further east. This results in a strong west-east precipitation gradient across the region (Matthews 2005; Støren et al. 2008), which in turn is clearly manifested on Jotunheimen's glaciers in the increase of the mean equilibrium line altitude (ELA) with distance from the coast. The ELA is about 1160 m a.s.l. for Ålfotbreen in the west, and about 2130 m a.s.l. for Gråsubreen in the east (Andreassen et al. 2005). Negative volume change is more pronounced towards the east and southeast, with area losses of 10% on many glaciers between 1930s and 2003 (Andreassen et al. 2008). Furthermore, the lower limit of mountain permafrost altitude decreases towards the east. The regional lower permafrost limit in the Jotunheimen region is calculated to be at around 1450 m a.s.l. (Etzelmüller et al. 2003). On Juvasshøe, a peak (1840 m.a.s.l) located approximately 12 km north of Hellstugubreen, the altitudinal limit for permafrost was delineated between 1410 and 1480 m.a.s.l (Hauck et al. 2004). Permanently frozen ground can be found both at top areas and on inter-valley plateaux (Etzelmüller et al. 2003).

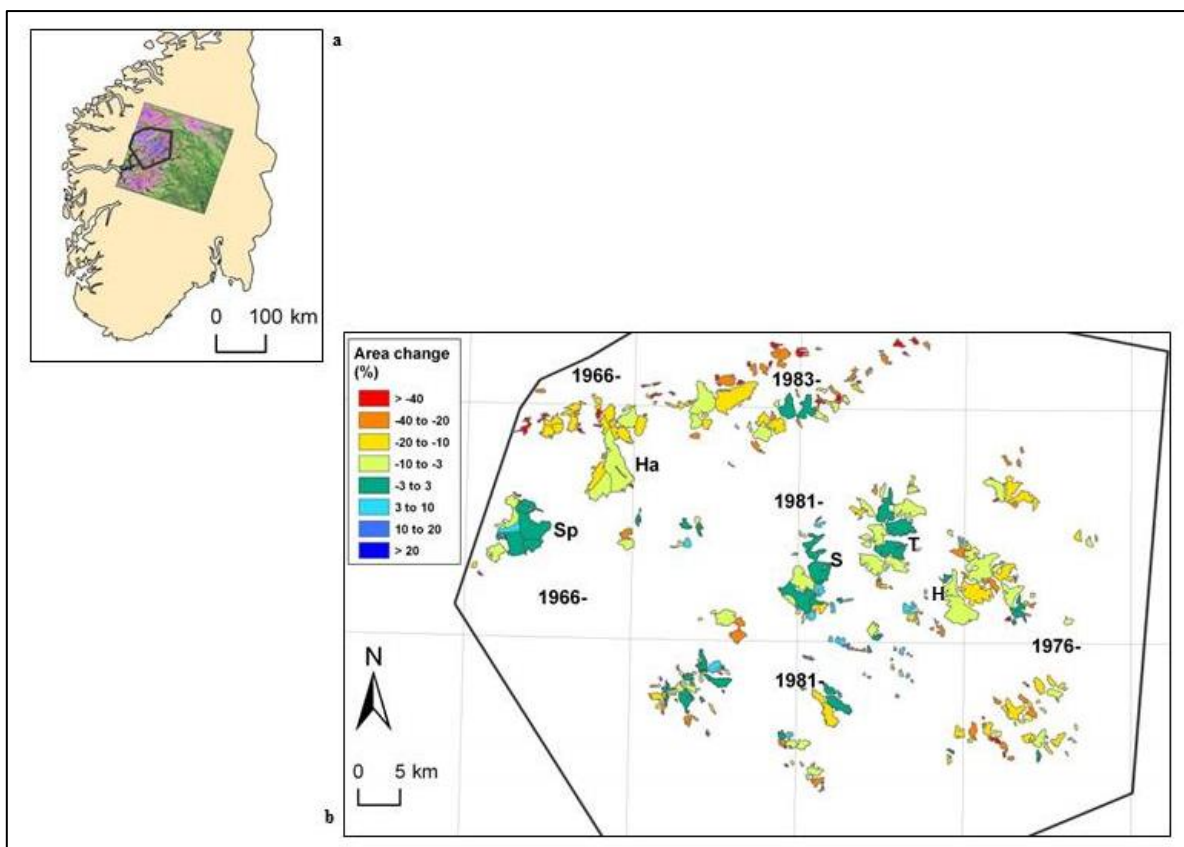


Figure 2.2. Relative area change per glacier from 1966-1993 to 2003. Lettercodes stand for glacier names: SP (Spørteggbreen), Ha (Harbardsbreen), S (Storbreen), T (Tverråbreen), H (Hellstugubreen). Glacier change within the uncertainty of the area change estimate ($\pm 3\%$) are displayed in green (after Andreassen et al. 2008).

Hellstugubreen (61°34' N, 8°26' E) is a north facing valley glacier situated in central Jotunheimen. To the south, its accumulation area borders that of Vestre Memurubreen. To the north, Hellstugubreen debouches into the Visdalen valley. Dominating peaks constrain the glacier and force its northward flow: the nine peaks of the Hellstugu-traverse to the west and the Memurutindene to the east all peak above 2000 m a.s.l. (Figure 2.3 and 2.4). Hellstugubreen has an area of 2.9 km². The elevation of the glacier ranges from 1482 to 2230 m a.s.l. (Figure 2.5) and thus it is located well within the permafrost limits (Etzelmüller et al. 2003; Hauck et al. 2004). In 2010, its ELA was calculated to be located at ~2230 m a.s.l., resulting in an accumulation area ratio of 0% (Kjøllmoen 2010), an indication of the glacier's confirmed negative mass balance.

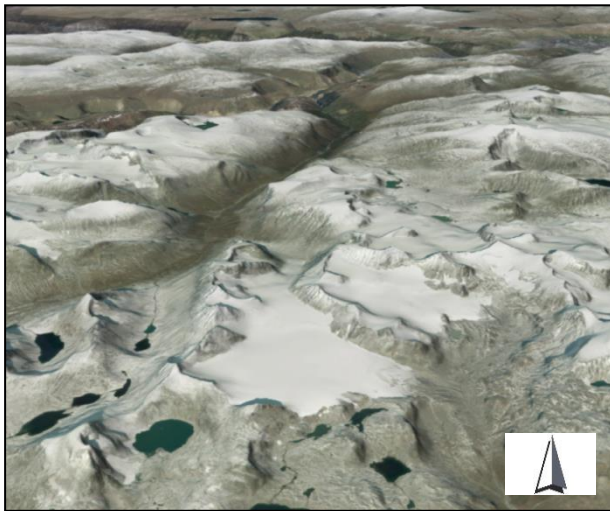


Figure 2.3. View from the south across Vestre Memurubreen and Hellstugubreen. Østre Memurubreen to the east (Image: www.norgei3d.no).

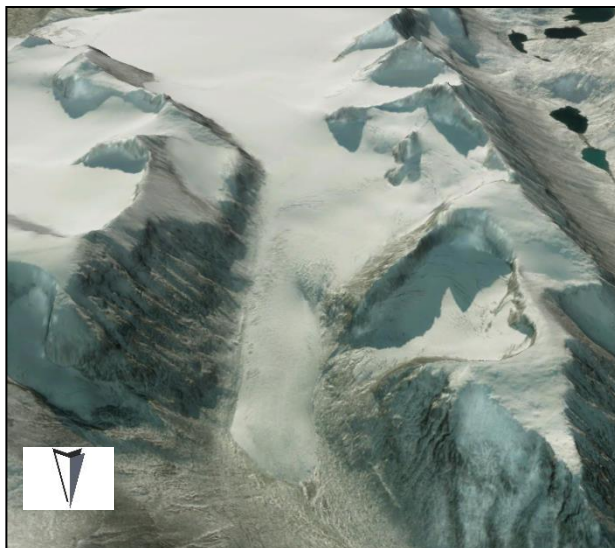


Figure 2.4. View from the north across Hellstugubreen and Vestre Memurubreen. Hellstugutindene to the west, Memurutindene to the east. The image clearly shows the small cirque to the west and how it is cut off from the main ice stream flowing south-north (Image: www.norgei3d.no).

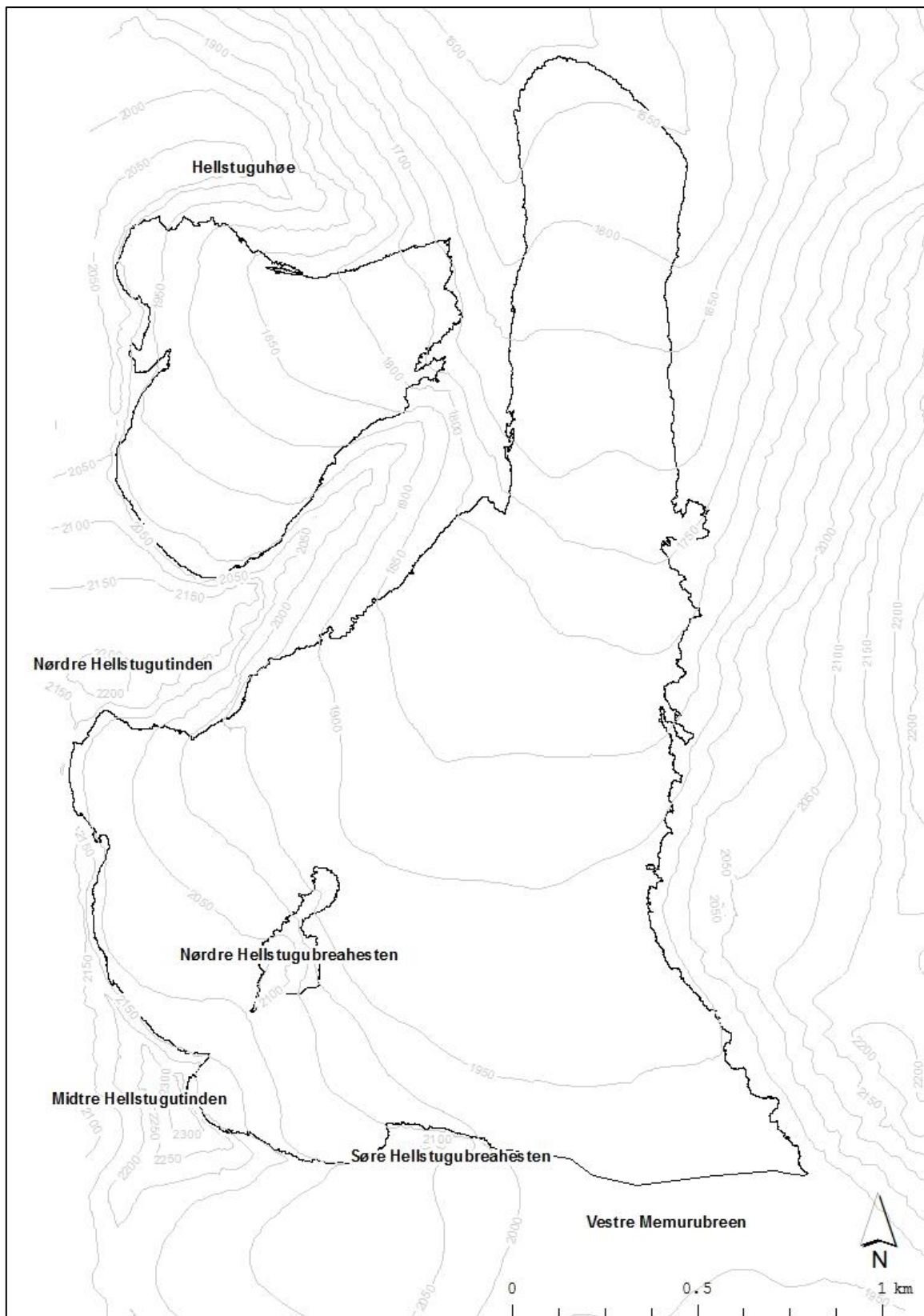


Figure 2.5. Hellstugubreen, Jotunheimen. Glacier outline from 2009. Ice divide from this investigation.

3. Background

3.1. Driving stresses and volume changes

The rate and spatial distribution of flow is known as the *flow field* of a glacier (Cuffey and Paterson 2010). In order to get a full description of the flow field in a glacier, the horizontal and vertical components of the velocity at every point have to be known (Hooke 2005). Glacier flow is controlled by driving and resisting stresses. This research focusses solely on the driving stresses behind the horizontal surface movement component of flow.

3.1.1. Driving stresses

Figure 3.1 explains the gravitational forces composing the driving stress. A model glacier is considered in Figure 3.1a: a parallel-side ice mass, with thickness H , resting on slope α . The weight of a column of ice perpendicular to the plane and of unit cross-section has a driving stress (τ_d) component $\rho g H \sin \alpha$, where ρ is the density of the ice and g the gravitational acceleration. The largest resisting force on most glaciers is the basal drag: shear stress τ_b across the base of the column. Thus,

$$\tau_d = \rho g H \sin \alpha \quad \text{and} \quad \tau_b = f' \tau_d ;$$

Equation 3.1.

where f' denotes a number usually of order one (Cuffey and Paterson, p. 295).

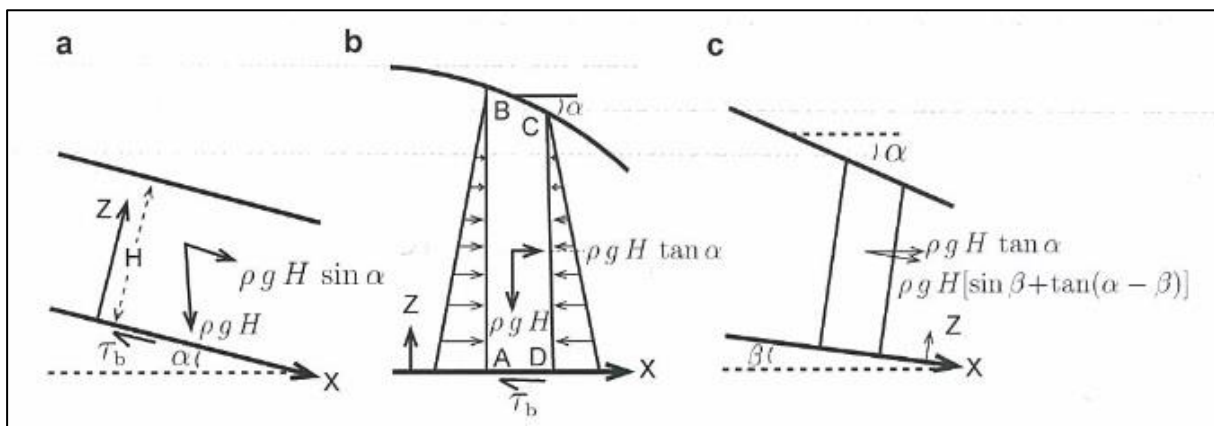


Figure 3.1. Gravitational forces composing the driving stress: (a) down-slope component of weight, (b) the pressure gradient force, (c) the combination (Cuffey and Paterson 2010, p. 295).

A slab of ice with a surface slope α , resting on a horizontal plane (Figure 3.1b) is more realistic to an ice sheet or the lower areas of a large mountain glacier. Because ice plastically, ice column ABCD of unit thickness is subjected to a pressure equalling the hydrostatic head

by a very close approximation. This pressure is defined as the ice overburden pressure. The pressure increases from 0 in B to $\rho g H$ in A, with $AB = H$. Normal force on AB therefore becomes $\frac{1}{2} \rho g H^2$. The normal force on CD becomes $\frac{1}{2} \rho g H^2 + d/dx \left[\frac{1}{2} \rho g H^2 \right] \delta x$. The driving stress for the body of ice, a horizontal force moving it to the right, is the difference between the two (against balanced by basal drag):

$$\tau_d = \rho g H \frac{dH}{dx} = \rho g H \tan \alpha \quad \text{and} \quad \tau_b = f' \tau_d ; \quad \text{Equation 3.2.}$$

where f' denotes a number usually of order one (Cuffey and Paterson, p. 296).

A real glacier does not match either of these idealised models, but the exact shape has little influence on the driving forces behind flow. At depth, there always exists a horizontal gradient of the hydrostatic head proportional to $-dS/dx = \tan \alpha$, where S is the surface elevation and α the surface slope.

Figure 3.1c considers a wedge-shaped slab of ice with sides perpendicular to the glacier bed. H is measured perpendicular to the slope, and α is a small bed slope. In the downward direction, $[\rho g H \sin \beta] \delta x$ should be added to the hydrostatic gradient force to give the driving force $\tau_d \delta x$. As before, τ_d is balanced by the basal drag $\tau_b \delta x$:

$$[\rho g H \sin \beta] \delta x - \rho g H [dH/dx] \delta x = f' \tau_d \delta x . \quad \text{Equation 3.3.}$$

For smaller angles, $dH/dx = \beta - \alpha$ and $\sin \beta = \beta$. Thus,

$$\tau_d \approx \rho g H \alpha \quad \text{and} \quad \tau_b = f' \tau_d . \quad \text{Equation 3.4.}$$

Thus, when the slopes are small, τ_d is the same as for a parallel-sided body of ice or a flat bed, as long as α refers to the surface slope (Ibid.).

From Equations 3.1 to 3.4 several conclusions can be drawn (Cuffey and Paterson 2010):

- 1) The driving stress, and hence the shear stress at the bed, are determined by the surface slope. Therefore, ice will always flow in the direction of the maximum surface slope, even when the bed slopes in a different direction. This has been confirmed by observations. Thomas et al. (2004) indicated that Pine Island glacier crosses a basal rise with a height of nearly 1 km;

- 2) Flow lines can be determined from the contour map of a glacier, if slope is considered to be the average value over distances of several times the ice thickness;
- 3) Driving stresses can therefore be determined from measurements of ice thickness H and surface slope α ;
- 4) Measured driving stresses provide an estimate for shear stress τ_b , as $0.5 < f' < 1.5$. Because τ_b values estimated from this assumption ($\tau_b = \tau_d$) normally lie between 50 and 200 kPa; and because the deformation rates in ice increase strongly as the effective stress rises to about 100 kPa and ice can be considered a perfectly plastic material, slow glacier flow can be considered to be a process of perfectly plastic deformation. τ_b therefore becomes equal to τ_0 (the yield stress for ice), at usually $\tau_0 = 100$ kPa;
- 5) From 4) follows:

$$H = \frac{1}{f'} \frac{\tau_0}{\rho_i g \alpha} \quad , \quad \text{Equation 3.5.}$$

and if $\tau_0 = 100$ kPa and $f' = 1$, then $\frac{\tau_0}{\rho_i g \alpha} = 11$ m. From this, a rough estimate of ice thickness can be made from the measurements of surface slope;

- 6) In Equation 3.5 a roughly constant value for $H \alpha$ is assumed. Therefore, a glacier is relatively thin where it is steep and thick where the surface flattens;
- 7) If $H \alpha$ is constant, glacier profiles acquire certain predictability. Surface slope α is the sum of ice thickness gradient dH/dx and bed slope β . If a glacier resting on a bed with a total elevation range of ΔB , with a thickness small compared to ΔB (as is the case on many mountain glaciers), then $\alpha \approx \beta$. The glacier can then be pictured as a long slab of ice of nearly uniform thickness. However, if the glacier is thick compared to ΔB , then $\alpha \approx dH/dx$, the glacier will assume the form of a parabola;
- 8) With a constant density, driving stress τ_d acting at a depth $H - z$ increases linearly from zero at the surface to τ_d at the base:

$$\tau_d(z) = \tau_d \left[1 - \frac{z}{H} \right] \quad . \quad \text{Equation 3.6.}$$

It should be noted that approximations like $\tau_d \approx 100$ kPA and $H \alpha \approx \text{constant}$ are appropriate for many glaciers. However, they should not be made for large and fast-flowing

glaciers. The driving stress τ_d on polar ice streams, for example, ranges from 15 to 410 kPa. In order to gain understanding of flow on these glaciers, other factors need to be considered. Resisting forces will greatly influence their dynamics.

3.1.2. Volume changes

From Section 3.1.1, it is clear that ice thickness and the slope of the glacier surface are important parameters influencing the driving forces behind glacier flow. Traditionally, volume changes have been calculated through the analysis of MB data acquired in the field (Andreassen 1999; Dyurgerov and Meier 2000). MB is measured through investigations of snow density and depth and ablation on a stake network on the glacier (Andreassen 1999).

This glaciological method of MB measurements is both time consuming and expensive, and for many glaciers direct MB data are not available (Andreassen 1999). Therefore, the comparison from surveys of glacier surface topography has been applied to evaluate changes in net balance in several studies (Østrem and Tvede 1986; Andreassen 1999; Dyurgerov and Meier 2000; Berthier et al. 2003; Rignot et al. 2003; Aizen et al. 2006; Surazakov and Aizen 2006; Larsen et al. 2007; Schiefer et al. 2007). Zemp et al. (2013) analysed the glaciological and geodetic balance records for 12 European glaciers and found that they are both subject to errors. Errors cumulate due to the law of error propagation and therefore become more detectable in longer time series. They propose the consistent re-analysis of existing mass balance series to become a standard procedure.

The geodetic method overlays maps of the glacier in order to calculate how much mass has been gained or lost between the two years of comparison (Andreassen 1999). Older studies make the calculations by manually placing an identical grid over the maps in question (e.g. Pytte 1964; Haakensen 1986). Newer methodology is described in several studies and while the software may differ – e.g. Andreassen (1999) uses ARC/Info software, Bauder et al. (2007) employ PV-WAVE software package (Visual Numerics, Inc., 2001) and Rivera and Casassa (1999) stick to the Windows version of IDRISI – the general procedure differs little between studies.

Analogue maps are digitised and converted to the UTM coordinate system. Next, digital triangular networks (TINs) are constructed for each of the maps. Regular grids are then generated from the TINs for further overlay analysis. Grid spacing is chosen, depending on the resolution of the input data and the size of the glacier (Kjøllmoen 1997; Andreassen 1998;

Bauder et al. 2007). Andreassen (1999) tested several interpolation techniques for creating DTMs, but found only small variations to exist between different methods, much in line with other studies (e.g. Kjølmoen 1996; Andreassen 1998). Bauder et al. (2007) note that the procedure is challenging and that several algorithms exist. Newer methodology suggests creating the DTMs by direct interpolation (without first creating TINs) from the contour maps in order to minimize errors that occur during interpolation (Andreassen et al. 2012, L. Andreassen, *NVE*, personal communication).

Ice thickness change for the periods between two maps is calculated by subtracting the regular grids. The resulting grid represents altitude differences in glacier ice, firn and snow, (ΔG_{xx-yy}). By multiplying ΔG_{xx-yy} with the glacier area, volume changes (ΔV) can be determined (Dyrgerov and Meier 2000; Bauder et al. 2007; Paul and Haeberli 2008). Mass change, ΔV_{xx-yy} , can be calculated by multiplying the difference grid by the density of ice and firn. Because field data is not always available, several studies (e.g. Kjølmoen 1997; Andreassen 1998; Andreassen 1999; Bauder et al. 2007; Paul and Haeberli 2008) assume the density of the ice and firn to be constant at 0.9 g cm^{-3} , the usual density of ice (Cuffey and Paterson 2010). This assumption is considered reasonable when no major changes in the firn layer are expected (Bauder et al. 2007). Thus,

$$\Delta V_{xx-yy} = \Delta G_{xx-yy} \times 0.9 \quad \text{Equation 3.7.}$$

However, more recent literature finds that assuming constant density at 0.9 g cm^{-3} affects the accuracy of the geodetic method with an overestimation of mass change of roughly 2-15% (Huss 2013). Huss (Ibid.) suggests a $0.85 \pm 0.06 \text{ g cm}^{-3}$ to be used for periods longer than 5 years and volume changes different from zero, stable mass balance gradients and the presence of a firn area. This lower density corresponds with findings by Sapiano et al. (1998). However, there will always be a significant uncertainty in geodetically determined mass balances, and Huss (2013) claims it might be larger than previously assumed.

Because surveys are rarely taken on exactly the same date for each of the years, Andreassen (1999) suggests converting ΔV given in m^3 to the average MB change expressed in water volume (water equivalent, w. eq., expressed in m) in order to correct the total ΔV for additional melting between mapping or photographing dates. Arendt et al. (2002) note the same need for adjustment when early-period measurements are made. On Storbreen, there was a 16 day gap between observations on 24 August 1984 and 8 August 1997. When temperature

data suggest that a lot of additional melting has occurred the between dates of observation, as was the case in this instance, the additional melting needs to be determined and added to the overall volume changes (Andreassen 1999).

Andreassen (1999) evaluated the two different methods of measurement of ΔV between 1940 and 1997 on Storbreen, Sweden. The computation of ΔV on Storbreen from maps gave more positive (or less negative) MB data compared to the annual field measurements, except for one period. The difference can be explained by the inaccuracy of the available maps (this is problematic especially for the earliest periods). The issue was raised in Bauder et al. (2007) as well. The latter study also found that a varying scale of the maps results in large differences in the contour-line interval and thus the accuracy of the obtained digital elevation model (DEM). Paul and Haeberli (2008) found that direct measurements of MB in the Swiss Alps agree well with the mean change derived from DEM differencing. Contrastingly, Berthier et al. (2006) and Schiefer et al. (2007) found a systematic underestimation of elevation to exist in their SRTM DEMs¹, leading to an overestimation of the mean thickness change.

Global loss of glacier volume started in the middle of the 19th century (Dyurgerov and Meier 2000). However, the loss of mass on glaciers cannot be regarded as a simple adjustment to the end of the Little Ice Age, as time series of glacier volume changes show great spatial and temporal variability (Ibid.). These variabilities exist on different scales. Temporally, Bauder et al. (2007) established a volume loss of 8.73 km³ in the Swiss Alps since 1920, 40% of which occurred since 1980. This corresponds with other finds that established extreme ice losses from the 1980s, both for the same region (Haeberli et al. 2007; Paul and Haeberli 2008) and on a global scale (Dyurgerov and Meier 2000). For the Swiss Alps, Paul and Haeberli (2008) calculated a loss of more than 80 m between 1985 and 1999, which means a cumulative MB of -10.8 m w. eq. However, even if there is a clear trend of great volume losses on a century timescale, the loss and gain of volume seems to fluctuate greatly within shorter decadal time frames (Dyurgerov and Meier 2000; Bauder et al. 2007). For the Swiss Alps, for instance, decadal net balances fluctuated from -0.29 (1920-1960) to -0.03 (1960-1980), to drop again down to -0.53 (1980 – 2007) m yr⁻¹ w. eq.

Geographically, variations of volume changes occur on individual glaciers, regionally and globally. Volume losses seem to be more significant closer to the glacier tongue, with

¹ SRTM: Shuttle Radar Topography Mission. DEMs based the SRTM have a smaller error margin than other DEMs and provide an accurate means to assess elevation changes (Paul and Haeberli 2008).

accumulation areas often hardly affected over the course of the last century (Andreassen 1999; Bauder et al. 2007). Changes in volume will affect a glacier's hypsometry (Kjøllmoen 1997). By investigating changes in the glacier's area distribution, statements can be made about how different areas of the glacier are affected by net mass changes in different ways. Regionally, glaciers located close together don't necessarily undergo mass changes to the same degree (Dyurgerov and Meier 2000). Bauder et al. (2007) could not establish a geographical pattern for the Swiss Alps. Rivera and Casassa (1999) found that the Pio XI glacier, Patagonia, experienced an advance and thickening between 1945 and 1995, while all neighbouring glaciers were retreating, making it quite unique in this region. However, also on Pio XI, the ELA is being shifted upwards, reaching the tipping point when the glacier would begin to retreat. Furthermore, while glaciers in more continental regions are losing volume at an increasingly fast rate, the more maritime glaciers are experiencing increased snow accumulation and positive volume changes (Andreassen 1998; Dyurgerov and Meier 2000; Nesje et al. 2000; Andreassen et al. 2005). Kjøllmoen (1997) and Andreassen (1998) found however, that some glaciers (Harbardsbreen and Jostefonn, respectively) do not fit in this profile of decreasing net balance with more easterly location. Other factors, such as hypsometry, geometry, aspect, ice dynamics and local weather conditions, should therefore be considered (Kjøllmoen 1997; Andreassen 1998).

3.2. Glacier flow

At any location on a glacier, the quantity of ice conveyed per unit time, is the flux (q). Glacier flow, and thus flux, is determined by gravitational forces causing the ice to flow. Flow modulates resisting forces within the ice and along boundaries. Therefore, flow must be fast enough in order for the gravitational and resisting forces to balance. Resisting forces depend on the properties of the ice, the properties of the substrate and the geometry of the glacier (Cuffey and Paterson 2010). A second approach to understanding flux is to consider that a glacier will always tend towards a steady state. When mass is added to the glacier, flux will transport ice from locations of net accumulations to locations of net loss. When fluxes are too small, the glacier will build up and thickness will increase, until transport rates match the accumulation. Thus, fluxes are determined by the mass input and by the geometry of the outlet. The latter approach fails if the glacier is far from a steady state (e.g. during surges), but it can explain many observed characteristics of glacier flow (Cuffey and Paterson 2010).

An idealised glacier, which is in a steady state over a period of years, will not undergo mass or thickness changes. It transports as much ice out of the system as is brought in by accumulation on the surface. This pattern of flow will allow the glacier to reach its balance velocity (U_B), which is expressed as

$$u = \frac{1}{h(x)} \int_0^x b_n(x) dx \tag{Equation 3.8}$$

Where u is the balance velocity, $h(x)$ is the glacier thickness, and b_n is meters of ice per year. The equation is an expression of the conservation of mass in an incompressible medium: as much mass must be moved out by flow $u h(x)$, as enters it by its accumulation on the surface $\int_0^x b_n(x) dx$ (Hooke 2005, p. 78).

For a mountain glacier in balance, this means that the flux of ice through a cross-section must equal the total annual accumulation upstream. The flux through a cross-section in the ablation zone must equal the mass of ice lost downstream. This means that the flux must increase steadily with distance down-glacier up to the equilibrium line (ELA), and decrease from the ELA to the terminus. At the terminus, a steady state glacier will have a flux equalling zero, unless it calves or advances (Cuffey and Paterson 2010). The dependence of glacier flow on accumulation at the surface is illustrated in Figure 3.2.

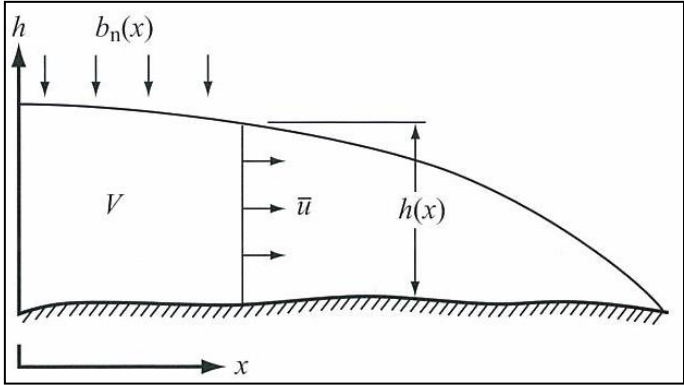


Figure 3.2. Diagram illustrating dependence of balance velocity u on accumulation b_n (Hooke 2005, p. 78).

Depth averaged velocities and surface velocities typically differ by less than 20%, which means that the balance velocity can be converted to a surface balance velocity for direct comparison to measurements of surface velocity (Cuffey and Paterson 2010). If the measured velocities differ significantly from the balance velocities, the glacier must be growing or shrinking. Thus, comparing the balance velocity to actual velocities becomes a way to assess the overall state of a glacier.

Because balance velocities approximate true velocities on many glaciers, they may reveal considerable amounts of information about the structure of flow fields, including typical rates and dominant spatial patterns (Cuffey and Paterson 2010).

Flux measurements have been undertaken along the centreline of many glaciers (see Table 3.1 for a few studies and their quantification of glacier flow). Much of the variation in ice fluxes between the various glaciers can be explained by variations in ice thickness and balance velocity.

3.2.1. Measurements of glacier velocity

The most accurate measurements of surface velocity are obtained during field campaigns (Cuffey and Paterson 2010). A network of metal stakes is constructed and their positions are surveyed at different times, generating displacements over time. Up to the 1990s positions of the stakes were determined by the use of a theodolite (e.g. Hoel and Werenskiold 1962; Brzozowski and Hooke 1981; Hooke et al. 1989). This optical technique was rather labour intensive and the number of data points were limited, or, in bad weather, even zero (Cuffey and Paterson 2010). The advent of Global Positioning Systems (GPS) in the 1990s has changed the nature of field expeditions dramatically, and since then nearly all field work has employed this method (Cuffey and Paterson 2010). Position accuracies better than 1 cm are typically achieved and measurements are fast and straightforward which means bigger areas can be covered. GPS trackers can be left on-site and thus provide a continuous signal recording.

The disadvantage of field expeditions is that they are time consuming and require considerable planning and funds. Moreover, not all glaciers can be accessed without problems due to their location and/or the political situation in the area (Lillesand et al. 2004). Also, they only yield data for a limited number of points in an established network. A more detailed map can be provided by remote sensing (Massonnet and Feigl 1998; Bamber 2007). Feature tracking and Interferometric Synthetic Aperture Radar (InSAR) are commonly used to determine surface velocity (e.g. Joughin et al. 1996; Bamler and Hartl 1998, Massonnet and Feigl 1998, Luckman et al. 2003; Ahn and Box 2010).

3.2.2. Temporal and spatial variations in glacier flow

In line with the general aim of this research, literature concerning characteristics and causes of temporal and spatial variations in the horizontal surface motion of glaciers at a medium-

interval (monthly and inter-seasonal) and inter-annual time frame will be reviewed. When relevant, references will be made to shorter interval (weekly and daily) phenomena, but they will not be discussed in great detail. With a starting point in the overall goal for this research, the focus of this review will be on the connection between glacier motion and climatic conditions (air temperature and precipitation). However, it is impossible to discuss glacier flow without touching upon glacier hydrology and characteristics like glacier thickness and longitudinal stress.

Cumulative changes in MB influence a glacier's thickness and volume that affect the flow of ice through internal deformation and basal sliding, which in turn results in fluctuations in glacier length. This whole process can take several years to decades and even centuries to complete. After a certain reaction time to the initial MB changes, which can range from a few years to decades, the glacier will go through a reaction time from several years to a century, to finally reach a new state of equilibrium (Haeberli 1995). This time taken to fully adjust to a change in its MB is the filling time or volume response time (Cuffey and Paterson 2010, p. 460). Volume response is related to an index of glacier thickness and ablation loss at the terminus (Jóhannesson et al. 1989). Oerlemans (1994) calculated the response time for most valley glaciers to be in the order of 10 – 50 years. The time between a change in MB and the first significant response at the terminus is called the lag time or terminus response time, which occurs many years before the volume response time. Glacier length fluctuations can therefore only give an indirect and delayed signal of climate perturbation (Bamber and Payne 2004; Imhof et al. 2012; Nesje and Matthews 2012). However, frontal position is easier to determine than MB and is therefore often the preferred method for studies examining the influence of climate fluctuations on ice masses (Imhof et al. 2012).

Both melt and rainfall have been identified as major factors influencing glacier motion on a monthly timescale. Similarly, daily and weekly variations in the glacier surface velocity are highly correlated with patterns of water input (Willis 1995; Cuffey and Paterson 2010). Speed-ups are caused when water accumulates on the bed and within the glacier, causing an increase in pressure and volume of water in voids at the base and within basal sediments. This results in lubrication of hard-bed sliding or weakens deformable sediments (Cuffey and Paterson 2010). However, this correlation only exists when the basal temperature is at melting point and a drainage system exists to transport the water to the glacier bed. Therefore, the relation between water input and glacier speed is not a consistent one (Willis 1995; Cuffey and Paterson 2010; Tedstone et al. 2013).

An increase in water input will enhance drainage by melting a larger and more efficient drainage system, or by expanding linked basal cavities. Increased drainage relieves water pressure and reduces water volume, and so reduces glacier motion (Cuffey and Paterson 2010). Hence, the maximum summer velocity is not always associated with the maximum meltwater production: the early-summer fast flow period often ends when an efficient drainage system develops. On many glaciers, the annual velocity maxima seem to precede the maximum ablation rates or the maximum proglacial discharge by about one month (Müller 1968; Müller and Iken 1973; Hodge 1974; Iken 1974, 1977; Brzozowski and Hooke 1981; Hooke et al. 1983).

The development of an efficient drainage system influences glacier motion on a shorter time scale as well. On Unteraargletscher, Switzerland, velocity increases during heavy rains, but after the extra water input has drained along the bed, the glacier flows more slowly than before the rain started (Gudmundsson et al. 2000). On Storglaciären, glacier velocity started to increase during periods of rising melt rates or rainfall and thus preceded peaks of water input (Brzozowski and Hooke 1981; Hooke et al. 1983; Hooke et al. 1989). On Greenland, more recent studies have found that while overwhelming of the hydrological system leads to an increase in glacier motion, this effect will die out later in the season as an efficient drainage system develops (Bartholomew et al. 2010; Tedstone et al. 2013).

In other cases, increased sliding destroys drainage channels that exist either englacially or in the subglacial sediment. Thus, a positive feedback exists between ice flow and water accumulation, leading to large and sustained increases in glacier speed. Surges are an example of this process (Willis 1995). On Variegated Glacier in Alaska, the release of intraglacial water pockets up-glacier seems to be the main source of water input (Harrison 1986), resulting in mini-surges lasting over a period of only a few days (Kamb and Engelhardt 1987). On rigid beds, increased glacier flow results in large and interconnected cavities that conduct water effectively. Thus, the positive feedback mechanism between rapid sliding and water accumulation seems to exist only for deformable beds.

Conversely, on a shorter time scale, different glaciers show a time lag between rates of surface water input and rates of movement. At White Glacier, Washington, USA, the upper ablation area showed a lag of 3-5 days in the early summer and a delay of about 1-2 days in the lower ablation area. At late summer, peaks in water input and velocity were synchronous (Müller and Iken 1973; Iken 1974). The large time lag at the beginning of the melt season is

caused by the drainage channels being closed during the winter. Over the course of the summer, the channels reopen, affected by an increase of overburden pressure, the accumulated heat in the melt water and the conversion of potential energy into heat once water has started to flow (Müller and Iken 1973).

Water inputs change the glaciers ice thickness as they influence glacier motion. In a simple scenario, because the velocity increases are proportional to the time-average velocity, the increases of flux gradient are proportional to the prevailing flux gradient. The rate of thickening and thinning is therefore proportional to the flux gradient. A speed-up along the entire glacier will thus cause thinning where the flux increases downstream.

However, spatial variation does not always follow a simple pattern. Thinning and thickening occur wherever the ice flow increases or decreases in speed respectively. Anywhere along the glacier where the speed-up decreases or increases down-glacier thickening and thinning are favoured, respectively. Furthermore, longitudinal stretching and compression will impact the movement of the ice.

3.2.2.1. Difference between summer and winter velocities

The majority of glaciers show greater spring and summer velocities compared to the autumn and winter (see e.g. Willis 1995, p. 65; Purdie et al. 2008). This suggests that, during the summer, more meltwater penetrates to the bed, thus increasing subglacial water pressures and therefore rates of sliding or bed deformation (Willis 1995). However, some glaciers seem to flow at the same speed all year, or even show the opposite behaviour. Blümcke and Finsterwalder (1905) found that the summer speeds in the upper accumulation area of Hintereisferner, Austria, are up to 20% smaller than the annual speeds. They attributed this exception to the general rule to the fact that very little (possibly no) meltwater penetrates to the bed of the accumulation basin during the summer, leaving subglacial water pressures and glacier speeds unaffected. Higher winter velocities are explained by increased ice deformation and/or basal deformation and regelation due to the increased glacier thickness during winter, resulting in greater internal and basal motion. Winter accelerations have also been observed on Nisqually Glacier, Washington, USA (Hodge 1974), and Variegated Glacier during the initial stages of its 1982-1983 surge (Kamb et al. 1985). Similar findings were made at the ELA of Saskatchewan Glacier, Alberta, Canada (Meier 1960), on one ice fall in Mittelbergferner, Austria (Pillewizer 1949), and in the accumulation area of Gornergletscher,

Switzerland (Elliston 1966), where summer and winter velocities are the same. On Jakobshavns Isbræ, it has been suggested that, surface-derived water during the summer travels englacially and does not reach the bed until the grounding line, accounting for the lack of monthly velocity variations in its ablation area (Echelmeyer and Harrison 1990). Mid-season accelerations have been described for Unteraargletscher (Iken et al. 1983) and Findenlengletscher, Switzerland, (Iken and Bindschadler 1986). On the latter, water pressure measurements demonstrated a clear connection between water pressure and speed.

3.2.2.2. *Occurrence of glacier motion events throughout the summer*

The relationship between high water inputs and rapid glacier motion appears to vary during the summer (Harrison 1986; Hooke et al 1989). Harrison et al. (1989) and Hooke et al. (1989) made observations of a sharp transition from low “normal” velocities to a higher background summer velocity on Variegated Glacier and Storglaciären, respectively.

3.2.2.3. *Decreasing seasonal velocity variations with distance up-glacier*

The difference between maximum and minimum velocities over medium- and long-term timescales decreases on many glaciers with distance up-glacier (Elliston 1966; Hooke et al. 1989; Willis 1991). For instance, the July velocities in the lower ablation area of Midtdalsbreen are 56% greater than those in March. 100 m higher up, the seasonal velocity increase is only 17% (Willis 1991). Similar observations were made on Storglaciären (Hooke et al. 1989). These results represent the degree to which subglacial water pressures are dependent on ice-overburden pressures. In the lower ablation area, melt rates are higher, snowpack is a lower influence and the hydrological system is more developed than higher up the glacier. Thus, ice thickness becomes a major parameter for glacial horizontal velocity. Additionally, with smaller ice thickness in the lower ablation area, water pressure will be a larger fraction of the overburden pressure, and will therefore have a larger influence on the glacier’s velocity (Hooke et al. 1989; Willis 1995).

3.2.2.4. *Kinematic waves of high summer velocity*

Kinematic waves of high summer velocity have been observed to move down-glacier on some glaciers. On Hintereisferner, this seasonal wave of maximum velocity moved at a speed of 18-

26 km yr⁻¹ (Schimpp 1958). At Nisqually Glacier, the wave moved at similar velocity (Hodge 1974), while on Columbia Glacier, the seasonal wave of high velocity moved down-glacier at speeds of 58-91 km yr⁻¹ (Krimmel and Rasmussen 1986; Krimmel and Vaugh 1987). The waves may be explained by fundamental aspects of the subglacial hydrological system, which influence spatial and temporal patterns of subglacial water pressures. The occurrence of the waves moving down-glacier requires a build-up of water pressure in up-glacier locations during the summer. Water could be stored subglacially during the winter when late-season supraglacial drainage water is trapped by early conduit closure. The build-up of subglacial water pressure may also occur when crevasses or moulins are located in up-glacier locations, or when water builds up within subglacial till or cavities. The mini-surges described for White Glacier (Iken 1974), Storglaciären (Hooke et al. 1989), Findelengletscher (Iken and Bindschadler 1986), Variegated Glacier (Kamb and Engelhardt 1987) can be explained in a similar manner. It seems that the surges are a way to evacuate this build-up water by the formation of pipes and channels within till or cavity linkages and tunnels over bedrock. Another explanation for the down-glacier propagation of waves of high glacier motion might be the result from an acceleration of blocks of ice in the upper part of a glacier, which will cause a longitudinal force on ice at progressively lower elevations. In contrast, the kinematic waves of high summer velocity moving up-glacier on Storglaciären, where the velocity increase in the middle ablation area occurred before the velocity increase in the upper ablation area (Hooke et al. 1983), might be expected when the restraining influence of ice at lower elevations has been reduced by the previous acceleration of flow in the lower areas (Willis 1995).

3.3. Previous work on Hellstugubreen

Work on Hellstugubreen has been extensive. A detailed description of the field campaigns and their methods can be found in Section 4, which tackles the data used in this research.

3.3.1. Volume

Volume investigations by Liestøl (1962) revealed that the glacier surface had lowered considerably since 1941. Longitudinal profiles and diagrams of cross sections show a general decline in surface elevation, with mass losses decreasing with distance from the front.

Haakensen (1986) investigated changes in volume on Hellstugubreen for the period 1962 – 1968 and 1968 – 1980 by placing identical grids over maps for each of these years. It was found that comparison of the maps from 1962 and 1968 did not provide sufficiently reliable data. For the other years, the contour lines coincide better, and with an error of less than 1 m, this comparison was considered to give reliable results. Between 1968 and 1980, Hellstugubreen decreased, and lost most mass on its tongue. In the accumulation area, a small increase in height was identified (Figure 3.3). It was concluded that Hellstugubreen showed a rather consistent pattern with an even decrease of displacement with height, making it straightforward to draw up the isotachs. Only in higher regions of the accumulation area some inconsistencies were found to exist, probably due to inaccuracies of the original maps. As noted in Section 3.1.2, Andreassen (1999) and Bauder et al. (2007) experienced the same problems with map accuracy.

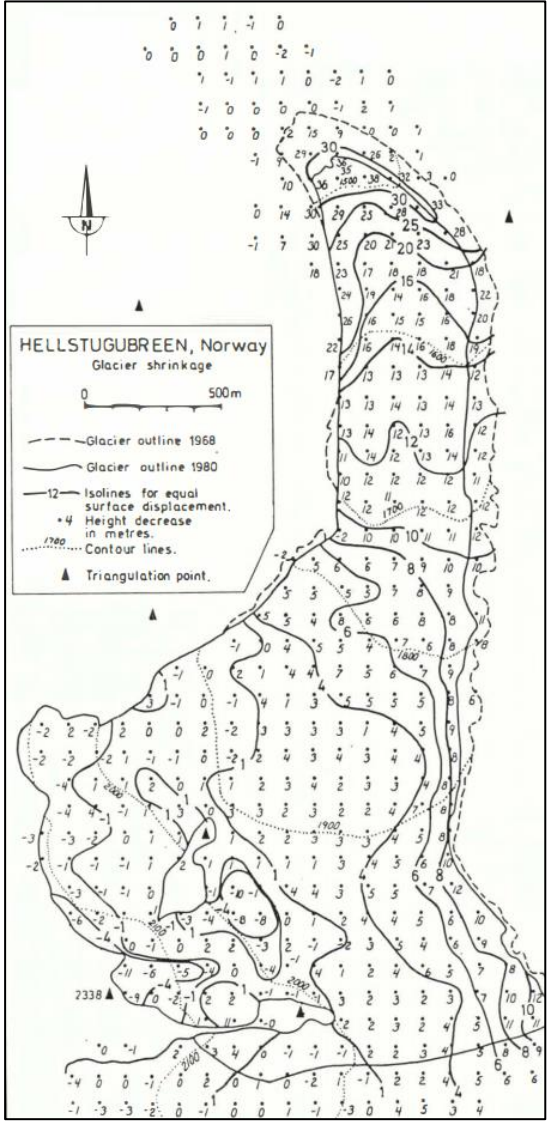


Figure 3.3. Surface elevation change between 1968 and 1980 in m. Dots indicate 100 m grid points. Positive figures indicate decrease in height and negative figures indicate growth (Haakensen 1986).

The total reduction of the glacier was found to be $19.7 \times 10^6 \text{ m}^3$, the average vertical reduction for the entire glacier being 5.98 m. Wielding an ice density of 0.9 g/cm^3 (as in Andreassen 1999, Bauder et al. 2007, Paul and Haeberli 2008), this corresponds to a negative MB of 5.39 m w. eq (Haakensen 1986). Andreassen et al. (2002) calculated volume changes on Hellstugubreen between 1966 and 1988 from traditional mass balance measurements and found a result of -7.7 m of cumulative volume change.

3.3.2. Extent and terminus

Liestøl (Hoel and Werenskiold 1962; Liestøl 1962) analysed the frontal and volume variations of Hellstugubreen since the beginning of the 21st century. Between 1901 and 1954, the glacier retreated 441.3 m (Hoel and Werenskiold 1962). Longitudinal profiles showing the glacier surface at specific times were constructed and these allowed the estimation of the total ice loss since 1750. Both frontal and volume changes on Hellstugubreen are summarized in Figure 3.5. Figure 3.4 shows the frontal changes on Hellstugubreen compared to the other glaciers in Jotunheimen for the same period. The advance of several glaciers in the early 1900s (1907 for Hellstugubreen), as well as the rather fast retreat of the front in the 1940s becomes apparent from the diagram.

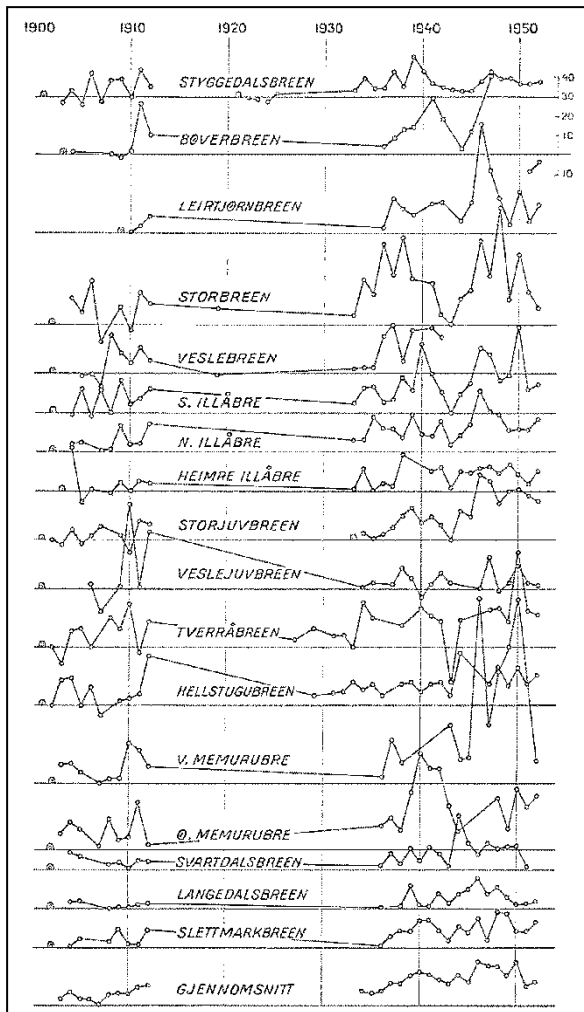


Figure 3.4. Annual frontal fluctuations of the glaciers of Jotunheimen (Liestøl 1962, p. 24).

3.3.3. Velocity

Liestøl (1962) concluded that Hellstugubreen is a glacier showing little dynamic action or variability. The glacier's maximum velocity was calculated to be less than 6 cm day^{-1} . The observed velocities are often less than the errors of observation. However, because of the regular shape of the tongue, Liestøl expects the flow on the lower areas of the glacier to be rather regular.

A clear difference between summer and winter velocities was established. The averages for the observation years 1938 – 1939 and 1941 – 1942 show the winter flow to be 73 and 83% of the preceding and following summer periods, respectively. Summer and winter velocities on Hellstugubreen seem to be independent of altitude, contrary to findings in the Alps (Elliston 1966), but in line with results from Midtdalsbreen (Willis 1991) and Storglaciären (Hooke et al. 1989 (see Section 3.1.2.3).

Figure 3.5 shows the isotachytes for 1942. Liestøl notes that even if the map would look the same for different years, the absolute values would be very different from year to year. Two waves of high velocity were identified. The first wave (1940) did not travel beyond 1650 m a.s.l. However, the wave recorded in 1943 travelled almost to the very front of the tongue the following year. Section 3.1.2.4 describes similar observations on other glaciers and in different areas. Liestøl (1962) finds a possible explanation for the speed up in 1942-1943 in the unusually large amount of snowfall during the previous winter.

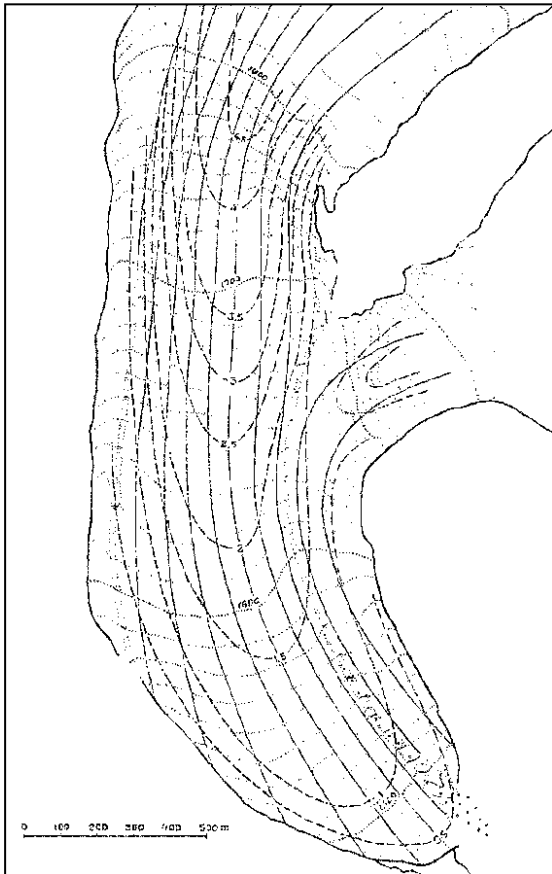


Figure 3.5. Map of Hellstugubreen with isotachs for 1942 (Liestøl 1962, p. 13).

Pytte (1964) found that stake velocities and their direction of movement were consistent during both years of her measurements (1961 – 1962 and 1962 – 1963). When comparing her own data to Liestøl’s analysis, Pytte sees similarities both in the direction of the flow-line and the pattern of the isotachs. Pytte (Ibid.) also found great velocity differences to exist between the ice flows on either side of the medial moraine² and thus considers the main Hellstugubreen and the small cirque located between Hellstuguhøe and Nørdre

² Until the smaller cirque between Hellstuguhøe and Nørdre Hellstugutinden (see Figure 3.5 for a map of Hellstugubreen and its surrounding peaks) got cut off from the main ice flow of Hellstugubreen between 1968 and 1980, a medial moraine formed by both ice streams was visible on Hellstugubreen. The moraine is still visible in the landscape today, but Hellstugubreen now flows to the east of the feature, while the cirque has retreated around 80 m in altitude.

Hellstugutinden to be separate ice flows that do not change their characteristics even below their point of merging.

Liestøl (1962) investigated the link between glacier fluctuations and variations in climatic conditions. At the time of his research, there were no meteorological stations within the Jotunheimen region, so he analysed data collected by stations located to the east, south and west of the region. Liestøl (Ibid) notes, however, that it is difficult to say how representative of the glaciated areas the data is, as local weather conditions vary greatly in the mountains. Figure 3.7 shows temperature and precipitation observation series for 4 stations.

Liestøl (1962, p.34) notes that the precipitation records for the Fannaråki station can be considered the most representative of the four, but that eastern Jotunheimen probably receives more precipitation with easterly winds. Only precipitation in the form of snow is considered in the time series, and is therefore reckoned from September 1st to June 1st.

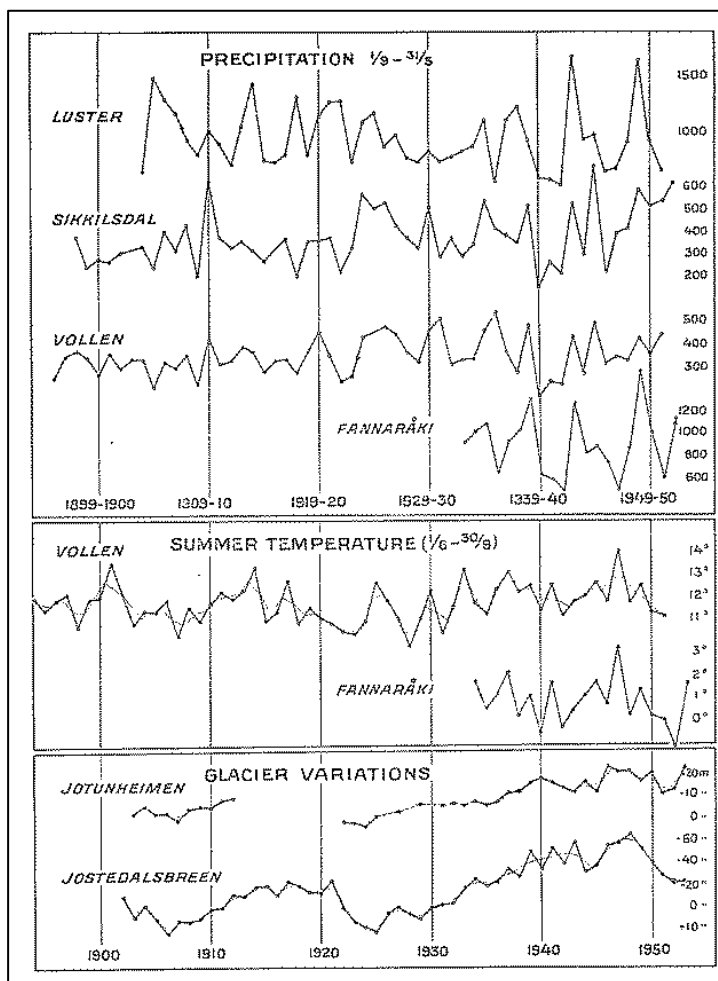


Figure 3.6. Winter precipitation and summer temperature for stations in the greater Jotunheimen region. Lower graph represents mean annual variations of 16 Jotunheimen glaciers and 12 outlet glaciers of Jostedalbreen, Norway. Dotted lines represent biannual means (Liestøl 1962, p.31).

Liestøl (Ibid.) states it is difficult to estimate how precipitation influences the advance or retreat of the glacier. In the summer of 1943, the tongue of Tverråbreen remained snow

covered because of unusually high winter precipitation. The effects of great accumulation may be registered already during the measurements the following summer. The effect on glacier flow may not be as straightforward to record, however, as it may be adjusted and delayed differently on individual glaciers. In addition, great winter precipitation can be cancelled out by high summer temperature, while the combination of little snow fall and a warm summer will cause more extensive melting. The station at Volden is considered the most representative for temperature observations. In order to study the relationship between meteorological factors and glacier variations, Liestøl (Ibid.) suggests that the combined effects of precipitation and temperature be considered.

The lower graph in Figure 3.7 shows glacier fluctuations in Jotunheimen, and for the sake of comparison, for the outlet glaciers of Jostedalsgreen, western Norway. No direct measurements exist for Jotunheimen between 1912 and 1933, but investigations of the proglacial landscape on Jotunheimen glaciers revealed that most glaciers experienced an advance during this period. Liestøl (1962, p.35) examined temperature and precipitation curves for the 1920s and established that the early 1920s had favourable conditions for glacier advance. He notes that great similarity is found, even in detail, between glacier fluctuation curves and the curves for the biennial temperature average. He concludes that temperature appears to have had the greatest influence upon glacier variations. However, he recommends a study of solar radiation rather than temperature as later investigations revealed that the incoming radiation on temperate glaciers normally accounts for more than 50% of the total ablation, while convection rarely accounts for more than 30% (Ibid.).

In 1964, Randi Pytte published her cand. real. thesis *Glaciological Investigations of Hellstugubreen* at the University of Oslo. Between the summer of 1962 and the autumn of 1963, Pytte spent about 100 days in the field divided over 10 field campaigns (Pytte 1964). The complete dataset will hereafter be referred to as PYT60. Both the original KOL40 and PYT60 can be found as hand written tables in the *NVE* archives in Oslo (Figure 4.1. Pytte published more concise tables in her doctoral thesis (Pytte 1964).

4.1. Maps

Maps constitute the basis for any glaciological investigation (Liestøl 1962; Pytte 1964). Maps (and photographs) allow the investigation of frontal and volumetric changes (e.g. Arendt et al. (2002). Mapping surveys of Hellstugubreen began as early as 1928 and many maps have been constructed since, some covering only the tongue, others covering the entire catchment area of the glacier. Some maps were never published, but were only used in the field and in order to set up trigonometric and stake networks. A detailed description of the mapping history on Hellstugubreen and in Jotunheimen can be found in Liestøl (1962). An overview of the maps used in this research is given in Table 4.1.

Source	Contours (m)	Scale	Type	Tongue, shape contours
Koller et al. 1941	10	1:10000	analogue, shape file contours	1931
Pytte 1962	10	1:10000	analogue, shape file contours	1932
Pytte 1968			shape file contours	1935
Liestøl 1980	10	1:10000	analogue, shape file contours	1938
NVE 1997			shape file contours	1940
NVE 2009			LAS, point cloud	1942
				1943

Table 4.1. Maps used in this thesis.

The 1941, 1962 and 1980 maps were used in this research as analogue maps as were their digitised versions. Analogue maps were digitized into ArcMap by *NVE* to make analysis possible, and they were made available as .shp-files (shape files) containing contour lines for the catchment area and glacier outline. For some maps the digital version was the only one consulted, even if they were not originally digitally constructed (e.g. the 1968 map). The 1941map was based on triangulation and terrestrial photogrammetry and was constructed in a

1:5000 scale with 10 m contour lines. It was printed in a 1:10000 scale with 10 m contour lines. When Pytte mapped the glacier in the summer of 1962, a Zeiss theodolite was used at both old (as used for the 1941 map) and new trigonometric positions (Pytte 1964). The former for the sake of reference, the latter were being used to measure in ablation stakes. 500 positions were used, their location dependent on density based on the glacier's topography. The resulting map was drawn in a 1:5000 scale, but it was printed in 1:10000 with contour lines at 10 m. The 1980 map was based on aerial photography, shot on 26. September 1980 by *Fjellanger Widerøe A.S.* O. Liestøl plotted the map for *NPI* and *NVE*.

In 1997, a DTM was constructed by *NVE* from remote sensing imagery (vertical aerial photography, August 1997) and was made available as a shape file containing contour lines. In 2009, orthophotos were obtained, providing information on the glacier's outline and retreat. The same year, a LiDAR (Light Detection And Ranging) survey was conducted, and a new DTM constructed. The data from the LiDAR investigations was made available to this research in the form of a .las-file containing elevations.

4.2. Volume changes and slope

For each stake, KOL40 contains data on the altitude change since the last position, the ablation since the last observation and the slope of the glacier's surface at that stake. Liestøl (1962) constructed several diagrams on volume changes on Hellstugubreen between 1929 and 1947, based on maps drawn up in a 1:2000 scale. The maps were based on tacheometric surveying and terrestrial stereophotogrammetry. Maps for each year are printed on transparent paper, one map is placed upon the other and the volume changes were calculated using a planimeter.

PYT60 contains calculations of volume changes for Hellstugubreen between 1941 and 1962, based on the KOL41 and PYT62 maps. In 2011, *NVE* conducted a radio echo sounding survey of Hellstugubreen and an ice thickness map of point data was made for that year (Figure 4.2). Each year, *NVE* digs a snow pit in the higher accumulation area to establish snow density.

It should be noted that the interpolated ice thickness (Figure 6.2) was based on a radar survey from 2011 while the DEM was derived from 2009 laserscanning. However, the surface

elevation difference between 2009 and 2011 can be assumed not to be of such an order that it would influence the driving stresses enough to compromise results.

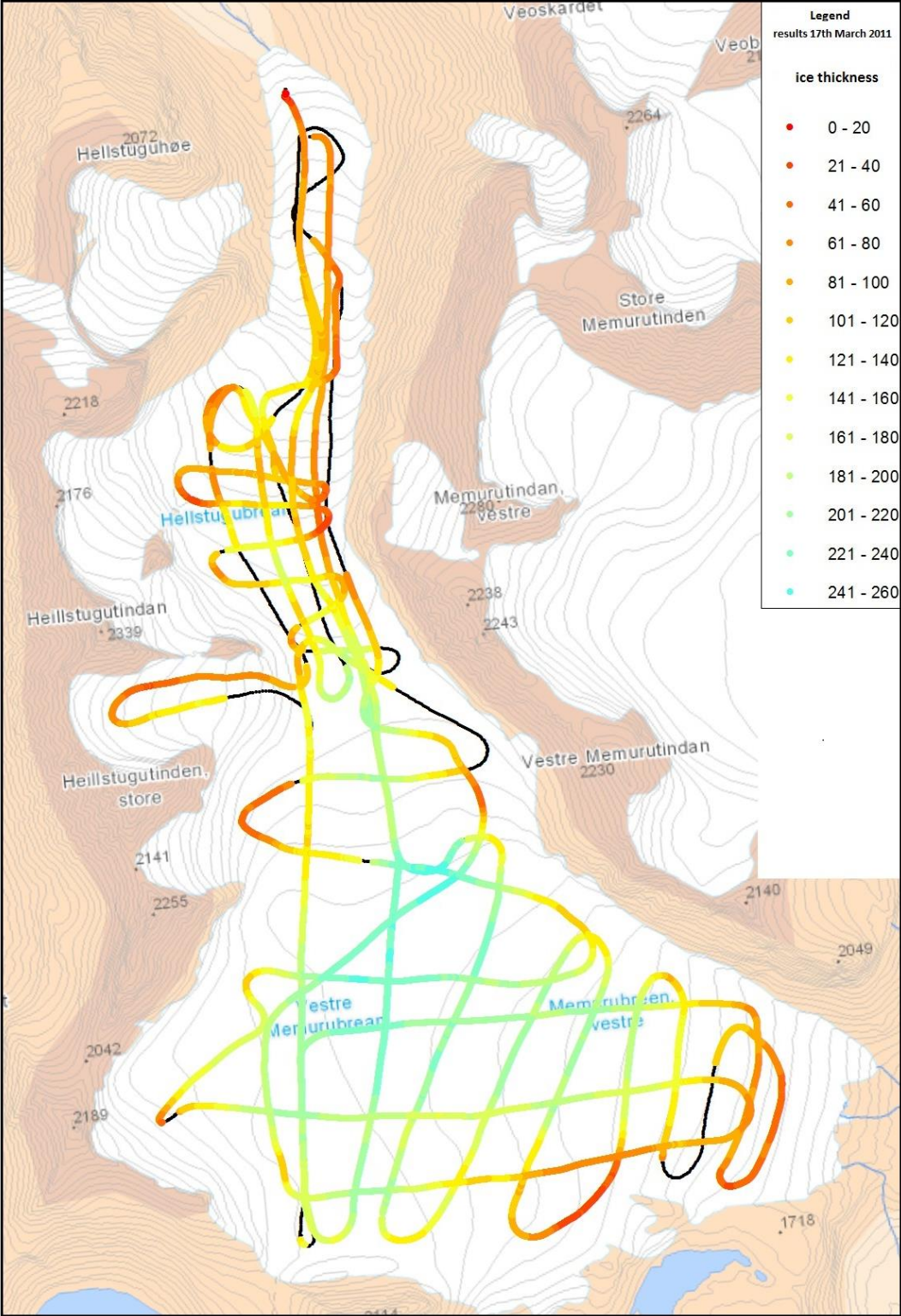


Figure 4.2. Ice thickness derived from radio echo sounding, March 2011 (Data: NVE)

4.3. Frontal changes and extent

The first surveys of Hellstugubreen's front were undertaken by P.A. Øyen, employed by the Geological Museum in Oslo (Hoel and Werenskiold 1962). Øyen conducted annual measurements of glacier variation between 1901 and 1912, when funding ran out. In order to measure the frontal position of the glacier, Øyen built a cairn at a suitable distance in front of the glacier tongue. Then, the distance from the cairn to the ice was measured with steel tapes along a fixed direction indicated by a second cairn. The cairns were placed so that the line would reach the ice at the most projecting point and in the middle of the front. The fieldwork was carried out once a year, usually towards the end of August (Hoel and Werenskiold 1962). Werenskiold resumed the work in 1933, but instead of cairns and lines he employed a tachymeter and a network of trigonometrical points (Liestøl 1962). His work continued until 1948 (Hoel and Werenskiold 1962). In 1949, *NPI* took over the survey (Hoel and Werenskiold 1962). Liestøl (1962, 23) includes a map of frontal retreat of Hellstugubreen between 1901 and 1948 (Figure 4.3).

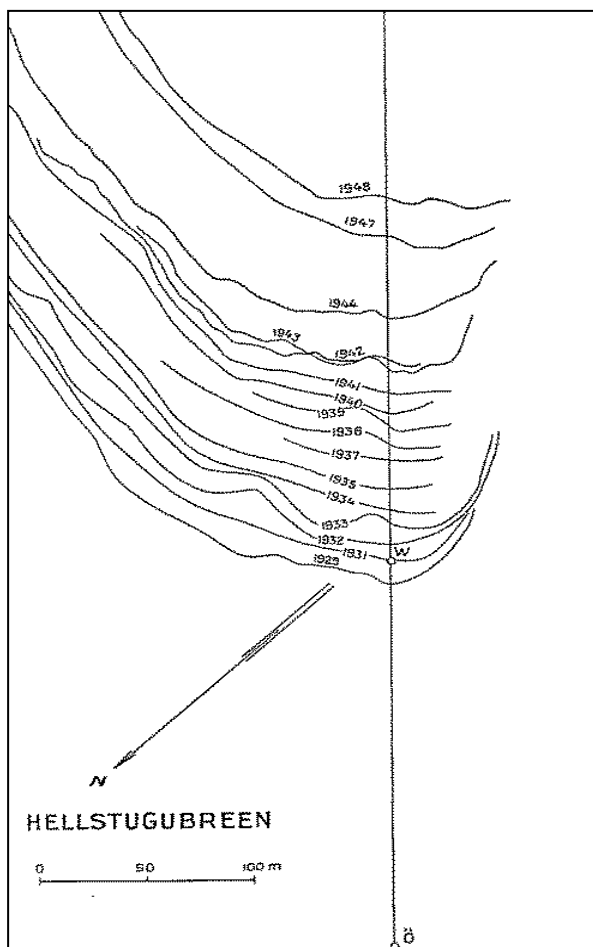


Figure 4.3. Frontal retreat on Hellstugubreen between 1901 and 1948. Points marked with $\text{\textcircled{O}}$ and W mark the cairns that Øyen and Werenskiold erected in 1901 and 1933, respectively (Liestøl 1962, p. 23).

Since the 1960s, *NVE* monitors the glacier front. Every year, measurements are made in late summer or early autumn, preferably before the first snow fall, usually in August or September. Distances are measured from along, or parallel to, the central flow line of the glacier. Traditionally, measuring tape was used to determine the distance between the glacier terminus and fixed landmarks such as big boulders or painted rocks, providing an accuracy of 2 m. Recently, a laser distance meter has been used, with an accuracy of 1 m (Andreassen et al. 2005). Apart from field investigations, remote sensing methods help determine glacier outline and frontal position. Ortophotography was used for the glacier outlines for 1997 and 2009.

4.4. Speed records

KOL40 comprises speed records for stakes between 1937 and 1944. In 1937, 41 holes in 9 rows were drilled into the surface of the lower part of Hellstugubreen. Rattan stakes equipped with barbs and numbered discs were placed in the holes. Stake positions were determined by sighting from two trigonometrical points with the aid of a precision theodolite. The lowest 24 points were also sighted from a third point. Until 1944, measurements of the stakes were carried out annually. The position of the stakes was determined by trigonometrical cross-bearing. Some years, the snow depth was determined by probing of the snow pack (Hoel and Werenskiold 1962).

1937	15.09
	10.10
1938	12.08
	28.09
1939	4.08
	18.09
1940	13.08
	16.09
1941	24.07
	13.09
1942	29.07
	15.09
1943	8.09
1944	3.08
	5.09
1945	3.09
1946	27.08
	11.09

Table 4.2. Observation dates for KOL40.

Velocity values were determined from the location of the ablation stakes. There usually exist 2 sets of observations for each year, with an interval of about six to eight weeks: one in late summer, the other when the snowline is highest, in September. Exceptions are 1943, 1945 and 1946. Liestøl mentions it is unfortunate that the measurements could not be made on the same date every year (Liestøl 1962, p. 6).

PYT60 consists of speed records for 1961-1962 and 1962-1963. The stakes were measured in August 1961, 1962 and 1963. The first year, a Baalsrud-instrument was used, while the following two years Pytte opted for a Zeiss DM-1 instrument (Figure 4.4). The latter was easier to move around in the field, but more importantly, it proved to be more accurate.

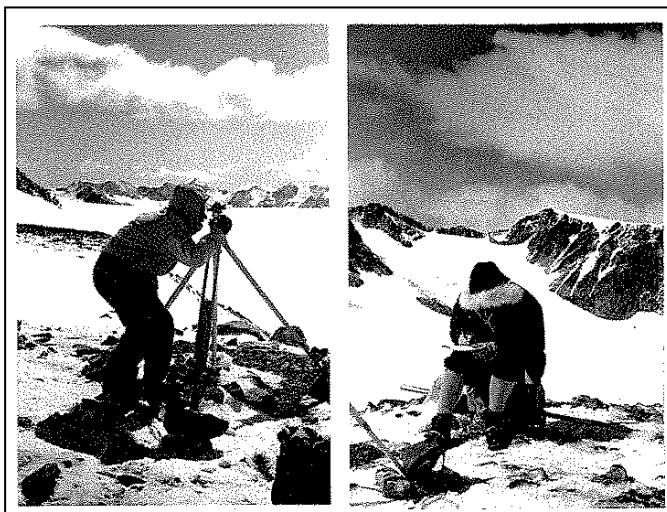


Figure 4.4. Measurements on Hellstugubreen, August 1962 (Images: Pytte 1964).

Seven measurement stations were established in the area, and the position of most stakes were measured from three of these. The position was determined based on the position of the previous year. However, because of high ablation, several stakes had to be redrilled during the summer. In the winter of 1962 the stakes in the accumulation area got buried under the snow, and most of these didn't appear during the ablation season. For this year, only the movement of the stakes on the glacier tongue could be measured. The accuracy for the measurements Pytte made was influenced by limitations of the instruments used, the melting out of stakes from the ice during the summer and weather conditions. Pytte calculated the uncertainty for both measurement seasons. The results of her measurements were visualised in a map showing vectors representing the velocity and direction of movement for each stake (Figure 4.5).

NVE has been recording stake position during their MB surveys, resulting in a series of continuous data from the 1960s until present for the stakes located on the glacier. The data

consists of UTM coordinates, antenna height and snow cover thickness. Section 5.1.2 contains further information on how stake locations are recorded in the field, and processed after. In 2009, *NVE* resumed investigations of glacial dynamics.

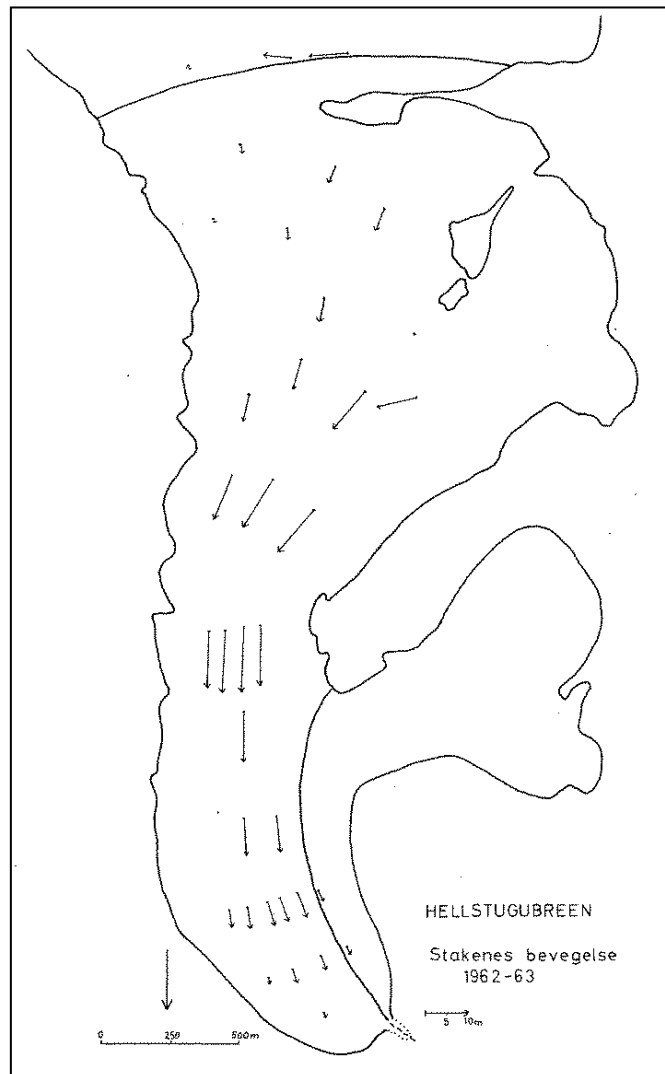


Figure 4.5. Map showing vectors representing the movement of the stakes as measured by R. Pytte for 1962-1963 (Pytte 1964).

4.5. Mass balance data

KOL40 contains MB measurements taken between 1937 and 1944. The length of the part of the canes protruding from the ice was measured, as well as the depth of the holes. Observation dates are the same as in Table 4.2. In spring, accumulation was measured and in autumn the ablation was determined. Autumn fieldwork also consisted of re-boring of the stakes that had melted out during the summer.

PYT60 has MB data for 1961 – 1962 and for 1962 – 1963. Stakes were measured in August. In order to calculate ablation, 36 stakes were drilled in the summer of 1961. In April 1962, 7 snow pits were dug in order to measure snow density and thus calculate accumulation. In the summer of 1963, accumulation was measured by probing. The stakes were measured in August 1961, 1962 and 1963.

NVE continued the MB measurements started by Pytte in the 60s and there exist annual MB records for Hellstugubreen from 1962, and 2010 was the 49th year of continuous MB measurements (Kjøllmoen et al. 2011). Accumulation and ablation measurements are usually performed in May, August and September each year. Snow depth soundings are made in May. For 2010, soundings were made at 138 locations (Ibid.).

5. Methodology

5.1. Field methods: glaciological method

The primary data for this research was gathered from 2010 to 2012 in assisting *NVE* on their annual fieldwork. *NVE* conducts field measurements three times a year on Hellstugubreen: the first measurements of the year are conducted at the end of the accumulation season (usually May), followed by a maintenance visit in July or August. A third campaign measures ablation at the end of the melt season, and preferably before the first snow, in mid-September. The dates for the fieldwork for this research (in assistance to *NVE*'s investigations) are listed in Table 5.1. The fieldwork in July 2013 consisted solely of photographing the glacier and surrounding country, and was performed independently of *NVE*.

year	date	fieldwork	participants
2011	Aug.04	MB, stake locations, frontal position	L.M. Andreassen, S. Windsvold, I. Pay
2012	May 02	MB, stake locations, frontal position, ice depth, snow depth	L.M. Andreassen, O. Repp, I. Pay, I. Pande Braathen
	Sep.20	MB, stake locations, frontal position	S. Windsvold, E. Barfod, I. Pay, I. Pande Braathen, B. Driessens
2013	July 7 – 8	photographs	I. Pay, T. Shaw

Table 5.1. Overview of the fieldwork gathering primary data.

During their field campaigns, *NVE* records accumulation and ablation at the stakes on the glacier. In addition, the position of the glacier front is determined. In winter, a snow pit is dug in the upper accumulation area. For each stake, the coordinates are recorded. Stakes that are at risk or that have already melted out from the ice are redrilled, and the new position is noted. For each year, a stake network map is made.

5.1.1. Determining the stake network

The stake network used is the one set up by *NVE*. From the extensive investigations in the 1960s, the measurement network was simplified gradually, based on experience and without affecting the accuracy of either the measurements or results (Andreassen et al. 2005; Kjøllmoen et al. 2011). A stake map for NVE10 can be found in Figure 5.1. A total of 13 stakes have been located on Hellstugubreen since 2011.

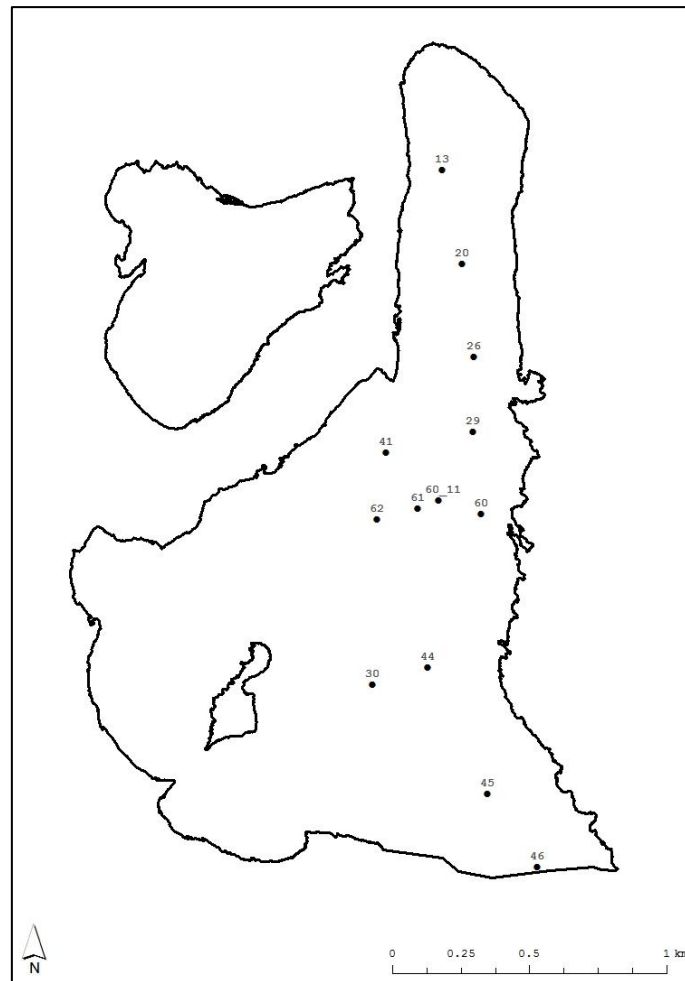


Figure 5.1. Stake map for the NVE10 fieldwork.
Glacier outline from 2009.

The placement of the stakes is based on several considerations:

- In order to be able to extrapolate point data to the entire glacier, the location of the stakes is of great importance. The density of the stake network is dependent on the glacier's hypsometry, geometry and mass-balance gradient. All areas on the glacier should be represented, which means stakes need to be placed from tongue to upper accumulation area;
- When performing velocity measurements, stakes should be placed near the central flow line, but also to the sides of it for comparison;
- In order to have as continuous time series as possible, and for the sake of comparison to previous data, new stakes may be placed at, or close to, the location of an older stake that has been lost or removed over the years.

5.1.2. Stake coordinates

Stake positions are recorded on every field campaign and are an essential part of the data set. A differential GPS (dGPS) is used for accurate determination of the location of a stake. dGPS provides improved location accuracy, from the 15 m nominal GPS accuracy to about 10 cm, improving speed measurements. Since stake locations were recorded with several months between measurements, this 10 cm is negligible.

A fixed, ground-based reference station is used in order to calibrate an antenna unit carried on the glacier. The base broadcasts the difference between the position of the roving receiver (henceforth referred to as Rover) indicated by the satellite systems and the known fixed position (Chivers n.d.) The base station records the position of the Rover every 2 seconds, generating long tables containing the time of measurement, coordinates and elevation. The data file will show at what position the Rover was standing still long enough for the logging to be completed. In order to get an accurate measurement, the Rover is positioned as close to the borehole as possible (Figure 5.2). In order to hold the dGPS still in one place, it is positioned in the snow when possible (Figure 5.2). When there is not enough snow, it is sometimes taped fixed to the stake. However, sometimes it is impossible to hold the Rover completely still in the field, and readings may vary during this “stable” period of coordinate readings. Therefore, an average is made both for the northings and eastings of the stake. Altitude is averaged the same way.

The obtained coordinates are then compared to those computed after the previous field work. In order to facilitate data analysis, a nominal, hand-held GPS unit (Garmin X) is carried on the glacier. With this unit, a coordinate is determined at every stake, together with the time of measurement (Figure 5.2). By comparing the Garmin GPS coordinates to the long lists of coordinates received by the dGPS, the dGPS data becomes more manageable. The elevation (Z-coordinate) of the stake has to be adjusted for antenna height (Figure 5.3). At NVE, Bjarne Kjøllmoen does all the processing of the Rover data.

At Hellstugubreen, a large boulder was chosen as the position for the fixed base. The boulder is big enough to be easily identified in the field, and its size ensures that it stays snow free during winter. A threaded metal rod was permanently drilled into this rock, which allows the dGPS base to be screwed into exactly the same place on the way to the glacier (Figures 5.4 and 5.5).



Figure 5.2. Recording handheld GPS data while the Rover is positioned as close to the stake as possible (Image: personal collection, May 2nd 2012).

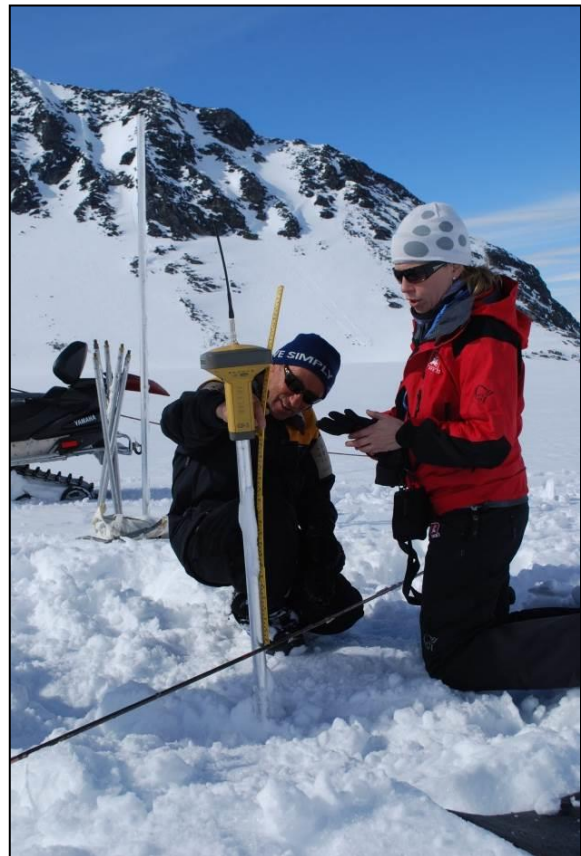


Figure 5.3. Measuring of antenna height above the snow surface (Image: personal collection, May 2nd 2012).



Figure 5.4. The boulder used to position the dGPS base station. Red circle indicates the threaded metal rod fixed into the rock used to screw the base in place. Hellstugubreen can be seen in the background (Image: personal collection, July 8th 2013).



Figure 5.5. The dGPS base in place, view towards Visdalen. Svellnosbreen in the background (Image: personal collection, Aug 4th 2011).

5.1.3. Glacier front

In late summer, changes in the position of the glacier front are measured by using a laser range finder in front of the ice body. The laser distance meter is held to the eye and pointed at a target at the ice edge. It then measures the time it takes a pulse of laser light to be reflected off of the target and returned to the sender. The time of flight measurement technique has proven to be useful the times it was employed at Hellstugubreen, thanks to favourable weather conditions. Accuracy is achieved within 1 m (Andreassen et al. 2005).

Part of the front was plotted on 20th September 2012 with the Garmin GPS by walking along the ice edge and measuring at 10 metre intervals.

5.2. Data analysis procedure

Data analysis was done in Microsoft Excel 2010 and with the use of GIS software. All maps were produced using ArcGIS software by Esri, more specifically ArcMap and ArcScene.

The handwritten tables from KOL40 as well as the relevant tables found in PYT60 were digitised for further analysis. All available mapping data was imported into ArcMap in order to facilitate analysis. First, stake coordinates from KOL40 were converted from the NGO_1948 (Oslo, Norway, Zone 2) coordinate system to GCS_WGS_ using ArcMap. Shape files were made per observation date, as well as per stake, both for KOL40 and NVE10. PYT60 does not contain stake coordinates and therefore the stake map for this dataset was scanned and digitized in ArcMap. From the 2009 LiDAR image, a DEM was created.

With all the elevation data in ArcMap, the quality of the data could be considered. The 1962 contour lines proved to be rather inaccurate for off-glacier areas, with elevation sometimes several dozen meters off compared to both the contours from 1941 and the more recent ones. Data based on maps with little accuracy give less reliable results, as suggested by the literature (Andreassen 1999; Bauder et al. 2007). The comparison of the contour maps and DEMs led to the estimation of the accuracy of the maps at $\pm 1.0 - 2.0$ m. The 2009 DEM is assumed to have the highest accuracy since it was made from LiDAR data. Andreassen (1999) uses the same level of accuracy.

Stakes relevant for comparison of KOL40, PYT60 and NVE10 were selected. To this purpose, an overlying stake map for all three datasets was constructed (Figure 5.6.). KOL40 and NVE10 contain coordinates for all stakes, which were imported into ArcMap. With a starting point is the overlying stake map, stakes from all three datasets were chosen according to their relative position on the glacier as well as according to how they overlap on the map (Table 5.2.). Stakes will henceforth be referred to as stake#_{dataset} (e.g. 11_{KOL40} for stake 11 from the KOL40 dataset). Another consideration when selecting stakes, was the quality of the data series available for each stake, especially for NVE10 as not all stakes have consistent records. For some stakes, like 45_{NVE10} and 46_{NVE10}, observations are questionable, as too many alternative locations have been recorded in the field.

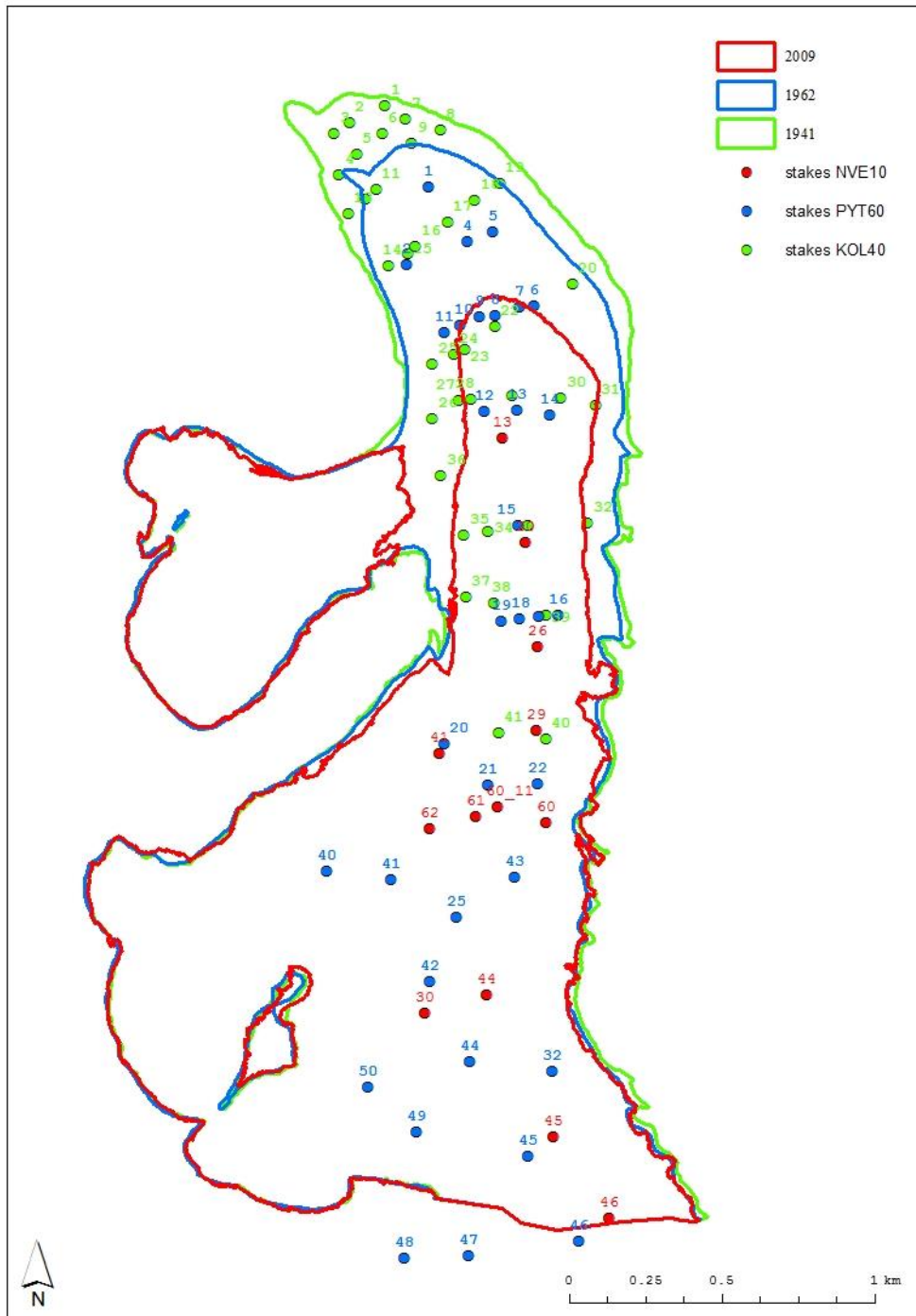


Figure 5.6. Overlaying stake maps and glacier outlines for KOL40, PYT60 and NVE10.

Stakes 11_{KOL40}, 2_{PYT60} and 13_{NVE10} were selected for analysis based on their position in relation to the glacier's front at the time of their initial set-up (Table 5.3). This approach was chosen in order to investigate if velocities at the glacier's tongue have changed over time, and to what magnitude. The other stakes were selected based on their proximity to each other. In

some instances, e.g. 33_{KOL40}, 15_{PYT60} and 20_{NVE10}, the location is almost identical. In others, e.g. 39_{KOL40}, 17_{PYT60} and 26_{NVE10}, the stakes are slightly further removed from each other.

	KOL40	PYT60	NVE10
relative location from front	11	2	13
overlap	28	12	13
	33	15	20
	39	17	26
	40	22	60

Table 5.3. Relative distance from front at time of observation for selected stakes.

Table 5.2. Selected stakes for comparison.

stake	distance from front (m)
11 _{KOL40}	314
2 _{PYT60}	313
13 _{NVE10}	422

5.2.1. Glacier outline

Even though it was cut off from the main ice body, the small cirque confined between Hellstuguhøe and Nørdre Hellstugutinden (Figure 2.5) has been included in all measurements of glacier extent and volume. Its exclusion from the 1980, 1997 and 2009 maps would result in unnaturally high changes in both volume and area extent. Also, other literature on Hellstugubreen includes the cirque in results, which makes comparison more straightforward (e.g. Kjøllmoen 2011).

As Hellstugubreen's accumulation area borders that of Vestre Memurubreen, the ice divide had to be determined. It was drawn at an elevation of around 1950 m.a.s.l. from the foot of the Nørdre Hellstugubreahesten nunatak to the west to the foot of the Vestre Memurtindan ridge to the east. The divide was based on the contour lines alone, without considering the drainage of the higher located cirques. Other literature operates with a different ice divide (e.g. Kjøllmoen 2011, NVE 2014), since part of the higher areas drain onto Hellstugubreen (Figure 5.7).

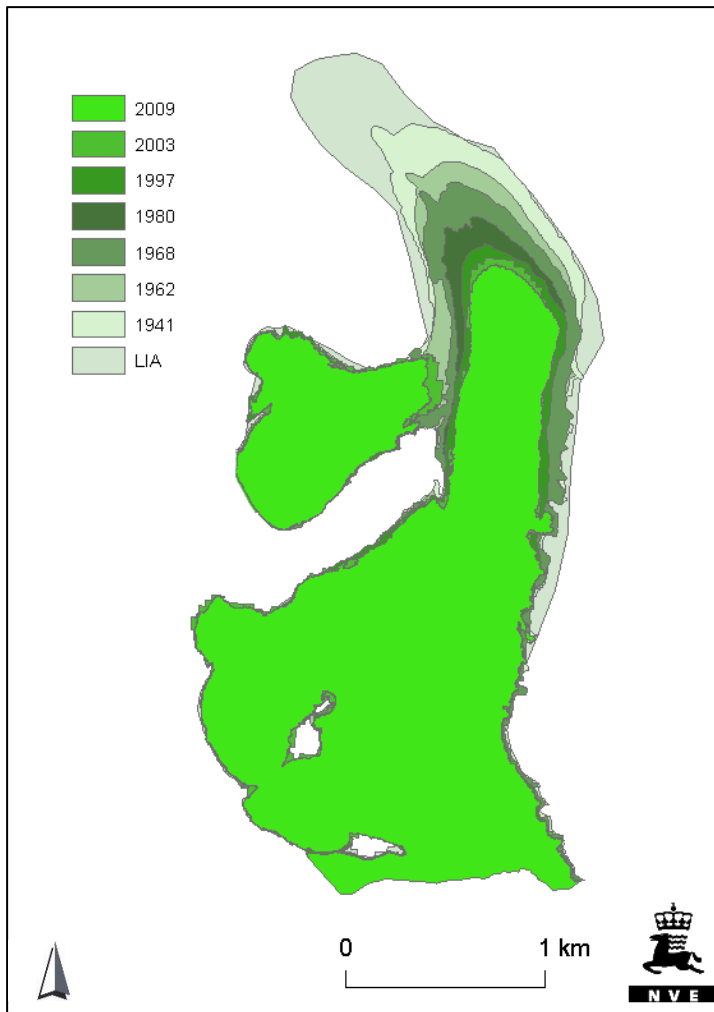


Figure 5.7. Glacier outline used by NVE, the ice divide between Hellstugubreen and Vestre Memurubreen should be noted (NVE 2014).

5.2.2. Elevation and volume changes

From the contour lines from 1941, 1962, 1968, 1980 and 1997, surface elevation maps (also known as digital elevation models, or DEMs) were constructed in ArcMap, according to known methodology (Andreassen 2009; Bauder et al. 2007). The TopoToRaster-tool was used, with the contours for the entire catchment as input. The DEM for 2009 was generated directly from the LiDAR data, using the LASToMultipoint-tool. To facilitate comparison between maps, each DEM was then cut using the Clip-tool down to match the glacier extent from the previous year: the 1962 DEM was cut to the 1941 extent, the 1968 DEM to the 1962 extent, etc. Table 5.4 shows an overview of the DEMs constructed for use in this research.

entire glacier	1941, 1962, 1968, 1980, 1997, 2009
tongue	1931, 1932, 1935, 1938, 1940, 1942, 1943

Table 5.4. DEMs constructed.

All DEMs all have a pixel size of 1 m. This cell size was considered to give accurate results, without making processing time impractically long. Other studies achieved good results wielding cell sizes of 10 m (Andreassen 1998) and 25 m (Kjøllmoen 1997). The disadvantage of small cell size, however, is that the DEMs might show unnaturally high maximum and minimum elevation.

Volume changes were computed from the raster DEMs by subtracting the surface elevation for one year from another, again following the methods used in the literature (Andreassen 2009; Bauder et al. 2007). From the DEMs, maps visualising the gradient of the glacier surface were created.

A polygon ranging from the 1941 front to ~1600 m a.s.l. was created in order to compare volume changes on the glacier tongue (Figure 5.8.). This area was selected based on the fact that between 1941 and 1968 most volume was lost in this area of the glacier.

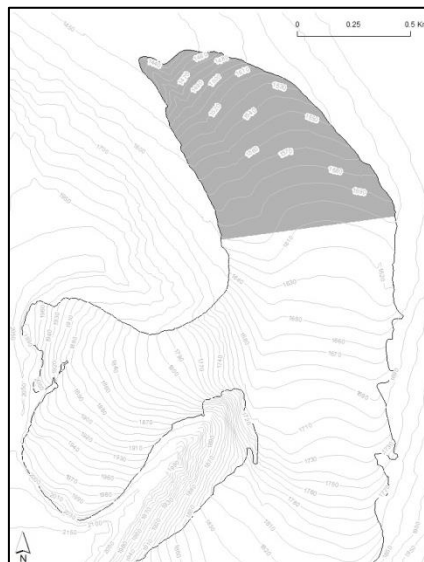


Figure 5.8. Polygon showing the outline used for area and volume calculations on the tongue. Glacier outline and contours from 1941.

5.2.3. Frontal changes

Analyses of Hellstugubreen's frontal changes were made by constructing overlaying maps of the glacier's outline in ArcMap. The change was measured as the distance for the different years between the most protruding point of the glacier tongue. However, the most protruding point on the tongue might not always reflect the retreat or advance of the entire glacier front, and measurements will always be a simplification of actual fluctuations.

5.2.4. Velocity data

ArcMap and Excel were used to compute movement (m) for the NVE10 stakes. The measure tool in ArcMap was used to determine the distance between coordinates for the different observations, which equals the movement (m). The measurements were recorded in Excel and the velocity was calculated according to Equation 5.1.

$$velocity = \frac{movement (m)}{\# \text{ days since last observation}} \quad \text{Equation 5.1.}$$

KOL40 contains measurements of velocity for each stake, as well as a computed average daily velocity since the last measurement. Average summer and winter velocities were calculated from this data. It should be noted that KOL40 usually contains measurements for July or August, and September. This means that the winter average contains averages for June and July as well. NVE10 winter averages do not include these months since observations were made in May each year. Since there only exists an annual average for 1943, this value has not been included in the calculations of winter and summer averages.

PYT60 contains average daily velocities for each stake per year, and does not differentiate between summer and winter measurements.

5.2.5. Driving stresses

Driving stresses were calculated according to Equation 3.1. This method was deemed to be accurate enough, even if the glacier does not match the idealized model. Cuffey and Paterson (2010) state that the exact shape of the glacier will have little influence on the driving forces behind flow.

6. Results

6.1. Driving stresses

6.1.1. Surface elevations and volume changes

During the processing of the DEMs, it became apparent that the 1962 map displays incorrect contour lines for non-glacierized areas, attributing elevations sometimes several dozen meters off compared to the 1941 and 1968 contour maps, and thus rendering the 1962 DEM generated from these contours not reliable enough to be used for further analysis in this research. Therefore, all further analysis based upon DEMs will disregard the 1962 map.

Surface elevation changes are represented in Figure 6.1. Figure 6.2 represents the interpolated ice thickness based on the 2011 radar survey. From this grid, volume changes could be calculated. Computed volume changes for the entire glacier can be found in Table 6.1.

Between 1941 and 2009, Hellstugubreen lost 58% of its mass, a reduction of $82 \times 10^6 \text{ m}^3 \text{ yr}^{-1}$, or the equivalent to a water layer of almost 20 m. The period between 1997 and 2009 had the highest average annual volume change ($-2 \times 10^6 \text{ m}^3 \text{ yr}^{-1}$ or almost 9 m of water), almost twice as that for the entire period from 1941 to 2009. Between 1980 and 1997, the glacier gained volume ($4 \times 10^6 \text{ m}^3$ or almost 5 m of water). However, that entire mass was added solely onto the small cirque to the west of the main ice body.

The first period (1941 – 1968) saw extreme ice losses over the glacier tongue. Between 1980 and 1997, losses are again greatest on the tongue. Between 1980 and 1997, middle regions of the glacier stayed relatively stable, with virtually all volume lost at the glacier tongue (1440 to ~1600 m a.s.l.), while volume changes are randomly distributed higher up-glacier. Between 1997 and 2009, however, the intense volume loss is the result of a thickness reduction for the entire glacier area, even if the loss is greatest on the tongue. For the entire 1941 – 2009 period, 40% of volume changes occur on the tongue, which accounts for 13% of the total glacier area (Table 6.2). Evidence of volume increase can be seen in the upper regions of the glacier and close to the mountain sides (Figures 6.1a, b and c).



Figure 6.1. Surface elevation changes (m) on Hellstugubreen between a) 1941 – 1968, b) 1968 – 1980, c) 1980 – 1997 and d) 1997 – 2009.

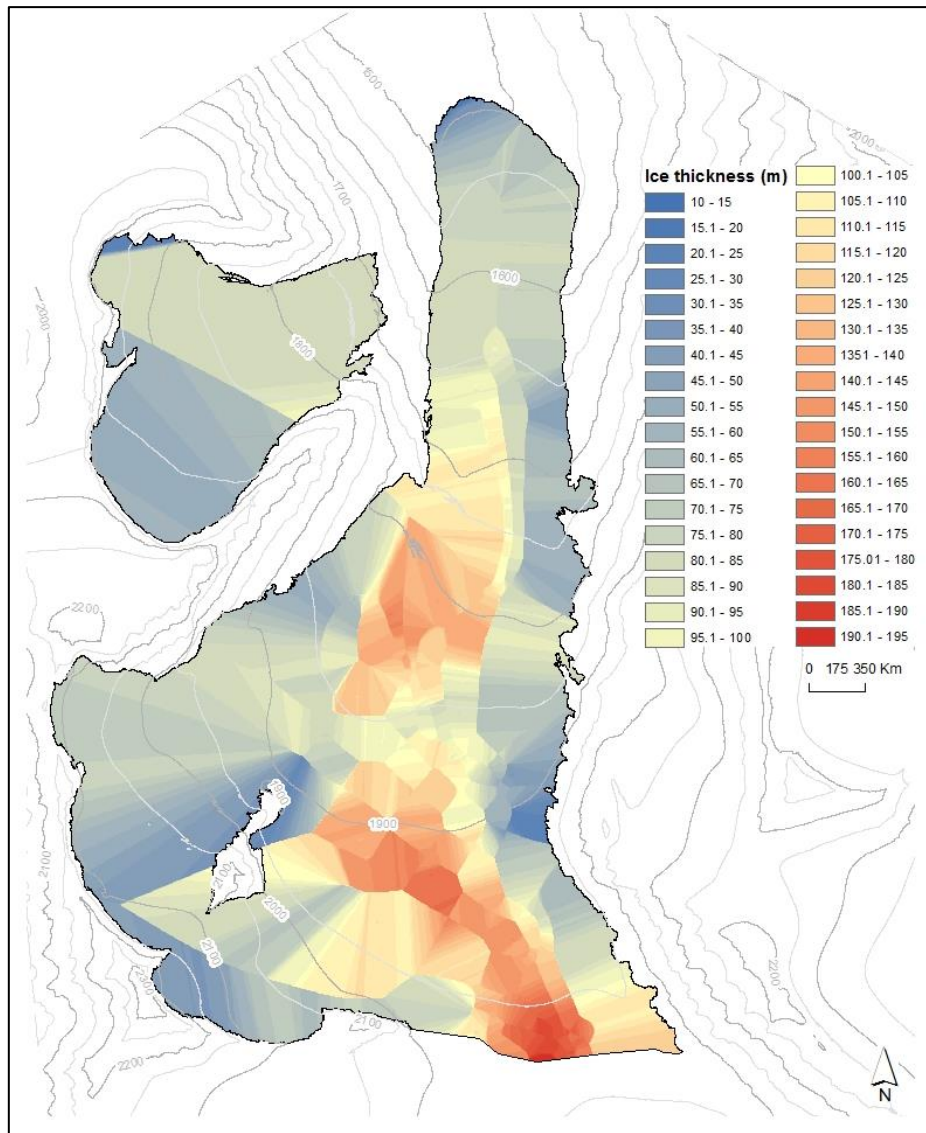


Figure 6.2. Interpolated ice thickness on Hellstugubreen as recorded by an echo sounding survey in May 2011 (Data: NVE).

Years	Total volume (km ³)	ΔV (m ³)	ΔV (%)	Annual ΔV (m ³)	Cummulative ΔV (total volume change / area) (m)
1941	0.57				
1968	0.33	-38×10^6	-42	-1.4×10^6	-8.92
1980	0.27	-18×10^6	-18	-1×10^6	-4.66
1997	0.3	4×10^6	11	0×10^6	0.63
2009	0.24	-30×10^6	-20	-2×10^6	-8.22
1941-2009	-	-82×10^6	-58	-1×10^6	-19.67

Table 6.1. Volume changes (m³) for Hellstugubreen since 1941.

Years	ΔV on tongue (m^3)	% of ΔV entire glacier
1941 - 1968	-24×10^6	63
1968 - 1980	-6×10^6	31
1980 - 1997	3×10^6	-
1997 - 2009	-6×10^6	19
1941 - 2009	-33×10^6	40

Table 6.2. Volume changes (m^3) for Hellstugubreen's tongue (up to ~1600 m a.s.l.) since 1941.

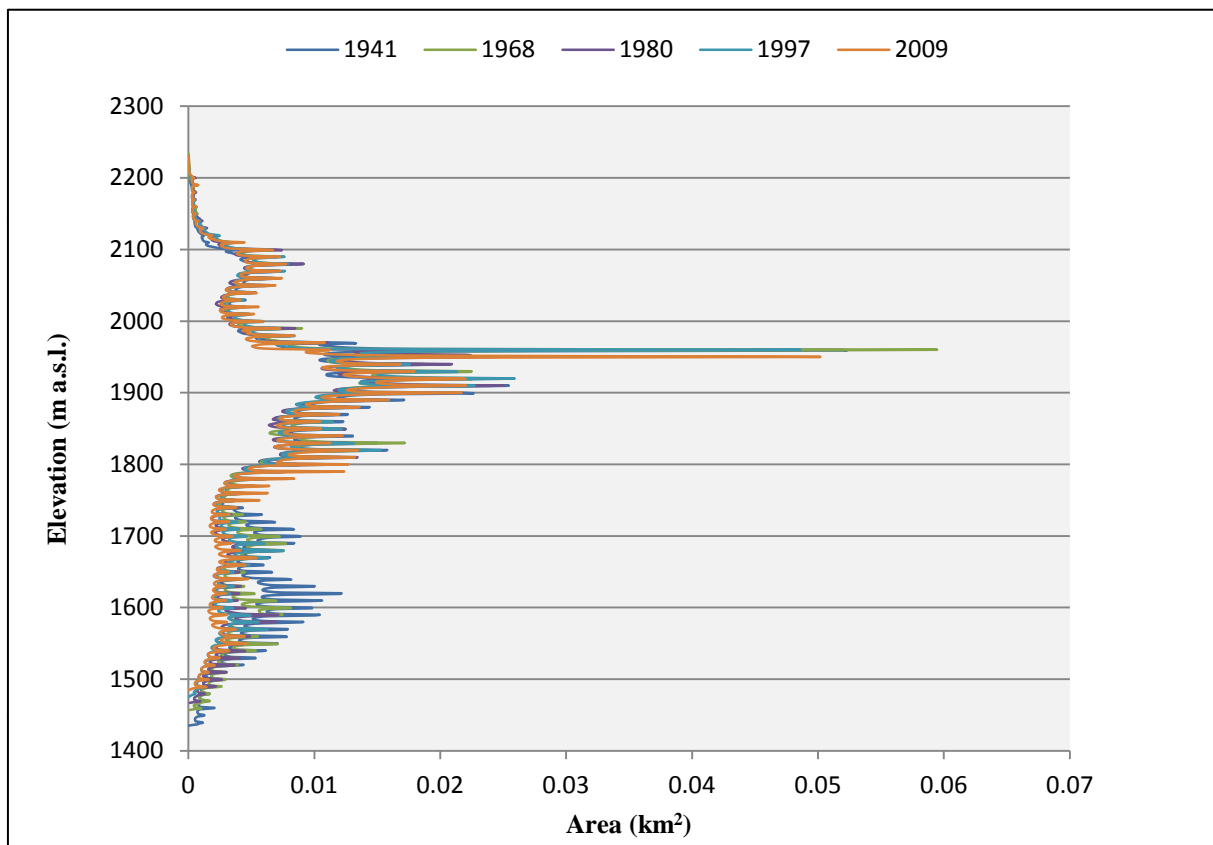


Figure 6.3. Hellstugubreen's hypsometry between 1941 and 2009.

Absolute elevation change for the selected stakes, from the DEMs, are given in Table 6.3. Between 1980 and 1997, five locations saw an elevation rise, but by 2009, all of them had gone down again to elevations lower than those from 1980.

When comparing the stakes across the three datasets (Table 6.4), all stakes have dropped in altitude since the 1940s, 48 m on average. The locations for the stakes closest to the glacier terminus in 1941 and 1968 are no longer located on the ice body and have kept a constant elevation since the late 1960s and 1980, respectively. When only taking into account stakes that were still located on the glacier in 2009, it is clear that the period between 1997 and 2009

Stake	1931	1932	1935	1938	1940	1941	1942	1943	1968	1980	1997	2009
11 _{KOL40}	1539	1539	1534	1530	1525	1520	1519	1516	1459			
2 _{PYT60}		1581		1572	1565	1567	1563	1561	1512	1490		
13 _{NVE10}						1642			1620	1609	1604	1584
28 _{KOL40}						1623			1590	1573	1575	1537
12 _{PYT60}						1631			1603	1590	1580	1560
13 _{NVE10}						1642			1620	1609	1604	1584
33 _{KOL40}						1683			1663	1653	1648	1636
15 _{PYT60}						1683			1665	1654	1647	1637
20 _{NVE10}						1692			1674	1664	1658	1648
39 _{KOL40}						1720			1707	1696	1693	1682
17 _{PYT60}						1720			1708	1696	1695	1684
26 _{NVE10}						1731			1720	1712	1716	1700
40 _{KOL40}						1788			1776	1769	1772	1760
22 _{PYT60}						1812			1804	1798	1799	1790
60 _{NVE10}						1830			1822	1816	1820	1809

Table 6.3. Elevation (m a.s.l.) for given stake locations on Hellstugubreen.

Stake	Total el. change 1941 - 2009 (m)	1941 - 1968		1968 - 1980		1980 - 1997		1997 - 2009	
		El. change (m)	% of total						
11 _{KOL40}	-61	-61	100	-	-	-	-	-	-
2 _{PYT60}	-77	-55	71	-22	29	-	-	-	-
13 _{NVE10}	-58	-22	38	-11	18	-5	9	-20	34
28 _{KOL40}	-85	-32	38	-17	20	2	-3	-38	44
12 _{PYT60}	-71	-27	38	-14	19	-10	14	-20	28
13 _{NVE10}	-58	-22	38	-11	18	-5	9	-20	34
33 _{KOL40}	-47	-19	40	-11	23	-4	9	-12	27
15 _{PYT60}	-46	-19	41	-10	22	-7	16	-10	21
20 _{NVE10}	-44	-16	36	-10	23	-6	14	-10	24
39 _{KOL40}	-37	-12	32	-12	31	-3	8	-10	28
17 _{PYT60}	-36	-12	33	-12	33	-1	3	-11	30
26 _{NVE10}	-31	-12	39	-9	29	4	-14	-16	50
40 _{KOL40}	-28	-11	39	-7	25	3	-10	-12	44
22 _{PYT60}	-22	-9	41	-6	28	1	-6	-9	40
60 _{NVE10}	-20	-8	40	-7	34	4	-21	-10	51

Table 6.4. Elevation changes for the compared stakes from 1941 to 2009.

saw the greatest volume losses, with stakes losing an average of 35% of the 1941 – 2009 total in this last period. Elevation loss decreases with distance up-glacier: stakes located on the upper tongue seem to have lost the most elevation, with the altitude loss averaged for 28_{KOL40}, 12_{PYT60} and 13_{NVE10} averaged to 71 m. The highest located stakes (40_{KOL40}, 22_{PYT60} og 60_{NVE10}) had an elevation change of 23 m between 1941 and 2009. Between 1980 and 1997,

five stake locations had an increase in elevation, while the others saw the smallest drop in the 1941 – 2009 period.

From Figure 6.2 and the elevation data in Table 6.2, ice thickness at each stake was computed and reconstructed back to 1941 (Table 6.5). Only ice depth at stake locations that were still located on the glacier at the time of the radar survey could be calculated. It is important to note that the radar investigations were done in 2011, while the elevations were taken from the 2009 DEM.

Stake	1941	1968	1980	1997	2009
28 _{KOL40}	165	132	115	117	79
12 _{PYT60}	149	121	108	98	78
13 _{NVE10}	140	118	107	102	82
33 _{KOL40}	123	103	93	88	76
15 _{PYT60}	141	123	112	105	95
20 _{NVE10}	134	116	106	100	90
39 _{KOL40}	119	106	95	92	81
17 _{PYT60}	118	106	94	93	82
26 _{NVE10}	136	125	117	121	105
40 _{KOL40}	84	72	65	68	56
22 _{PYT60}	106	98	92	93	84
60 _{NVE10}	113	105	99	103	92

Table 6.5. Recorded (2011) and reconstructed ice thickness for the compared stakes from 1941 to 2009.

6.1.2. Slope

Slope changes can be found in Table 6.6. Values (in degrees) are for a 20 m radius around each stake. This radius was chosen with the rather even surface of Hellstugubreen in mind. Cuffey and Paterson (2010) state that slope should be considered over distances several times the ice thickness. However, since glacier thickness has changed considerably, polygons of constant size were chosen for comparison across the decades. It was believed that a 20 m radius would give a sufficiently accurate idea of the surface slope around the stakes. There does not seem to be a pattern as to how the surface slope changes at stake locations, but when comparing surface at the compared stakes, the surface slope at the NVE10 stakes has increased by 46% that at the KOL40 stakes.

Stake	1941	1968	1980	1997	2009
11 _{KOL40}	8	-	-	-	-
2 _{PYT60}	9	13	-	-	-
13 _{NVE10}	10	9	10	7	11
28 _{KOL40}	10	10	21	10	21
12 _{PYT60}	10	13	9	8	15
13 _{NVE10}	10	9	10	7	11
33 _{KOL40}	5	3	12	10	12
15 _{PYT60}	7	8	9	11	11
20 _{NVE10}	10	10	8	10	10
39 _{KOL40}	11	12	8	11	8
17 _{PYT60}	8	13	7	12	8
26 _{NVE10}	14	10	11	12	12
40 _{KOL40}	9	12	10	16	10
22 _{PYT60}	22	17	9	9	8
60 _{NVE10}	13	14	10	8	8

Table 6.6. Changes in slope (°) for the compared stakes, from 1941 to 2009.

6.1.3. Driving stresses

Driving stresses τ_d were calculated according to Equation 3.1 (Table 6.7). Since the exact shape of a glacier has little influence on the driving forces behind flow, and because Hellstugubreen generally slopes gently, this equation was deemed to give sufficiently accurate results. Because f' denotes a number usually of order one, basal drag (or shear stress) τ_b can be derived from these results.

Stake	Slope (°)	Ice thickness (m)	Driving stress (kPAa)
28 _{KOL40}	10	165	253
12 _{PYT60}	10	121	185
13 _{NVE10}	10	82	126
33 _{KOL40}	5	123	95
15 _{PYT60}	7	123	132
20 _{NVE10}	10	90	138
39 _{KOL40}	11	119	200
17 _{PYT60}	8	106	130
26 _{NVE10}	14	105	224
40 _{KOL40}	9	84	116
22 _{PYT60}	22	98	324
60 _{NVE10}	13	92	183

Table 6.7. Driving stresses (kPa) for the compared stakes, from 1941 to 2009.

Driving stresses show great variation, both within the same period and when comparing the three datasets. No geographical or temporal pattern becomes apparent from the results. While the driving stress from stake 28KOL40 has decreased by 50% to 126 kPa at stake 13NVE10, the driving stress has increased by 45% from 33KOL40 to 20NVE10.

6.2. Velocity

6.2.1. Annual velocity

Average daily velocities for NVE10 are given in Table 6.8 and represented in Figure 6.3. It should be noted that the time series for some stakes (29_{NVE10}, 30_{NVE10}, 41_{NVE10}, 44_{NVE10}, 45_{NVE10}, 61_{NVE10}, 62_{NVE10}) consist of three consecutive observations or less, rendering them less suited for an analysis of inter-annual velocity changes. The time series for 13_{NVE10}, 20_{NVE10}, 26_{NVE10} and 60_{NVE10} are more complete. Results for September 2013 represent the average daily velocity since September 2012.

When the results are averaged over the entire glacier, Hellstugubreen moved at a velocity of 0.0261 m d⁻¹, or 9.53 m yr⁻¹. between May 2010 and September 2013. Results for September 2013 are annual velocities. The glacier's maximum average daily velocity in the 2010s was recorded at 0.0556 m d⁻¹ on August 4th 2010 at stake 26_{NVE10}. Stake 26_{NVE10} had the highest average velocity for the entire period, at 0.0449 m d⁻¹, while 45_{NVE10} did not show any displacement at all during this period with an average displacement of 0.0025 m d⁻¹.

In the 2010s, 6 stakes show a general downward trend (Figure 6.4): 13_{NVE10}, 20_{NVE10}, 26_{NVE10}, 41_{NVE10}, 61_{NVE10} and 30_{NVE10} slowed down between 2010 and 2013. Over the same period, five stakes accelerated: 29_{NVE10}, 60_{NVE10}, 62_{NVE10}, 44_{NVE10} and 45_{NVE10}. Stakes 26_{NVE10}, 41_{NVE10}, 29_{NVE10} and 20_{NVE10} have the highest average velocity when the whole period is considered (Figure 6.5).

Stakes 20_{NVE10} and 26_{NVE10} have the highest velocities until the summer of 2012. From August 2011 26_{NVE10} decelerates significantly, even during summer. Only a year later, between August and September 2012, its velocity stabilizes again. Figure 6.6 shows the direction of flow for the NVE stakes.

Date of observation \ Stake #	13	20	26	29	30	41	44	45	60	61	62
07.05.2010		0.0313	0.0438		0.0152		0.0108	0.0031	0.009		0.028
04.08.2010	0.02062	0.0416	0.0556		0.0155	0.042	0.0136				
28.09.2010	0.0371	0.0513	0.0526		0.0109		0.0092				
05.05.2011	0.0154	0.0336	0.04						0.0105		
04.08.2011	0.0164	0.0416	0.0446						0.0244		
14.09.2011	0.0237	0.0369	0.053						0.0215		
02.05.2012	0.015	0.0307	0.0399				0.0108	0.0035	0.0237		
09.08.2012	0.01	0.0252	0.0356	0.0395			0.0119		0.0278		
20.09.2012	0.0162	0.0255	0.0472	0.0421				0.001	0.0275	0.0296	0.0268
10.09.2013		0.0271	0.0369	0.0429				0.0023	0.0288	0.029	0.0275

Table 6.8. Calculated velocities (in m d^{-1}) for the NVE10 stakes.

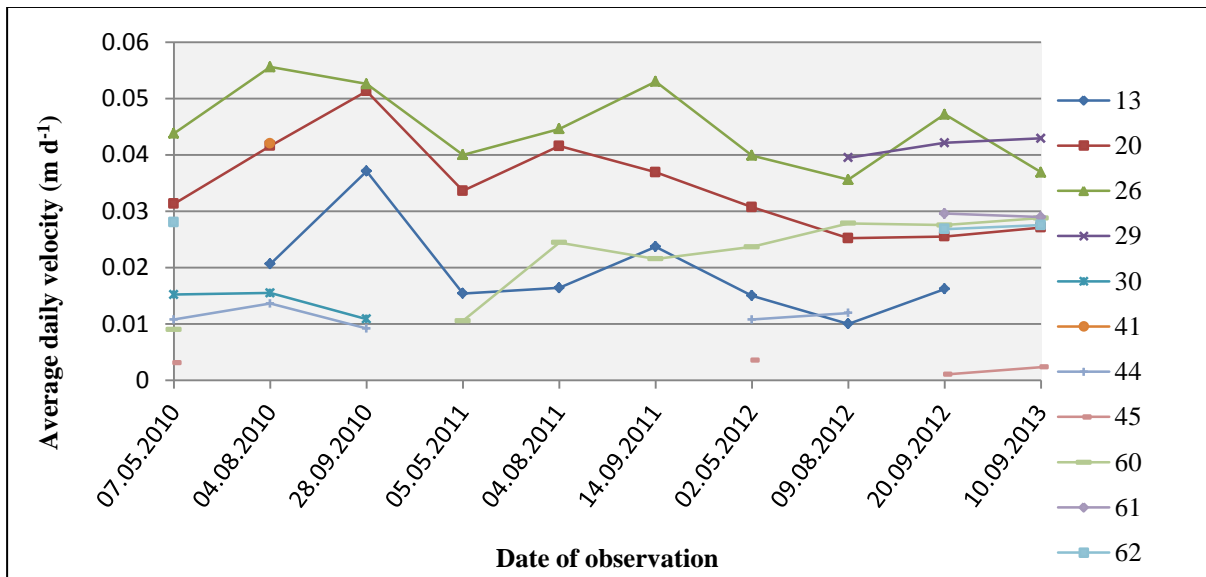


Figure 6.4. Average daily velocities (in m d^{-1}) for the NVE10 stakes. Note how the time interval between observations is not of equal length.

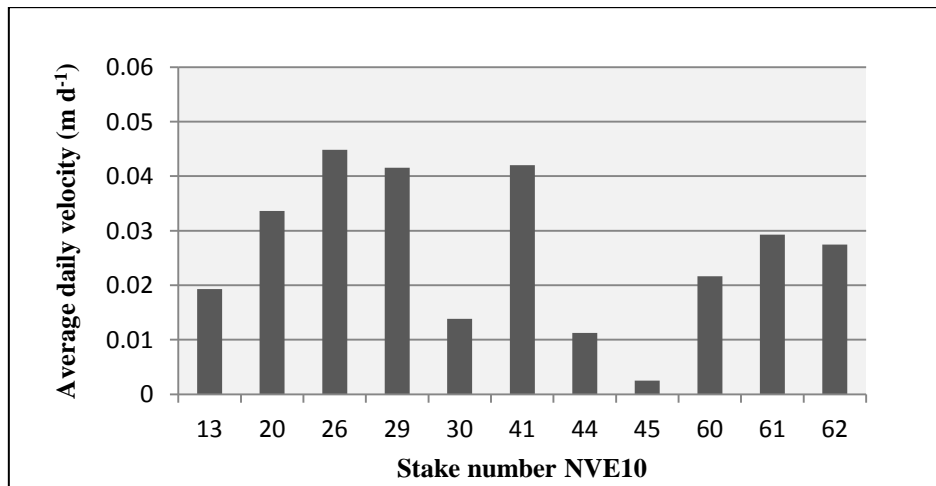


Figure 6.5. Average daily velocities (in m d^{-1}) for 2009–2013, as calculated from NVE10 stake positions.

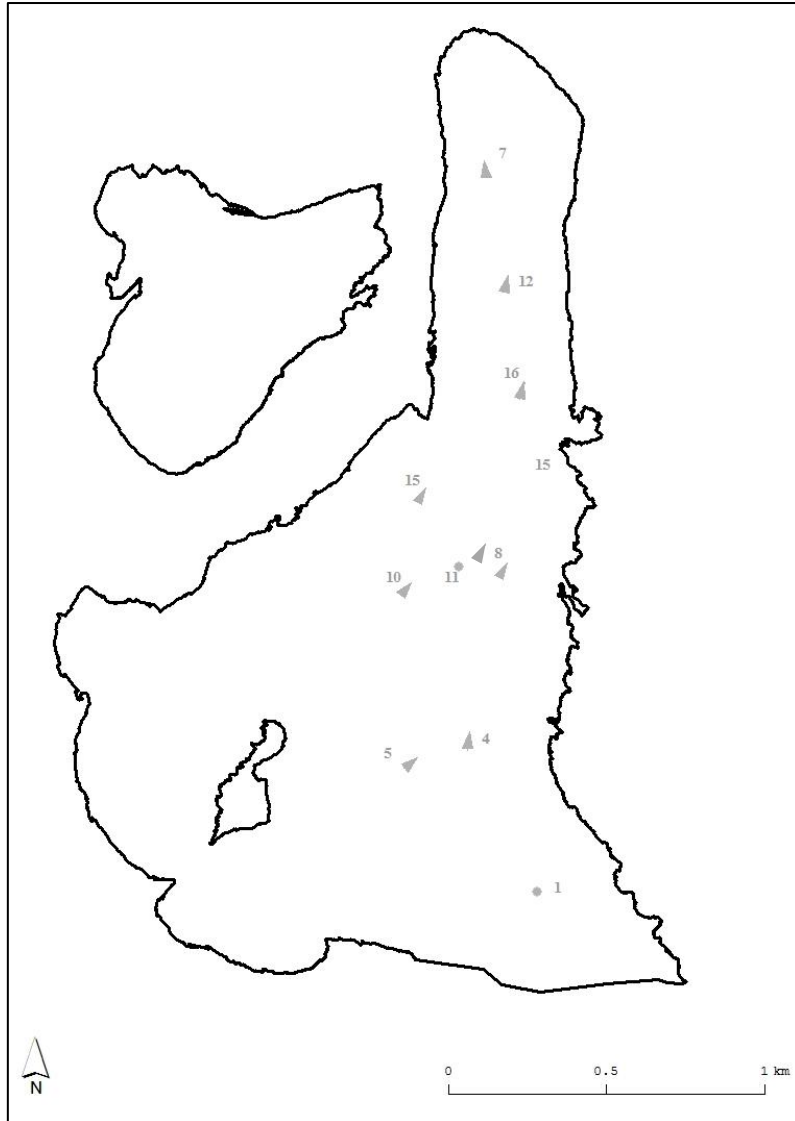


Figure 6.6. Vector map showing the direction of movement from 2009 to 2013 for NVE10. Vector size does not represent the magnitude of movement. Numbers are for displacement in m yr^{-1} .

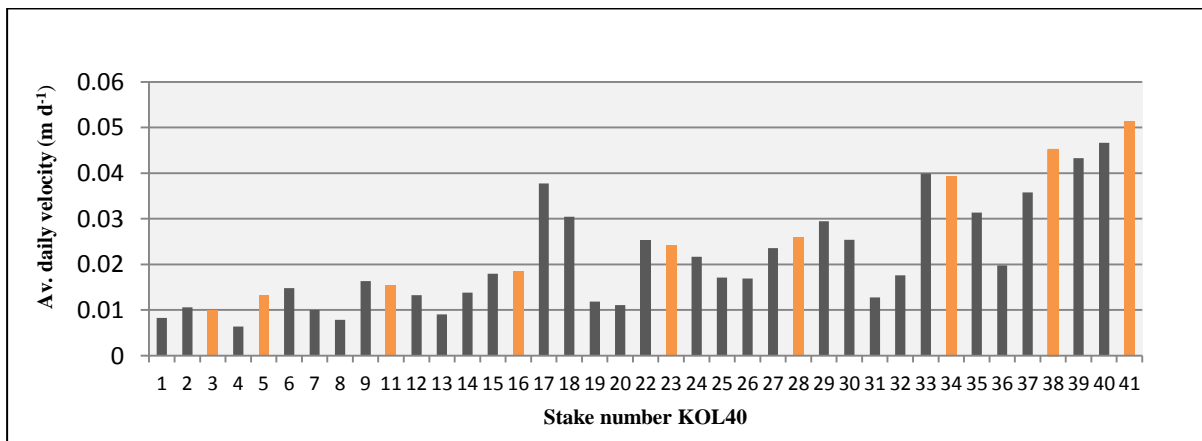


Figure 6.7. Average daily velocities (in m d^{-1}) for 1937–1946, calculated from KOL40. Stakes marked in orange are located on the center line of the glacier, with 3_{KOL40} located closest to the terminus and 41_{KOL40} furthest removed from the tongue.

Average daily velocities for each year between 1937 and 1946 for each of the observation years for each stake can be found in Figure 6.8. Figure 6.7 displays the averages for each stake for the entire KOL40 dataset. It should be noted that the first observation for KOL40 was made in October 1937 and the last one at the end of August 1946. Both observations were included in the calculations for both the annual velocities and for the entire KOL40 dataset. The highest annual velocity on Hellstugubreen for this period was calculated for stake 41_{KOL40} at 0.0515 m d⁻¹ in 1938.

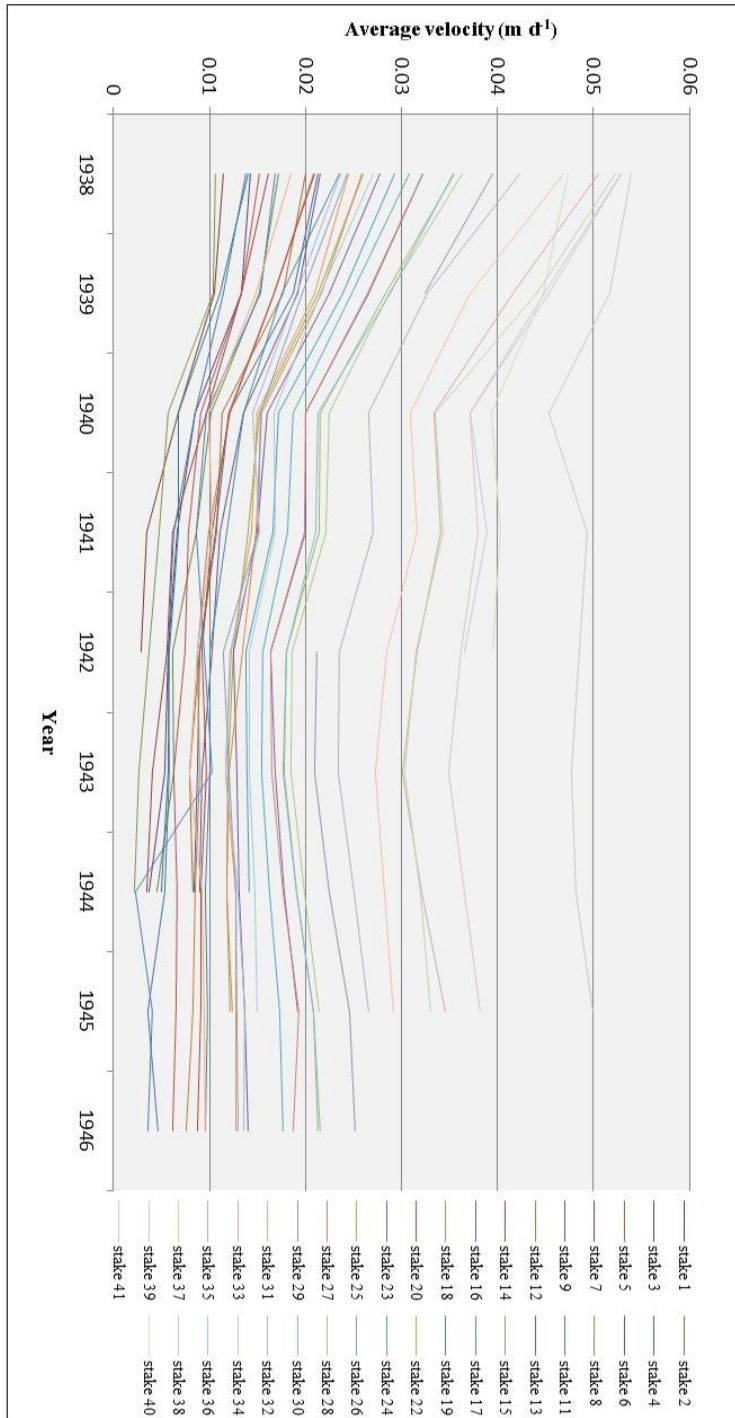


Figure 6.8. Average daily velocities for each year (m d⁻¹) for the KOL40 stakes.

Figure 6.9 gives the average daily velocities for the period 1961 to 1963 calculated from PYT60. As Pytte (1964) concluded, stake velocities were quite consistent during both years of measurements. The lowest velocity for this period was calculated for stake 32_{PYT60} which hardly showed any movement at 0.002 m d⁻¹, while stake 18_{PYT60} had the highest velocity at 0.042 m d⁻¹, in the last year of observations. The stake with the highest average daily velocity for both years of observation was 21_{PYT60} at 0.0385 m d⁻¹. When considering averages for both years of measurements, the stakes with the highest velocity are 16_{PYT60} to 22_{PYT60},

moving at slightly less than 0.04 m d^{-1} . 16_{PYT60} to 19_{PYT60} constitute a cross profile at approximately 1700 m a.s.l.

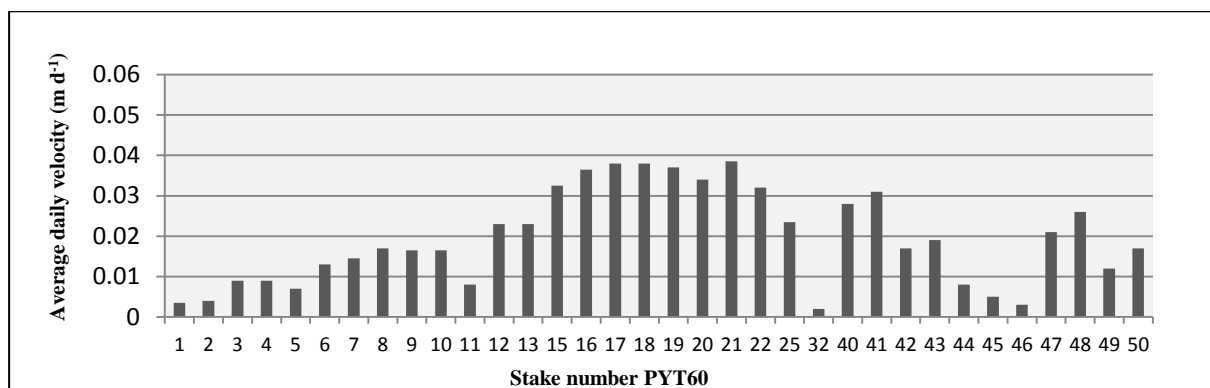


Figure 6.9. Average daily velocities (in m d^{-1}) for 1961 – 1963, calculated from PYT60.

Table 6.10 gives average daily velocities for all stakes for all three datasets. When the calculated velocities for all stakes are averaged for the entire glacier and for each of the time series, there appears to have been little change in velocity over the past 80 years (Table 6.9). This is contradictory initial expectations. In the 1940s, the average velocity for the entire glacier was 0.0223 m d^{-1} . In the 2010s, the glacier showed a 15% increase in velocity at 0.026 m d^{-1} .

	Average daily velocity (m d^{-1})	Average annual velocity (m yr^{-1})
KOL40	0.0223	8.14
PYT60	0.0195	7.12
NVE10	0.0261	9.53

Table 6.9. Average velocities for the entire glacier for all three datasets.

KOL40		PYT60		NVE10	
Stake #	Average daily velocity (m d^{-1})	Stake #	Average daily velocity (m d^{-1})	Stake #	Average daily velocity (m d^{-1})
1	0.0083	1	0.0035	13	0.0193
2	0.0106	2	0.004	20	0.0336
3	0.0099	3	0.009	26	0.0449

4	0.0064	4	0.009	29	0.0415
5	0.0133	5	0.007	30	0.0138
6	0.0148	6	0.013	41	0.042
7	0.01	7	0.0145	44	0.0113
8	0.0079	8	0.017	45	0.0025
9	0.0164	9	0.0165	60	0.0217
11	0.0155	10	0.0165	61	0.0293
12	0.0132	11	0.008	62	0.0275
13	0.009	12	0.023		
14	0.0138	13	0.023		
15	0.0179	15	0.0325		
16	0.0184	16	0.0365		
17	0.0377	17	0.038		
18	0.0305	18	0.038		
19	0.0118	19	0.037		
20	0.0111	20	0.034		
22	0.0254	21	0.0385		
23	0.0243	22	0.032		
24	0.0217	25	0.0235		
25	0.0171	32	0.002		
26	0.0169	40	0.028		
27	0.0236	41	0.031		
28	0.026	42	0.017		
29	0.0295	43	0.019		
30	0.0254	44	0.008		
31	0.0128	45	0.005		
32	0.0176	46	0.003		
33	0.0399	47	0.021		
34	0.0394	48	0.026		
35	0.0314	49	0.012		
36	0.0198	50	0.017		
37	0.0358				
38	0.0451				
39	0.0433				
40	0.0467				
41	0.0515				

Table 6.10. Average daily velocities for the periods 1937 – 1946 (KOL40), 1961 – 1963 (PYT60) and 1997 – 2013 (NVE10). Note that a complete dataset does not exist for all stakes. Averages were calculated from the observations available and rounded to the fourth decimal.

Date of observation	11 _{KOL40} / 2 _{PT60} / 13 _{NVE10}	28 _{KOL40} / 12 _{PT60} / 13 _{NVE10}	33 _{KOL40} / 15 _{PT60} / 20 _{NVE10}	39 _{KOL40} / 17 _{PT60} / 26 _{NVE10}	40 _{KOL40} / 22 _{PT60} / 60 _{NVE10}
15.09.1937	-	-	-	-	-
10.10.1937	0.0309	0.0438	0.0583	0.0563	0.0612
12.08.1938	0.023	0.0396	0.049	0.0506	0.0461
28.09.1938	0.0269	0.0387	0.0606	0.0676	0.0555
04.08.1939	0.017	0.032	0.041	0.0442	0.0442
18.09.1939	0.0215	0.035	0.046	0.0494	0.0492
13.08.1940	0.0132	-	0.0331	0.0367	0.0385
16.09.1940	0.0176	-	0.0363	0.0411	0.0481
24.07.1941	0.0114	-	0.0333	0.037	0.0392
13.09.1941	0.0141	0.0276	0.0393	0.0437	0.0468
29.07.1942	0.01	0.0206	0.0301	0.0356	0.0385
15.09.1942	0.0101	0.0257	0.0417	0.0401	0.0463
08.09.1943	-	0.021	0.0301	0.035	-
03.08.1944	0.0093	0.022	0.032	0.0366	-
05.09.1944	0.0131	0.0273	0.033	0.0374	-
03.09.1945	-	0.0246	0.0346	0.0382	-
27.08.1946	0.0096	0.0252	-	-	-
1962	0.004	0.022	0.0003	0.0004	0.032
1963	0.004	0.024	0.0003	0.0004	0.032
07.05.2010	-	-	0.0313	0.0438	0.009
04.08.2010	0.0206	0.0206	0.0416	0.0536	-
28.09.2010	0.0371	0.0371	0.0513	0.0526	0.0105
05.05.2011	0.0154	0.0154	0.0336	0.04	0.0244
04.08.2011	0.0164	0.0164	-	0.0446	0.0215
14.09.2011	0.0237	0.0237	0.0369	0.053	0.0237
02.05.2012	0.015	0.015	0.0307	0.0399	0.0278
09.08.2012	0.01	0.01	0.0252	0.0356	-
20.09.2012	0.0162	0.0162	0.0255	0.0472	0.0275
10.09.2013	-	-	0.0271	0.0369	0.0288

Table 6.11. Average movement of stakes ($m \cdot d^{-1}$), rounded to the fourth decimal, since the last observation, for the compared stakes of all datasets. Observations in red are for redrills.

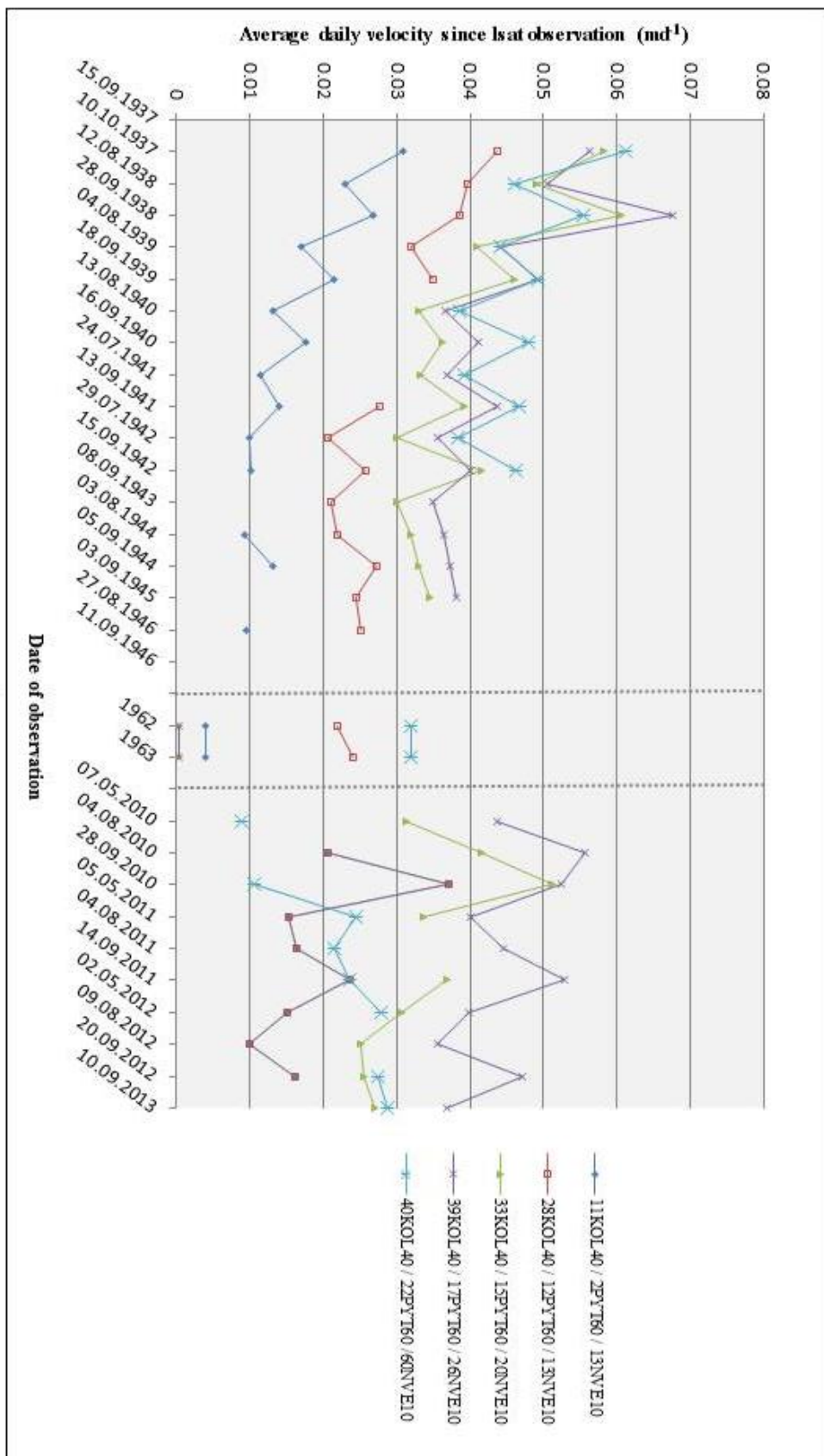


Figure 6.10. Average movement of stakes (m d⁻¹) since the last observation for the compared stakes from all datasets.

The differences that do exist are so small that they are statistically insignificant. A Student's t-test performed on 10 observations for 39_{KOL40} (12.08.1938 – 15.09.1942) and 26_{NVE10} (07.05.2010 – 10.09.2013) showed no significant difference between the two datasets at the commonly tested 95% confidence level. The same is true for the comparison of the selected stakes from KOL40, PYT60 and NVE10 (Figure 6.8 and Table 6.11).

When looking at the stakes along the flow line, KOL40 shows a clear increase in velocity with distance up-glacier (Figure 6.5). 3_{KOL40} moved at an average speed of 1 cm d⁻¹, while the topmost stake, 41_{KOL40} displayed velocities more than five times greater. However, this relationship is no longer apparent from PYT 60 (Figure 6.6) or NVE10 (Figure 6.4).

6.2.2. Summer and winter velocities

As expected, there are clear differences between winter and summer velocities. Table 6.12 shows the average daily velocities for NVE10 for the summer season (May to September). Average summer velocity for all stakes for the 2010s was 0.0292 m d⁻¹. Averaged over the entire period, 26_{NVE10} had the highest summer velocity (0.0468 m d⁻¹) while 30_{NVE10} moved the slowest at 0.0136 m d⁻¹ (Table 6.14). The highest summer velocity was calculated to be 0.0544 m d⁻¹ at stake 26_{NVE10} in the summer of 2010. The lowest summer velocity was recorded the same year at stake 60_{NVE10} at 0.0105 m d⁻¹.

Year	13	20	26	29	30	41	44	60	61	62
2010	0.023	0.0453	0.0544		0.0155	0.042	0.0136	0.0105		
2011	0.0186		0.0471					0.0222		
2012	0.0118	0.0284	0.039	0.0403				0.0275	0.0296	0.0268

Table 6.12. Average daily summer velocities (m d⁻¹), rounded to the fourth decimal, for NVE10.

Year	13	20	26	30	44	60	62
2009-2010		0.0312	0.0437	0.0152	0.0108	0.009	0.028
2010-2011	0.0154	0.0335	0.04	0.0109	0.0092	0.0244	
2011-2012	0.015	0.0306	0.0398		0.0108	0.0278	

Table 6.13. Average daily winter velocities (m d⁻¹), rounded to the fourth decimal, for NVE10.

	13	20	26	29	30	41	44	60	61	62
Av. daily summer vel. (m d ⁻¹)	0.0178	0.0369	0.0468	0.0403	0.0155	0.042	0.0136	0.0201	0.0296	0.0268
Av. daily winter vel. (m d ⁻¹)	0.0152	0.0318	0.0412		0.0131		0.0103	0.0204		0.028
diff winter/summer (%)	14.8	13.8	12.1		15.7		24.6	-1.6		-4.4

Table 6.14. Average summer and winter velocities (in m d⁻¹), rounded to the fourth decimal, for NVE10.

Table 6.13 represents average daily winter (September to May) velocities for NVE. In winter, Hellstugubreen moved at an average velocity of 0.0233 m d^{-1} . On average, 62_{NVE10} has the highest winter velocity at 0.0257 m d^{-1} , while stake 30_{NVE10} has the lowest at just less than 0.0162 m d^{-1} . The highest and lowest winter velocities were recorded, as for the summer, to exist at stakes 26_{NVE10} and 60_{NVE10} , respectively. 26_{NVE10} moved at a speed of 0.0437 m d^{-1} in the winter of 2010-2012, while 60_{NVE10} was barely moving at 0.009 m d^{-1} that same winter.

From Tables 6.12 and 6.13 it may be concluded that winter velocities show more intra-annual stability than the velocities recorded for summer, as can be reasonably expected. Average winter velocities on Hellstugubreen in the period 2010 – 2013 were slightly more than 20% lower than the average summer velocities (Table 6.14). This result is in line with most studies of seasonal variability of surface velocities (e.g. Hodge 1974; Hooke et al. 1983; Hooke et al. 1989; Willis 1991). However, the seasonal differences are not equally clear for all stakes, nor do they occur at the same magnitude every year. The lowermost stake, 13_{NVE10} , shows clear summer peaks in September, with the summer acceleration less pronounced between May and August than between August and September. 60_{NVE10} shows minimal seasonal variation from the summer of 2011 onwards. The chart for 20_{NVE10} , 29_{NVE10} and 60_{NVE10} flattens out from August 2012, while both 13_{NVE10} and 26_{NVE10} still have a clear summer peak in September after that period. In the summer of 2012, only two stakes (44_{NVE10} and 60_{NVE10}) accelerated between May and August. The other stakes started accelerating only from August.

44_{NVE10} has the biggest difference between summer and winter velocities, with winter flow only 75% of values for the summer. Two stakes seem to experience winter accelerations: 60_{NVE10} flows 1.6 % faster in winter, while 62_{NVE10} speeds up to velocities 4.4 % higher than those in the summer months. The seasonal differences seem to be independent of distance up-glacier (Table 6.13), a confirmation of findings on Hellstugubreen made by Liestøl (1962), and in line with results on Midtdalsbreen (Willis 1991) and Storglaciären (Hooke et al. 1989), but contradicting findings in the Alps (Elliston 1966),

The initial speed-up after winter is followed by another abrupt acceleration between August and September. Generally, the summer speed up is 14% greater between August and September compared to the May – August period. There seems to exist a transition to higher summer background temperatures as the summer progresses. Similar observations were made on Variegated Glacier (Harrison et al. 1989) and Storglaciären (Hooke et al. 1989).

Average annual, summer and winter velocities (in m d^{-1}) for the 1940s, 1960s and 2010s are given in Figure 6.11. PYT60 lacks specific values for winter and summer and therefore only an average daily velocity is given.

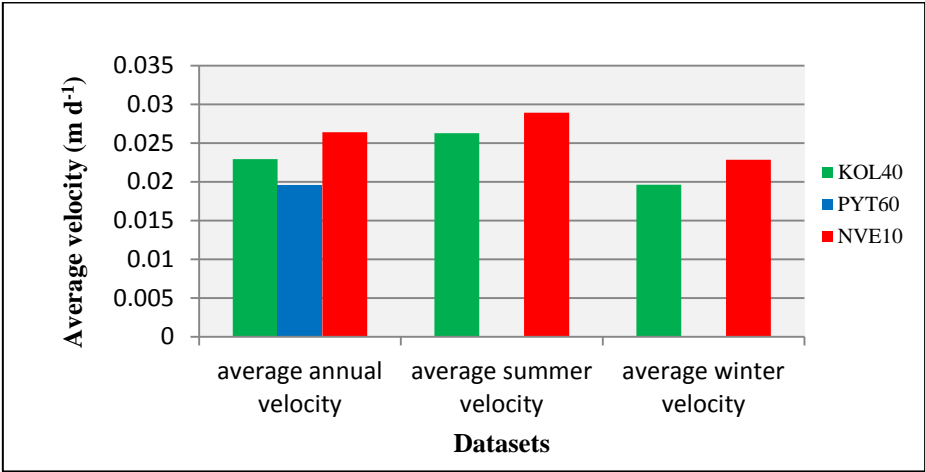


Figure 6.11. Average daily velocities for all three datasets.

Figure 6.12 shows average daily winter and summer velocities for KOL40. Table 6.7 contains average velocities for the compared stakes. Averaged over the entire glacier, the difference between winter and summer velocities has increased by 4% since the 1940s, with KOL40 showing winter velocities 24% lower than those in summer (Table 6.16). However, from Table 6.15, it becomes clear that the stakes chosen for comparison have been seeing a smaller summer/winter difference in daily velocity between 2010 and 2013 compared to the 1940s.

Stake #	Average summer velocity (m d^{-1})	Average winter velocity (m d^{-1})	Difference winter/summer (%)
11 _{KOL40}	0.017	0.0133	21.7
13 _{NVE10}	0.0178	0.0152	14.8
28 _{KOL40}	0.0291	0.0241	17
13 _{NVE10}	0.0178	0.0152	14.8
33 _{KOL40}	0.045	0.0364	19.1
20 _{NVE10}	0.0369	0.0318	13.8
39 _{KOL40}	0.0479	0.0401	16.3
26 _{NVE10}	0.0468	0.0412	12.1
40 _{KOL40}	0.0512	0.0413	19.3
60 _{NVE10}	0.0201	0.0204	-1.6

Table 6.15. Average summer and winter velocities (in m d^{-1}) for 1937 – 1946, rounded to the fourth decimal, calculated from KOL40.

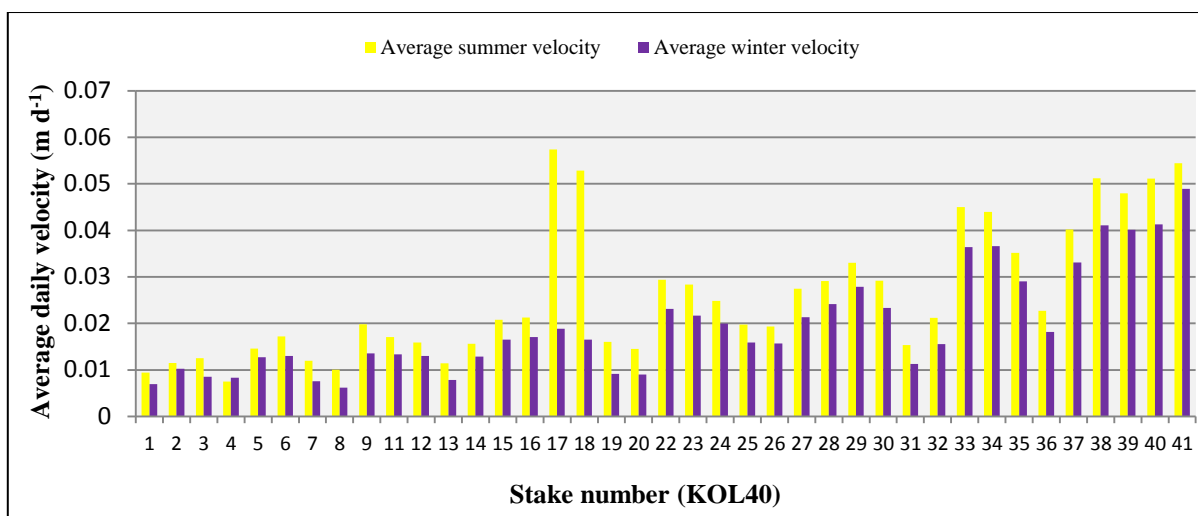


Figure 6.12. Average daily winter and summer velocities and average daily summer velocities (in %) for the KOL40 stakes.

Stake #	Average summer velocity (m d-1)	Average winter velocity (m d-1)	Difference winter/summer (%)
1	0.0094	0.0069	26.7
2	0.0115	0.0103	10.5
3	0.0125	0.0085	32.1
4	0.0075	0.0083	-11.3
5	0.0146	0.0127	13.1
6	0.0172	0.013	24.5
7	0.012	0.0075	37.1
8	0.0101	0.0062	38.5
9	0.0198	0.0136	31.4
11	0.017	0.0133	21.7
12	0.0159	0.013	18.2
13	0.0114	0.0078	31.5
14	0.0156	0.0129	17.5
15	0.0208	0.0165	20.5
16	0.0213	0.0171	19.7
17	0.0574	0.0188	67.2
18	0.0528	0.0165	68.7
19	0.016	0.0091	43.2
20	0.0145	0.009	38
22	0.0294	0.0231	21.3
23	0.0283	0.0217	23.5
24	0.0248	0.02	19.6
25	0.0197	0.0159	19.3
26	0.0193	0.0157	18.8
27	0.0274	0.0213	22.3
28	0.0291	0.0241	17
29	0.033	0.0279	15.6
30	0.0292	0.0233	20.2
31	0.0154	0.0113	26.5
32	0.0212	0.0155	26.6
33	0.045	0.0364	19.1
34	0.044	0.0366	16.7
35	0.0352	0.029	17.5
36	0.0227	0.0182	19.8
37	0.0402	0.0331	17.7
38	0.0512	0.0411	19.7
39	0.0479	0.0401	16.3
40	0.0512	0.0413	19.3
41	0.0544	0.0489	10.1

Table 6.16. Average summer and winter velocities (in m d^{-1}) for 1937 – 1946, rounded to the fourth decimal, calculated from KOL40.

6.3. Extent and frontal changes

Area changes on Hellstugubreen are given in Table 6.17, represented in Figure 6.13 and mapped in Figure 6.14. Since 1941, Hellstugubreen has lost 0.86 km^2 (or 20%) of its area. Between 1997 and 1980 Hellstugubreen did not suffer any area loss, and actually grew by 2%.

Year	Area (km^2)	Total area change (km^2)	Area change (%)	Average annual area loss ($\text{km}^2 \text{ yr}^{-1}$)
1941	4.24			
1962	3.99	-0.26	-6	-0.01
1968	3.92	-0.06	-2	-0.01
1980	3.53	-0.39	-10	-0.03
1997	3.6	0.06	2	0
2009	3.38	-0.22	-6	-0.02
1941-2009		-0.86	-20	-0.01

Table 6.17. Evolution of Hellstugubreen’s area coverage between 1941 and 2009. Western cirque included in calculations.

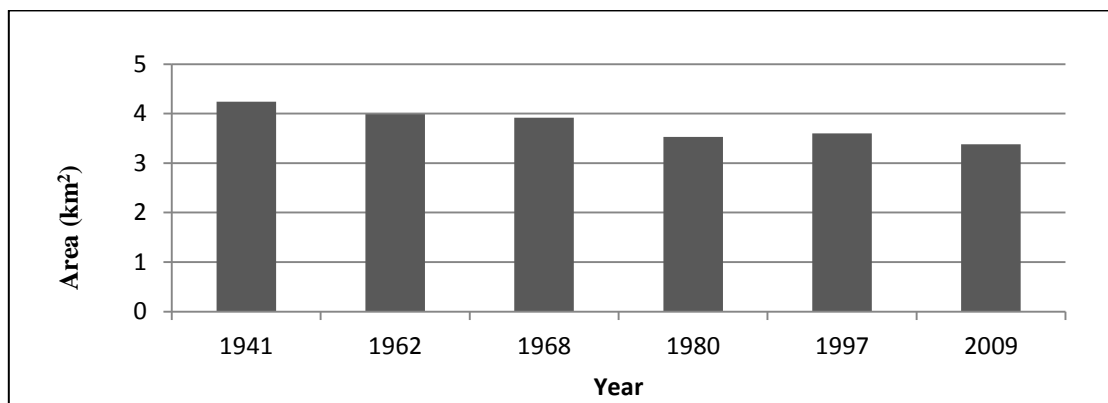


Figure 6.13. Hellstugubreen’s area (km^2). Western cirque included in calculations.

Comparison of these results to results from *NVE* (2014) show differences in total area, most likely due to the different location of the ice divide (see Section 5.2.1 and Table 6.18). The average difference between the results presented here and those from *NVE* (2014) is -2%, since the glacier outline used here is smaller than that used by *NVE*.

Year	Area (km²)	Area (km²) NVE 2014
LIA	-	4.7
1941	4.24	4.39
1962	3.99	4.08
1968	3.92	4.03
1980	3.53	3.62
1997	3.6	3.65
2003	-	3.6
2009	3.38	3.43

Table 6.18. Comparison of area extent results from this research and those from *NVE* (2014).

Between 1901 and 2011, 71 observations of frontal position exist for Hellstugubreen (Table 6.19, Figure 6.14). During this period, the glacier has retreated nearly constantly, with a total frontal change of 1107 m. Small positive changes in 1907 (2 m) and 1997 (5 m) are exceptions to the general trend, an observation made in the literature (Andreassen et al. 2005). Over the past 110 years, the glacier has retreated 1107 m. Between 1941 and 2009, the glacier retreated 845 m. From Figure 6.13, frontal changes occur coincidentally with volume changes.

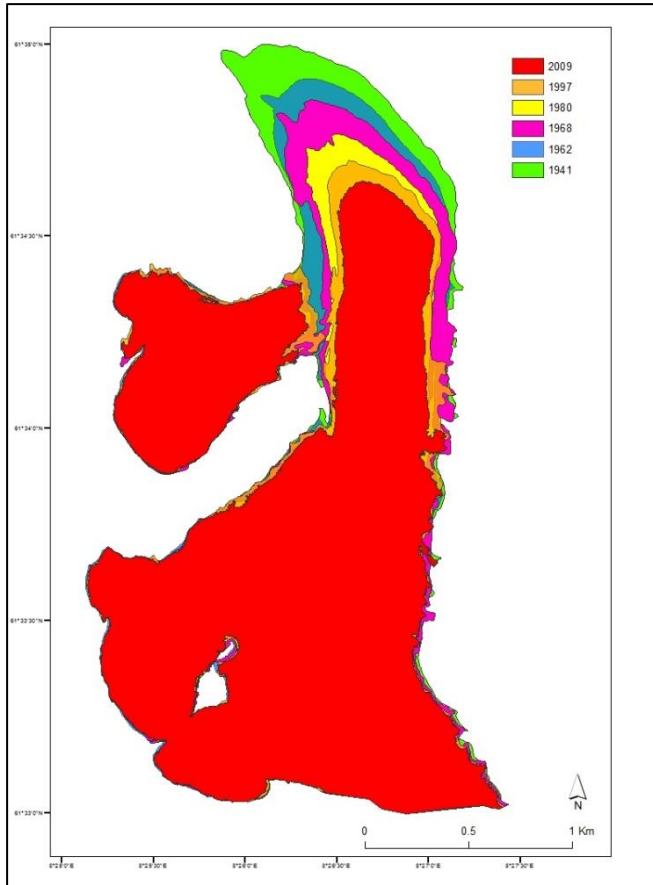


Figure 6.14. Evolution of Hellstugubreen's extent between 1941 and 2009.

year	m	cumul
1901	0	0
1902	0,01	0,01
1903	-12,7	-12,69
1904	-14	-26,69
1905	-0,3	-26,99
1906	-9	-35,99
1907	5	-30,99
1908	0	-30,99
1909	-4,4	-35,39
1910	-3,6	-38,99
1911	-5,7	-44,69
1912	-25,3	-69,99
1913	0	-69,99
1914	0	-69,99
1915	0	-69,99
1916	0	-69,99
1917	0	-69,99
1918	0	-69,99
1919	0	-69,99
1920	0	-69,99
1921	0	-69,99
1922	0	-69,99
1923	0	-69,99
1924	0	-69,99
1925	0	-69,99
1926	0	-69,99
1927	0	-69,99
1928	0	-69,99
1929	-87,3	-157,29
1930	0	-157,29
1931	-13	-170,29
1932	-7	-177,29
1933	-12	-189,29
1934	-8	-197,29
1935	-11	-208,29
1936	-5	-213,29
1937	-8	-221,29

year	m	cumul
1938	-11	-232,29
1939	-12	-244,29
1940	-7	-251,29
1941	-11	-262,29
1942	-12	-274,29
1943	-5	-279,29
1944	-27	-306,29
1945	0	-306,29
1946	0	-306,29
1947	-43	-349,29
1948	-20	-369,29
1949	-10	-379,29
1950	-19	-398,29
1951	-10,7	-408,99
1952	-15,3	-424,29
1953	-13	-437,29
1954	-14	-451,29
1955	-11	-462,29
1956	-18	-480,29
1957	-13	-493,29
1958	-4	-497,29
1959	-39	-536,29
1960	0	-536,29
1961	-14	-550,29
1962	-10	-560,29
1963	-12	-572,29
1964	-6	-578,29
1965	0	-578,29
1966	0	-578,29
1967	0	-578,29
1968	0	-578,29
1969	0	-578,29
1970	0	-578,29
1971	-90	-668,29
1972	0	-668,29
1973	0	-668,29
1974	0	-668,29

year	m	cumul
1975	-69	-737,29
1976	-31	-768,29
1977	0	-768,29
1978	0	-768,29
1979	0	-768,29
1980	0	-768,29
1981	0	-768,29
1982	0	-768,29
1983	-95	-863,29
1984	0	-863,29
1985	0	-863,29
1986	-49	-912,29
1987	-10	-922,29
1988	-18	-940,29
1989	-7	-947,29
1990	-8	-955,29
1991	-7	-962,29
1992	-9	-971,29
1993	-3	-974,29
1994	-9	-983,29
1995	-6	-989,29
1996	-3	-992,29
1997	2	-990,29
1998	-9	-999,29
1999	-7	-1006,29
2000	0	-1006,29
2001	-4	-1010,29
2002	-17	-1027,29
2003	-10	-1037,29
2004	-5	-1042,29
2005	-4	-1046,29
2006	-15	-1061,29
2007	-10	-1071,29
2008	0,01	-1071,28
2009	-10	-1081,28
2010	-5	-1086,28
2011	-21	-1107,28

Table 6.19. Absolute and cumulative frontal changes on Hellstugubreen from 1901 until 2011. During this period, the glacier retreated 1107 m. Years without measurements are marked 0 (Data: NVE).

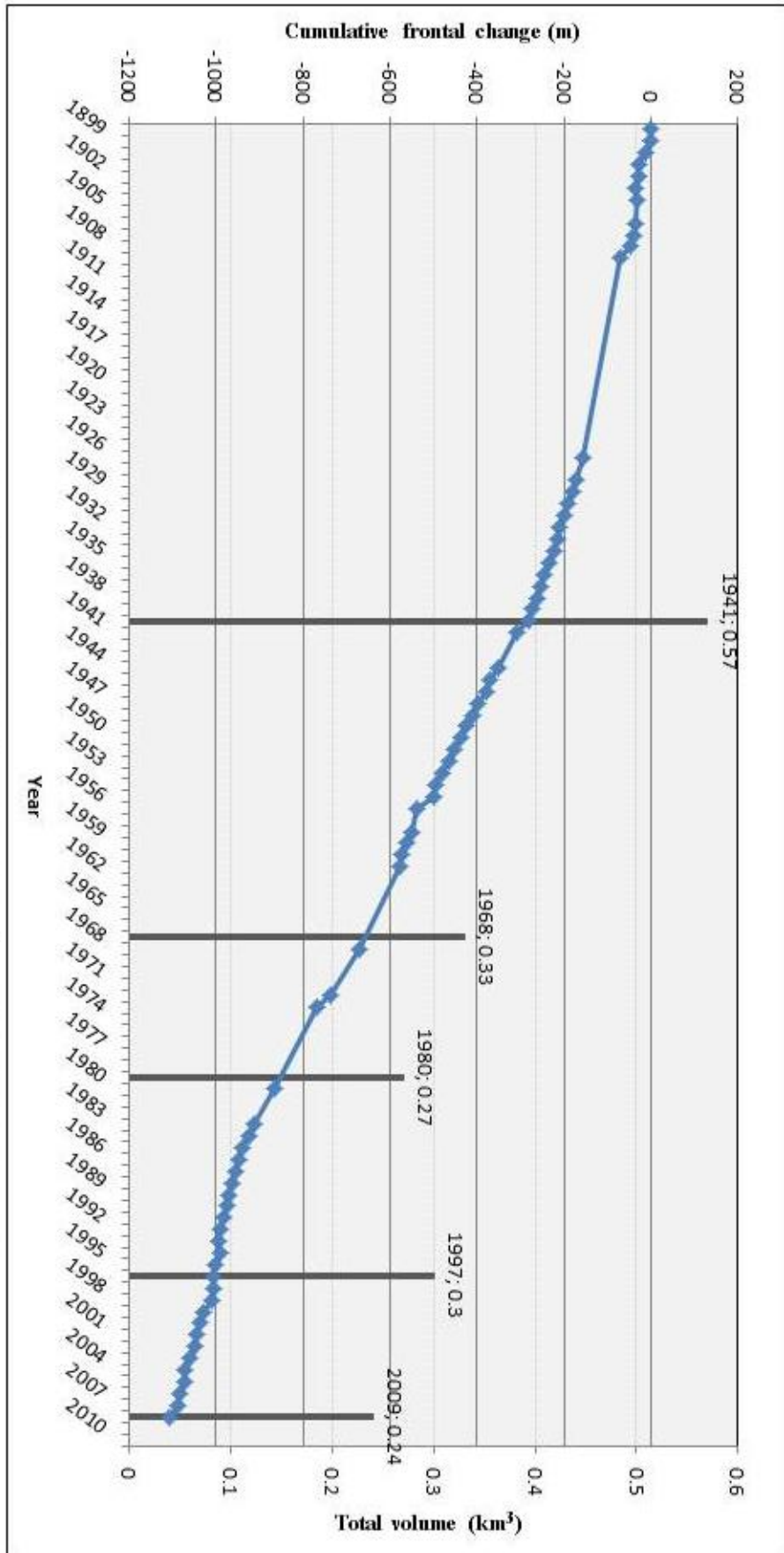


Figure 6.15. Cumulative frontal changes (m) and total volume (km³) on Hellstugubreen from 1901 until 2011.

When comparing the three decades that form the focus of this research (1940s, 1960s and 2000s); clear differences can be observed (Table 6.20). With an average retreat of 12.7 m yr⁻¹ between 1939 and 1951, the 1940s showed the fastest recession. In the 1960s, the retreat was 20% smaller compared to the 1940s. The difference in retreat between the 2000s and the 1960s is 23%. In the 2000s, the retreat was 39% smaller compared to that in the 1940s.

Period	Total change (m)	Annual change (m yr ⁻¹)
1939-1951	-164.7	-12.7
1959-1971	-132	-10.1
1999-2011	-101	-7.8
1941 - 1968	-367.2	-13.6
1968 - 1980	-193.1	-16.1
1980 - 1997	-167.7	-9.9
1997 - 2009	-91	-7.6

Table 6.20. Frontal retreat on Hellstugubreen.

When comparing the periods covered by the comparative DEMs (Table 6.18), the average annual retreat of Hellstugubreen's front was 44% smaller between 1997 and 2009 than in the first period (1941 – 1968). Between 1968 and 1980, the front moved back just over 16 m d⁻¹, amounting to a retreat of almost 200 m for that period.

7. Discussion

7.1. Volume, terminus and extent

The volume losses on Hellstugubreen seem to correspond with findings both on a global and more regional scale. While glaciers in moist, maritime regions across the world are growing, glaciers in cold and drier regions demonstrate trends of shrinkage (Dyurgerov and Meier 2000). Studies have established that this global trend is reflected on a regional scale in southwestern Norway, where glaciers constitute a west-east profile across the country (Andreassen 1998; Dyurgerov and Meier 2000; Nesje et al. 2000; Andreassen et al. 2005). Hellstugubreen fits into this west-east profile. However, it should be noted that Hellstugubreen is located near the watershed on the east–west divide and receives precipitation from both the west and the east. Both Nigardsbreen and Storbreen experience the same climatic setting, while Harbardsbreen receives most precipitation from the south and west (Kjøllmoen 1997; Andreassen 1998). Maritime glaciers Ålfotbreen and Nigardsbreen had a mass gain of more than 10 m between 1966 and 1993, while the glaciers in Jotunheimen to the east (Storbreen, Hellstugubreen, Gråsubreen) all shrank considerably during the same period. Ålfotbreen gained 13.3 m, while Grådubreen lost a -7.5 m water layer (Andreassen et al. 2005). Andreassen et al. (2005) calculated a volume change of -7.7 m during this period on Hellstugubreen. Results from this research are in correspondence with these findings: between 1968 and 1980, Hellstugubreen lost a volume of 4.66 m of water averaged over its entire surface.

Storglaciären lost an ice volume of $19 \times 10^6 \text{ m}^3$ (or 5.69 m w.eq, a mean annual loss of 0.14 m w.eq.) between 1959 and 1999 (Koblet et al. 2010). On average, Hellstugubreen lost 0.29 m of water column per year between 1941 and 2009, more than double the amount. For comparison, Harbardsbreen lost 8.5 m between 1966 and 1996 (Kjøllmoen 1997). Between 1968 and 1997, a layer equal to 4 m of water was lost from Hellstugubreen. Comparing datasets of unequal time scale poses problems, however, as Hellstugubreen lost 40% of its volume between 1941 and 1968.

The mass gain of $4 \times 10^6 \text{ m}^3$ on Hellstugubreen between 1980 and 1997 is in line with results for Storglaciären, which gained $7 \times 10^6 \text{ m}^3$ between 1980 and 1999 (Koblet et al. 2010). Since 2001, all monitored Norwegian glaciers have seen their mass reduced (Andreassen et al.

2005). Continuous extreme ice losses since 1980 have been established for the Alps (Haeberli et al. 2007; Paul and Haeberli 2008) and on a global scale (Dyurgerov and Meier 2000).

The total volume change on Hellstugubreen of $82 \times 10^6 \text{ m}^3$ compares to the loss of a nearly 20 m thick water layer. However, the removal of mass has not been equally distributed across the glacier surface. Hellstugubreen's tongue (from the ice front up to 1700 m a.s.l.) lost $33 \times 10^6 \text{ m}^3$ of mass between 1941 and 2009, accounting for 37% of the overall volume changes. On Storbreen, thinning has been most pronounced in the lower height intervals since the 1940s as well (Andreassen 1999). However, in small areas in the upper regions of both Hellstugubreen and Storbreen, there has occurred mass gain, probably as a result of a more positive net balance. The positive changes on Hellstugubreen that occur close to the mountain walls were at first assumed to originate from an input of materials from avalanching and rock slides. However, they are caused by errors in the contour lines (Liss M. Andreassen, personal communication). On Storglaciären, the great volume loss between 1959 and 1969 was the result of a general thickness reduction. The losses registered the following decade (1969 – 1980) were greatest on the tongue and upper accumulation area, while the ablation area gained mass in that period (Koblet et al. 2010).

Pronounced thinning on the tongue is confirmed by Hellstugubreen's frontal retreat, a conclusion supported by earlier findings by Liestøl (1962) (Figure 7.1.). For instance, at stake 33, velocity decreased during the first year of observation, concurring with a thinning of the glacier. In 19743 and 1944 the thickness increased again, and so did the velocity. In 1945, the situation was reversed. Tverråbreen and Hellstugubreen behaved in a very similar way, which can be expected considering they are located close ($\pm 6.5 \text{ km}$) together (Liestøl 1962).

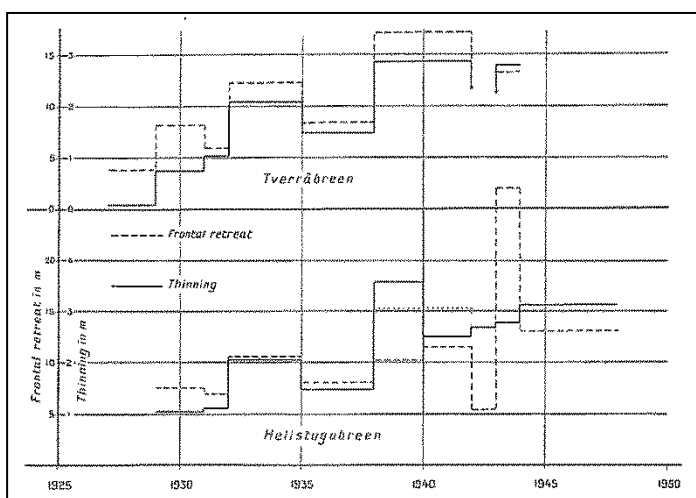


Figure 7.1. Thinning and frontal retreat of Tverråbreen and Hellstugubreen (Liestøl 1962, p. 28).

As the glacier retreats, exposed side moraines can become the source of dust transported onto the glacier tongue. Especially under warm and dry conditions, dust particles can be deposited tens to hundreds of meters away. Oerlemans et al. (2009) demonstrated that the accumulation of dust on the snout of the Vadret da Morteratsch lowers the albedo of the glacier surface, thus enhancing summer melt rate. Other studies have considered the same process to occur on other glaciers (Huss et al. 2009). The fine layer of dust that exists on Hellstugubreen's tongue might affect the local balance rate in a similar way, causing greater ablation on the glacier tongue (Figure 7.2).



Figure 7.2. Hellstugubreen's terminus with exposed debris. A fine layer of dust can be observed on the glacier tongue (Image: personal collection, July 8th 2013).

Located within a 15 km radius from Hellstugubreen, Storbreen and Styggedalsbreen retreated almost constantly, with the exception of small positive changes, as did Hellstugubreen. In the 1990s, maritime Norwegian glaciers advanced strongly (Andreassen et al. 2005). Storglaciären reacted to its positive volume change between 1980 and 1999 with a slow down, and eventually a halt, of its retreat (Koblet et al. 2010). Simultaneously, Hellstugubreen's retreat slowed down considerably, and in 1996 – 1997 the glacier front advanced by 2 m. Since the early 2000s retreat has again been faster.

The period of slow down of the frontal retreat and positive volume gain on Hellstugubreen between 1980 and 1997 coincides with mass surpluses on all monitored Norwegian glaciers except for Langfjordjøkelen, Northern Norway. Dyurgerov and Meier (200) showed differences between cumulative values between 1961 and 1997 for ΔV for individual glaciers to reach 30 m in Scandinavia, and suggest large-scale or meso-scale climatic conditions to be responsible for these differences. In addition, the fact that distant glaciers may correlate more strongly than neighbouring glaciers, is according to Dyurgerov and Meier (2000) a proof of the existence of teleconnections involving regional atmospheric circulation patterns.

Decadal- to millennial-scale glacier variations which reflect global, hemispherical, regional and local climate variations have been identified (Winkler and Matthews 2010). Oerlemans (2005) showed that glacier length records from all over the world reflect a distinct global

temperature signal. Climatic conditions in the Northern Hemisphere are related to patterns of natural variability that operate on several temporal and spatial scales. Wallace and Gutzler (1981) refer to these meteorological oscillations as teleconnection patterns due to the fact that they cause simultaneous reactions across the world in terms of geopotential heights at a given pressure surface. These teleconnection patterns consist of large-scale changes in atmospheric waves and jet stream patterns and influence mean wind speed and direction, as well as the position and intensity of the jet stream. Thus, they influence seasonal mean heat and moisture transport, the intensity and number of storms, as well as their paths and their weather. Fluctuations in ocean surface temperature and heat content, ocean currents and their related heat transport and sea ice cover are all related to changes in large-scale teleconnection modes. Such climatic fluctuations affect not only agricultural harvests, water and energy supply and demand and fisheries, but glacier behaviour as well (Hurrell 2003; NOAA 2012) .

The most important pattern of large-scale variability in the northern hemisphere influencing the regional climatic conditions at middle and high latitudes is the North Atlantic Oscillation (NAO) (Hurrell 1995). Initially identified by Walker and Bliss (1932), the NAO consists of swings in the atmospheric sea level pressure (SLP) difference between the Arctic and the subtropical Atlantic, more precisely between the Ponta Delgada in the Azores and Stykkisholmur in Iceland (Nesje et al. 2000; Hurrell 2003; Imhof et al. 2012). The NAO is quantified in the NAO index that is defined as the difference between the normalised mean winter (December-March) sea-level pressure anomalies in the Azores and Iceland. The indices of the teleconnection patterns considered are published by the National Oceanic and Atmospheric Administration (NOAA) Climate Prediction Center (CPC – available at: www.cpc.noaa.gov) (Figure 7.3). Positive NAO indices are associated with high SLP at both the Azores high and Icelandic low centres over the North Atlantic. The pressure variation creates a north-eastward shift in the Atlantic storm activity, with enhanced activity from Greenland across Iceland into northern Europe, influencing northern Europe and Scandinavia with warmer, yet wetter conditions during winter and intensifying the strength and frequency of storms in the vicinity of Iceland and the Norwegian Sea. At the same time, a positive phase of the NAO results in a modest decrease in activity from the Azores across the Iberian Peninsula and the Mediterranean, with drier and colder conditions in this region as a result (Hurrell 1995; Hurrell 2003). The NAO stays strong throughout the year, but is most prominent during the boreal cold season (November through April) when the atmosphere is dynamically the most active (Hurrell and Van Loon 1997; Nesje et al. 2000). McCabe et al. (2000) showed that

46% of the global winter balance variability can be explained by global climatic patterns, a percentage confirmed by Dyurgerov and Meier (2000). Dyurgerov and Meier (2000) note that, on short time scales (annual), ΔV of glaciers respond to change in climate with little delay. They calculated a time lag of one year between volume changes in consecutive years. Annual changes in volume can thus occur almost simultaneous with annual changes in weather.

In addition to the inter-annual variability, there have been several periods where the NAO index persisted in one phase over many years (Hurrell and Van Loon 1997). Periods of advance and retreat have previously been linked to fluctuations in the NAO index, among other regions in the Alps and South-western Norway (e.g. Hooke et al. 1983; Nesje et al. 2000; Reichert et al. 2001; Nesje and Dahl 2003; Imhof et al. 2012; Nesje and Matthews 2012). Between the early 1940s and the early 1970s, the NAO index showed a downward trend; with winter temperatures and precipitation in Europe frequently lower than normal (Van Loon and Williams 1976). The retreat of Hellstugubreen between 1941 and 1968 (316 m) can and its ΔV of $-38 \times 10^6 \text{ m}^3$ (-42%) can be explained by the low NAO index during the same period.

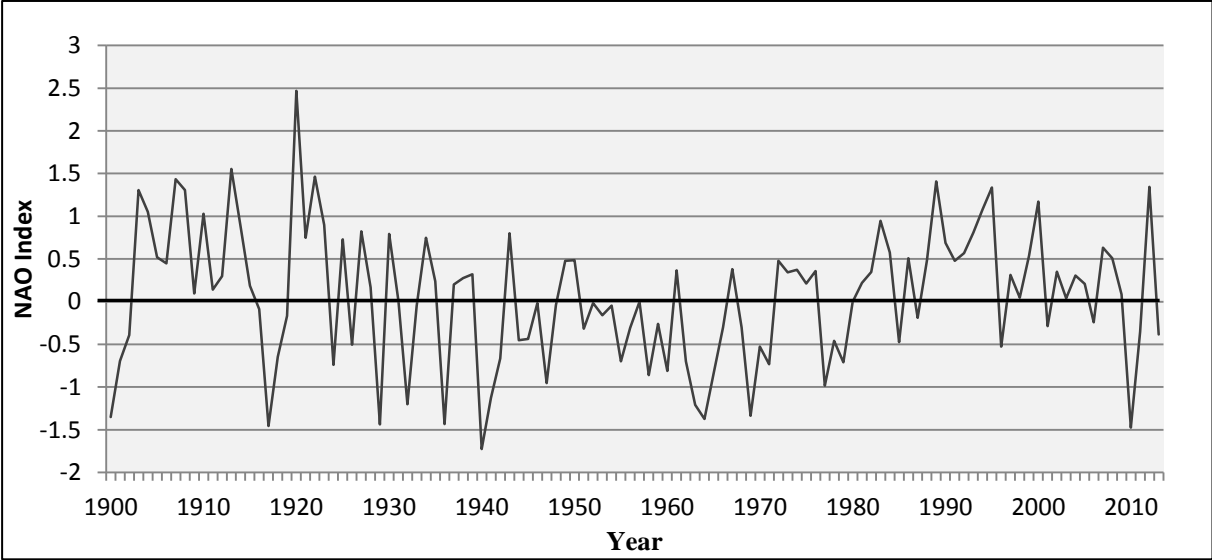


Figure 7.3. NAO index data from the CPCC (NOAA 2012), combined with reconstructed data from before January 1950 (Luterbacher et al. 2001). This produced a continuous time series from 1901 until February 2014.

Since 1980, the NAO has remained highly positive, with several winters marked by the highest positive values of the NAO index recorded since 1864 (Hurrell and Van Loon 1997), resulting in high amounts of precipitation and, with a certain time lag, higher-than-normal positive mass-balance to Norway. Matthews (2012) identified a positive NAO index in the

winters of between 1988 and 2000 as the main cause for the large glacier advances in Scandinavia in the 1990s. Other studies confirm these findings (Nesje et al. 2000; Nesje and Matthews 2012). The sudden advance of Norwegian maritime glaciers in the 1990s and the subsequent rapid retreat has been termed the Briksdalsbre Event, after Briksdalsbreen, south-western Norway, which saw a phenomenal advance of 285m in less than a decade, followed by an equally impressive retreat of 486 m between 1996 and 2009 (Nesje and Matthews 2012). The effects of this period of high winter precipitation affected several continental glaciers as well as the maritime ice bodies. The effect of the NAO on the winter balance gradually decreases with increasing continentality (Nesje et al. 2000; Andreassen et al. 2005), which explains why Hellstugubreen did not see the extreme volume gains and advance of some more coastal glaciers like Ålfotbreen and Nigardsbreen. Also located in Jotunheimen, Styggedalsbreen and Storbreen started advancing in 1989 and didn't retreat again until the late 1990s. Bøverdalen advanced between 1988 and 2001.

However, the correlation with the NAO is not always constant. Imhof et al. (2012) note that the classical correlation with the NAO was between 1962 and 1998 (they name Briksdalsbreen as an example), but that that correlation was significantly weaker or even inversed during other periods. They conclude that especially maritime glaciers in southern Norway will be influenced in a complex way by future fluctuations of the NAO. Local factors such as aspect (Hellstugubreen faces north), and exposure to the sun (it is often shaded) will influence the glacier's mass balance and volume changes to a great extent.

Regional weather trends are influenced by global signals, but can also reflect more local conditions. Figure 7.3 shows the mean summer (July) and winter (January) temperatures for weather stations located at Fokstua and Fokstugu, respectively. The stations carry different station numbers at the Norwegian Meteorological Institute, but they are located in approximately the same location on Dovrefjell, about 75 km north-east of Hellstugubreen. The two stations were combined to give a continuous time series. Figure 7.5 clearly shows the period of high winter precipitation in the 1990s, with a smaller peak at the beginning of the 20th century and in the 1950s. The high winter precipitation in the early 1900s is reflected in the slow retreat of Hellstugubreen in that period. In 1907, the glacier advanced 5 m, the only year outside of the 1990s with terminus advance in the entire time series. The slight increase in precipitation in the 1950s and 1970s did not seem to influence Hellstugubreen's mass balance much, probably due to high summer melt rates in those periods.

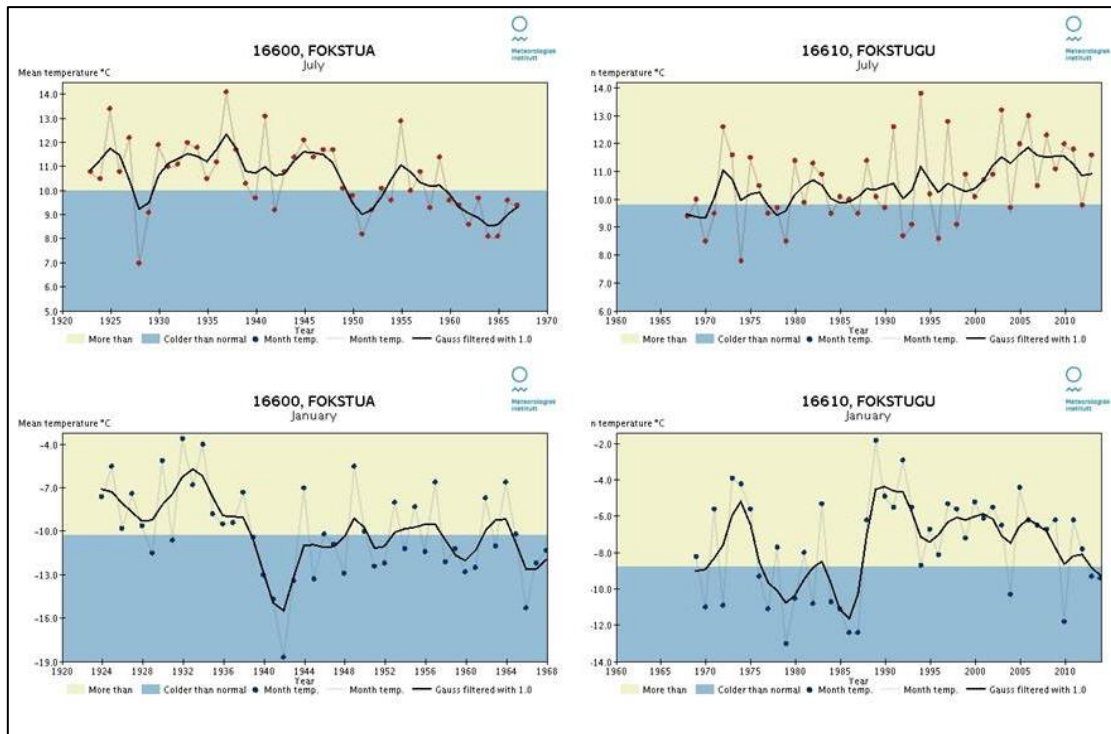


Figure 7.4. Mean summer (July) and winter (January) temperatures from 1920 -1970 (Fokstua) and 1970-2014 (Fokstugu) (Data: eKlima.no).

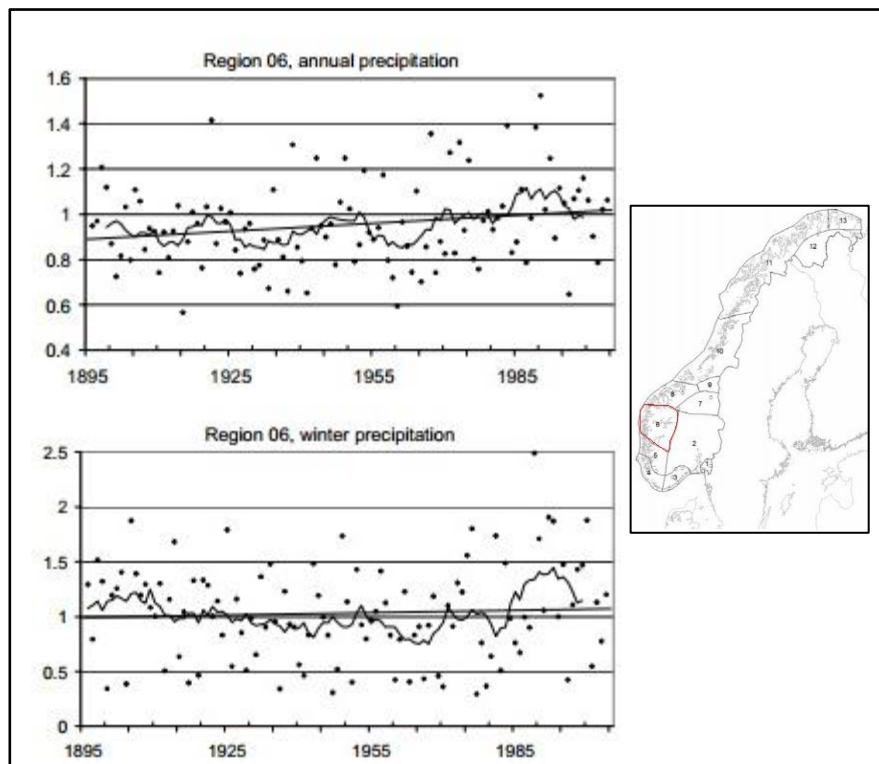


Figure 7.5. Annual and winter precipitation in south-western Norway. The precipitation is given as fraction of the 1961-1990 average. The diamonds show individual values, while the curves show 10-year running means dated on the 5th year. The straight lines indicate the linear trends (Hanssen-Bauer 2005).

7.2. Slope

Driving stresses are also dependent on the surface slope, and the fact that the glacier surface steepened by 46% on average for the compared stakes could have countered the effects of extreme volume loss, at least partly. On Pine Island Glacier, Antarctica, assuming constant basal drag and longitudinal stress gradients, a steepening surface (271%) caused an increase in gravitational driving stress and hence caused the glacier to accelerate (19%) between 2006 and 2008 (Scott et al. 2009).

7.3. Velocity

Between May 2010 and September 2013, Hellstugubreen moved at a velocity of 0.0261 m d^{-1} , which corresponds to 9.53 m yr^{-1} . Hanson and Hooke (1994) determined a velocity of 15 m yr^{-1} on Storglaciären, which is of similar size as Hellstugubreen. Table 7.1 shows surface velocities and flux rates for several glaciers.

Glacier	Type	Surface velocity (m yr^{-1})	Ice thickness (m)	Flux q ($10^4 \text{ m}^2 \text{ yr}^{-1}$)	Distance from front (km)	Literature
Storglaciären	mountain	15	200	0.3	2	Hanson and Hooke (1994)
McCall	mountain	15	170	0.26	3	Rabus and Echelmeyer (1997)
Blue	mountain	50	250	1.25	2	Meier et al. (1974)
Worthington	mountain	75	200	1.5	4	Harper et al. (2001)
Taylor	ice sheet outlet	17	1000	1.7	50	Kavanaugh et al. (2009)
Columbia	mountain, tide water	730	950	70	52	O'Neel et al. (2005)
		2900	800	230	52	Clarke and Echelmeyer (1996)
Jakobshavn*	ice sheet outlet	1050	2500	250	500	Clarke and Echelmeyer (1996)
Jakobshavn**	ice sheet outlet	3800	1760	670	530	Joughin et al. (2001)
NEGIS	ice sheet outlet	300	1200	36	620	Joughin et al. (2001)
Whillans	ice sheet outlet	440	1030	45	500	Engelhardt and Kamb (1998)
Pine Island	ice sheet outlet	1500	1800	270	300	Thomas et al. (2004)
Jutulstraumen	ice sheet outlet	550	1300	70	550	Rolstad et al. (2000)

* 40 km above grounding line

** 7 km above grounding line

Table 7.1. Example of measured surface velocities and fluxes for some glaciers (after Cuffey and Paterson 2010).

Table 7.1 clearly shows that flux q increases with distance from the head of the glacier X . The smallest glacier, Storglaciären, Sweden, has the smallest flux. The ice streams all have large fluxes, an expression of the large basins they drain. However, there are some discrepancies to this general rule. The Northeast Greenland Ice Stream (NEGIS) has a much smaller flux than Jakobshavn Isbræ, West Greenland, despite the fact that the former has a larger basin. This can be explained by the fact that Jakobshavn converges into a narrow channel. But it also reflects the climatic setting of the two ice streams. NEGIS drains the dry north east of Greenland, whereas Jakobshavn is situated in the much wetter west-central region of Greenland. Climate also explains why Blue Glacier, Washington, USA, and Storglaciären, that are nearly equal in size, have very different fluxes. Abundant snowfall in a coastal mountain setting allows for a flux four times larger at Blue Glacier. Columbia Glacier, Alaska, USA, drains a much larger basin than the other mountain glaciers and thus has a much greater flux, matching the flux seen on some the polar outlet glaciers. Draining a particularly dry region of Antarctica, Taylor Glacier carries a flux only a few per cent as large as Columbia, despite the fact that its basin is similar in size to that of Columbia.

When considering spatial variations in horizontal velocity, the stakes between 1700 and 1800 m a.s.l. (20_{NVE10}, 26_{NVE10}, 29_{NVE10} and 41_{NVE}) had the highest velocity in the 2010. The stakes that had the greatest velocities in the 1940s and 1960s, the fastest stakes were also located in this area. In the 1960s, the general velocity of the glacier was slightly smaller during the first year of Pytte's measurements, but the glacier flow in the 1960s seems similar to that in the 1940s. However, the glacier's lower areas slowed down significantly.

In the 1970s, *NVE* found that the greatest velocities on Hellstugubreen ($15 - 20 \text{ m yr}^{-1}$) are to be found in a small area between 1700 and 1800 m a.s.l. (*NVE* 1975). This area is notably steeper in this area, and the ice is forced through a narrowing in the valley. The report also notes a remarkable deceleration at the glacier front and in the south-eastern parts of the firn area. Between 1941 and 1972, no velocity changes could be detected in the areas above 1650 m a.s.l. However, the tongue has thinned noticeably and the glacier has slowed down in the areas located below 1650 m a.s.l. Between 1941 and 1962, the front retreated 250 m., and another 100 m. was lost during the subsequent six years.

The fact that stake 60_{NVE}, located in this area, has slower velocities might have to do with the fact that the mean horizontal velocity decreases near the valley sides due to drag. On Storglaciären, Hooke et al. (1983) concluded that the glacier must be frozen to the bed where

the ice is less than 40 m thick. Similar conditions probably exist on the sides on Hellstugubreen, as the ice thins towards the valley sides and calculated velocities for 60_{NVE10} can be considered a confirmation of this assumption. A more extensive stake network that includes cross profiles would provide more specifics. On Storglaciären, vertical velocity would sometimes compensate for the lack of horizontal velocity (Hooke et al. 1983). Similar processes might be at work on Hellstugubreen.

As do the majority of glaciers around the world, Hellstugubreen displays clear differences between winter and summer velocities, with summer velocities 20% higher on average in the 2010s. This suggests that in summer, more meltwater penetrates to the bottom, increasing rates of sliding and till deformation. The usual peak of summer velocity in September is in correspondence with findings on Midtdalsbreen and Storglaciären, where summer velocities increase mid-season (Hooke et al. 1989). Thus, the relationship between water input and rapid glacier motion seems to vary during the summer.

At 60_{NVE10}, winter velocity in the 2010s was 2% higher than the summer flow. Even if the difference is minimal, it might be an indication that other factors should be taken into account. Again, its location close to the valley sides could enhance ice deformation and regelation.

The difference between winter and summer velocities seems independent of altitude (see Section 6.2.2), a confirmation of findings by Liestøl (1962) and consistent with results from Storglaciären (Hooke et al. 1989) and Midtdalsbreen (Willis 1991). This increase of seasonality with distance down glacier might be explained by the fact that ice thickness decreases closer to the terminus. With thickness being a smaller fraction of the overburden pressure, water pressure will have more influence on the velocity.

Pytte (1964) speculates that the dramatic loss of ice thickness (40 – 60 m between 1941 and 1963) in the lower areas might be the cause of the slow down. Hellstugubreen lost 58% of its volume between 1941 and 2009. In the same period, surface velocities changed so little that they cannot be confirmed statistically. Based on this, initial expectations were for the glacier to respond to the volume changes by slowing down considerably, since the magnitude of the driving stresses are a function of ice thickness. Since this expected slow down does not seem to have occurred on Hellstugubreen, other factors must be considered.

7.4. Driving stresses and velocity

Driving stresses for stakes show great variation in their fluctuations. Velocities for the stakes in Table 6.20 have decreased by 22% on average. The greatest change was for 40KOL40 to 60NVE10 with a slow down of 54%. However, the driving stresses have increased by 19%.

Stake	Slope (°)	Ice thickness (m)	Driving stress (kPAa)	Average daily velocity (m d ⁻¹)	Average annual velocity (m yr ⁻¹)
28 _{KOL40}	10	165	253	0.026	9.49
12 _{PYT60}	10	121	185	0.023	8.4
13 _{NVE10}	10	82	126	0.0193	7.04
33 _{KOL40}	5	123	95	0.0399	14.56
15 _{PYT60}	7	123	132	0.0325	11.86
20 _{NVE10}	10	90	138	0.0336	12.26
39 _{KOL40}	11	119	200	0.0433	15.8
17 _{PYT60}	8	106	130	0.038	13.87
26 _{NVE10}	14	105	224	0.0449	16.39
40 _{KOL40}	9	84	116	0.0467	17.05
22 _{PYT60}	22	98	324	0.032	11.68
60 _{NVE10}	13	92	183	0.0217	7.92

Table 6.20. Calculated driving stresses compared to velocities.

Since τ_b values estimated from the assumption that $0.5 < f' < 1.5$ results in values between 95 and 324; and because the deformation rates in ice increase strongly when stress rates rise to about 100kPA (see section 3.2.1), the slow glacier flow can be considered to be a result of perfectly plastic deformation. τ_b therefore becomes equal to the yield stress for ice, at usually 100 kPA.

However, since the driving stress spans such a large range, but velocities remain fairly constant, other factors, like resisting forces and an increasing angle of the surface slope, are likely to counter the effect of the driving stresses.

7.5. Other factors

Another consideration should be the glacier's changing hydrology with changing climate and dynamics. Since so much mass was lost, the glacial meltwater discharge must have increased since the 1940s. This could increase velocities as more meltwater means better lubrication and easier deformation of the underlying sediments (Willis 1995). It is possible that increased

melt has countered the slow down due to loss of ice thickness. On the other hand, increased hydrological power can result in a more efficient drainage system, relieving water pressures (Ibid.).

8. Limitations and suggestions for future work

As seen in Section 5, this research employed a methodology that has been tested with good results in the literature. However, limitations did occur in the course of the research process. First of all, the quality of the analogue maps should be considered. The shape-files derived from the analogue map from 1962 showed elevations at off-glacier locations that did not correspond at all to the 1941 or 1968 shape-files. This is known to happen (Andreassen 1999) but often the DEMs derived from the erroneous contour lines can be corrected because the errors are constant across the maps. This is the case when the whole DEM is tilted at an angle compared to the actual surface. However, the 1962 map was not based on aerial photography and there was no consistency in the error rate. To correct the map would have encompassed going back to the original aerial photographs and field notes. Due to time limitations, the DEM from 1962 was excluded from this research. The contour map was used, however, in the analysis of glacier extent and frontal retreat. Digitising procedures (data transformations, interpolations and calculations) can also affect the final result. Converting projections, generating DEMs and overlay operations all introduce errors (Arbia et al. 1998; Andreassen 1999). It would be interesting to compare the methods used in this research to the mass balance method, as Andreassen (1999) did on Storbreen.

As pointed out in Section 5.2.1, and by Liestøl (1962), stake location (and thus velocity) was not recorded on the same dates each year; measurement dates can differ from the previous year by several days or even weeks. This means that summer and winter velocities are not measured over the same interval each year, which implies for instance that periods of extreme melt can be included in one year's calculations for summer velocity, but not the next. Ideally, observation should be made on the same date for each year, both in summer and in winter. However, field expeditions are dependent on good weather, logistics and the number of available hands, and compromises are inevitable. Another consideration is that velocity data was not available for the exact same geographical locations for the 1940s, 1960s and 2010s, and therefore the comparison of the stakes across the decades does over a general idea of the evolution of glacier velocity, but accurate results were difficult to generate. If the stake network was to be extended, stakes located more closely to those from KOL40 and PYT60 would provide a better basis for comparison. A more extensive survey on Hellstugubreen would also shed light on the differences between stakes located close to the flow line and those closer to the lateral margins. Cross-profiles could be compared to those from the earlier

datasets, and could provide data on the temperature regime of the glacier.

Velocities for the 2010s were calculated from data covering the period between 2009 and 2013. The results would have been considerably more accurate had a 2011 map been available. Constant density of ice was assumed at 0.9 g cm^{-3} . To improve ΔV calculations, ice density profiles should be taken in the accumulation area at the time of photography.

In order to establish the complete flow field of the glacier, vertical velocities should be investigated. Factors like basal drag, longitudinal stress should be considered at different locations. A study of discharge would shed light on the development of Hellstugubreen's melt water channel development, both on an intra-annual time scale as on a decadal one.

A climate scenario for 2071 – 2100 would cause the melting of a surface layer of $140 \pm 30 \text{ m}$ by 2100 a rise of the average ELA of $260 \pm 50 \text{ m}$, reducing the number of Norwegian glaciers from 1627 to ~27, a reduction of ~98% (Nesje et al. 2008). Andreassen and Oerlemans (2009) suggest that, on Storbreen, a 1°C temperature rise must be compensated by a 30% increase in precipitation to keep Storbreen in balance. It would increase the length of the ablation season by 20 (50) days. The model used on Storbreen can be applied to Hellstugubreen as Hellstugubreen has long records of mass balance. It only needs daily precipitation and temperature data as input, which can easily be obtained from online databases. Such modelling would make it possible to assess the impact of possible climate change on Hellstugubreen and predict its future fluctuations. Furthermore, investigations of the bedrock of the glacier basin would give a better estimate of total volume change. An outline of the glacier bed would allow for greater understanding of how long Hellstugubreen can survive under varied climate conditions.

9. Conclusions

Investigations of glacier flow are essential to the understanding of several glaciological problems. The main interest of this research has been the response of Hellstugubreen's response to its changing geometry between 1941 and 2009. From the observation of significant frontal retreat, it was expected that Hellstugubreen had lost a considerable amount of mass since the 1940s, and that this volume change would influence driving stresses and thus glacier flow. Three datasets were compared: one from the 1940s (KOL40), one from the 1960s (PYT60), and the most recent one from the 2010s (NVE10). Contour maps and stake data formed the basis for this research. From each dataset, stakes were selected for comparison.

Driving stress is controlled by ice thickness, surface slope, gravitational acceleration (9.81 m s^{-2}) and ice density (assumed constant at 0.9 g cm^{-3}). Ice thickness and surface slope had to be calculated for each of the selected stakes based on DEMs. The DEMs were constructed from contour lines for 1941, 1962, 1968, 1980, 1997 and 2009. The quality of the DEMs was a major concern, as the original contour maps showed discrepancies for non-glacierized areas. The 1962 DEM was considered to be of too poor quality to be used further in the analysis. Volume changes were calculated, according to known methodology, by overlaying the elevation grids and subtracting them. From the 2011 radar survey, ice thickness was interpolated and reconstructed for each of the DEMs. Between 1941 and 1997, Hellstugubreen lost 58% of its volume and 20% of its areal extent. Averaged over the entire glacier, Hellstugubreen lost the equivalent of a nearly 20 m water layer over the course of 68 years. Volume losses have been greatest at the tongue, with 40% of the total mass lost on 13% of the total glacier area. Results are in line with other glaciers in the region, like Storbreen and Harbardsbreen. While Hellstugubreen lost more than half of its volume since 1941, losses have not been constant over time. Between 1980 and 1997, the glacier gained mass ($4 \times 10^6 \text{ m}^3$) as result of several winters with high precipitation. Hellstugubreen's surface seems to have steepened when considering the compared stakes for the three datasets, a result that could be expected as thinning glaciers will change their gradients in order to keep the system in balance. With changes in both ice thickness and surface slope, driving stresses changed considerably for the compared stakes. However, no pattern to the changing of driving stresses was found to exist.

Calculations established that frontal and volume changes coincided and that frontal fluctuations are a reliable indicator of mass changes. Since 1901, Hellstugubreen has retreated 1107 m. Between 1941 and 2009, its front moved back 845 m and its area was reduced to 3.38 km², a reduction of 20%. Frontal and area changes seem to reflect volume changes, as the glacier's retreat slowed down from the 1980s, and the glacier even advanced by 2 m between 1996 and 1997. Most other glaciers in Norway saw an advance or at least a slow down of their retreat in the same period. There seems exist a relationship between frontal fluctuations on Hellstugubreen and other Jotunheimen glaciers and patterns of large-scale climatic variability, quantified in the NAO index, a result that can be considered to be in line with the literature (Nesje 2000; Imhof 2012; Nesje 2012). The most distinct period with a high NAO index (meaning periods with warmer but wetter conditions) occurred in the 1990s, when all but one of the monitored Norwegian glaciers had both mass gain and frontal advance. When comparing the changes in volume and extent on Hellstugubreen to glaciers in the same region, Hellstugubreen fits into a west-east profile across south-west Norway, where Jotunheimen is transitional between maritime western Norway and the more continental conditions found further east.

Velocity for NVE10 was calculated from changing stake locations with time. Between 2009 and 2013, Hellstugubreen flowed at an average speed of 0.0261 m d⁻¹ (9.53 m yr⁻¹), a change that is too small compared to the 0.0223 m d⁻¹ (8.14 m yr⁻¹) for the 1940s to be statistically significant. In the 2010s, summer velocities ranged from 0.0105 m d⁻¹ to 0.0544 m d⁻¹, while winter velocities varied from 0.009 m d⁻¹ to 0.0437 m d⁻¹. The difference between winter and summer velocities was -20% in the same period, compared to -24% for the KOL40 dataset.

This research confirmed initial expectations of great amounts of volume loss and changes in the glacier's geometry, as well as the consequent changes in driving stresses. However, even though driving stresses changed for the compared stakes between 1941 and 2009, average annual velocities have remained relatively constant, pointing to other reasons for the lack of change in velocity. A study of factors that might influence glacier flow, such as longitudinal stress, vertical velocities and the glacier's hydrology, would greatly benefit future research into this area and permit greater accuracy of conclusions. Applying existing models on Hellstugubreen would allow for the assessment of impact of possible climate change on the glacier.

References

- Ahn, Y., and J. E. Box. 2010. Glacier velocities from time-lapse photos: technique development and first results from the Extreme Ice Survey (EIS) in Greenland. *Journal of Glaciology* 56 (198):723-734.
- Aizen, V. B., V. A. Kuzmichenok, A. B. Surazakov, and E. M. Aizen. 2006. Glacier changes in the central and northern Tien Shan during the last 140 years based on surface and remote-sensing data. *Annals of Glaciology* 43 (1):202-213.
- Andreassen, L., F. Paul, A. Kääb, and J. Hausberg. 2008. Landsat-derived glacier inventory for Jotunheimen, Norway, and deduced glacier changes since the 1930s. *The Cryosphere* 2 (2):131-145.
- Andreassen, L. M. 1998. Volumendringer på Jostefonn 1966–93, 10: NVE.
- Andreassen, L. M. 1999. Comparing Traditional Mass Balance Measurements with Long-term Volume Change Extracted from Topographical Maps: A Case Study of Storbreen Glacier in Jotunheimen, Norway, for the Period 1940–1997. *Geografiska Annaler: Series A, Physical Geography* 81 (4):467-476.
- Andreassen, L. M., H. Elvehoy, and B. Kjöllmoen. 2002. Using aerial photography to study glacier changes in Norway. *Annals of Glaciology* 34 (1):343-348.
- Andreassen, L. M., H. Elvehoy, B. Kjöllmoen, R. V. Engeset, and N. Haakensen. 2005. Glacier mass-balance and length variation in Norway. *Annals of Glaciology* 42 (1):317-325.
- Andreassen, L. M., B. Kjöllmoen, A. Rasmussen, K. Melvold, and O. Nordli. 2012. Langfjordjokelen, a rapidly shrinking glacier in northern Norway. *Journal of Glaciology* 58 (209):581-593.
- Andreassen, L. M., and J. Oerlemans. 2009. Modelling long-term summer and winter balances and the climate sensitivity of Storbreen, Norway. *Geografiska Annaler* 91 A (4):233-251.
- Andreassen, L. M., and S. H. Winsvold. 2012. *Inventory of Norwegian Glaciers*. Oslo: Norwegian Water Resources and Energy Directorate.
- Arbia, G., D. Griffith, and R. Haining. 1998. Error propagation modelling in raster GIS: overlay operations. *International Journal of Geographical Information Science* 12 (2):145-167.
- Arendt, A. A., K. A. Echelmeyer, W. D. Harrison, C. S. Lingle, and V. B. Valentine. 2002. Rapid wastage of Alaska glaciers and their contribution to rising sea level. *Science* 297 (5580):382-386.
- Bamber, J. 2007. Remote sensing in glaciology. *Glacier Science and Environmental Change*:370-382.
- Bamber, J. L., and A. J. Payne eds. 2004. *Mass balance of the cryosphere*. Cambridge: Cambridge University Press.
- Bamler, R., and P. Hartl. 1998. Synthetic aperture radar interferometry. *Inverse problems* 14 (4):R1.
- Bauder, A., M. Funk, and M. Huss. 2007. Ice-volume changes of selected glaciers in the Swiss Alps since the end of the 19th century. *Annals of Glaciology* 46 (1):145-149.
- Benn, D. I., and D. J. A. Evans. 1998. *Glaciers & Glaciation*. London: Arnold.
- Berthier, E., Y. Arnaud, C. Vincent, and F. Remy. 2006. Biases of SRTM in high-mountain areas: Implications for the monitoring of glacier volume changes. *Geophysical Research Letters* 33 (8).
- Berthier, E., B. Raup, and T. Scambos. 2003. New velocity map and mass-balance estimate of Mertz Glacier, East Antarctica, derived from Landsat sequential imagery. *Journal of Glaciology* 49 (167):503-511.

- Blümcke, A., and S. Finsterwalder. 1905. Zeitliche Änderungen in der Geschwindigkeit in der Gletscherbewegung. Sitzungsberichte der Mathematisch-physikalischen Klasse der Kgl. . *Bayerischen Akademie der Wissenschaften zu München* 35:109-131.
- Brzozowski, J., and R. L. Hooke. 1981. Seasonal Variations in Surface Velocity of the Lower Part of Storglaciären, Kebnekaise, Sweden. *Geografiska Annaler. Series A, Physical Geography* 63 (3/4):233-240.
- Cuffey, K. M., and W. S. B. Paterson. 2010. *The Physics of Glaciers*. Burlington: Elsevier Science.
- Dyurgerov, M. 2003. Mountain and subpolar glaciers show an increase in sensitivity to climate warming and intensification of the water cycle. *Journal of Hydrology* 282 (1):164-176.
- Dyurgerov, M. B., and M. F. Meier. 2000. Twentieth century climate change: Evidence from small glaciers. *Proceedings of the National Academy of Sciences* 97 (4):1406-1411.
- . 2005. *Glaciers and the changing earth system: a 2004 snapshot*: Institute of Arctic and Alpine Research, University of Colorado Boulder, CO.
- Echelmeyer, K. A., and W. D. Harrison. 1990. Jakobshavns Isbræ, west Greenland: seasonal variations in velocities - or lack thereof. *Journal of Glaciology* 36:82-88.
- Elliston, G. R. 1966. Glaciological studies on the Gornergletscher: III. Changes in surface speed with time. Unpublished manuscript.
- Etzelmüller, B., I. Berthling, and J. L. Sollid. 2003. Aspects and concepts on the geomorphological significance of Holocene permafrost in southern Norway. *Geomorphology* (52):18.
- Gardner, A. S., G. Moholdt, J. G. Cogley, B. Wouters, A. A. Arendt, J. Wahr, E. Berthier, R. Hock, W. T. Pfeffer, and G. Kaser. 2013. A reconciled estimate of glacier contributions to sea level rise: 2003 to 2009. *Science* 340 (6134):852-857.
- Haakensen, N. 1986. Glacier mapping to confirm results from mass-balance measurements. *Annals of Glaciology* 8:73-77.
- Haeberli, W. 1995. Glacier fluctuations and climate change detection. *Geografica Fisica e Dinamica Quarternaria* 18 (2):191-199.
- Haeberli, W., M. Hoelzle, F. Paul, and M. Zemp. 2007. Integrated monitoring of mountain glaciers as key indicators of global climate change: the European Alps. *Annals of Glaciology* 46 (1):150-160.
- Hanson, B., and R. L. Hooke. 1994. Short-term velocity variations and basal coupling near a bergschrund, Storglaciären, Sweden. *Journal of Glaciology* 40 (134).
- Hanssen-Bauer, I. 2005. Regional temperature and precipitation series for Norway: analyses of time series updated to 2004. *Met. no report* 15 (2005):1-34.
- Harrison, W. D. 1986. Short period motion events on Variegated Glacier as observed by automatic photography and seismic methods. *Annals of Glaciology* 23:321-334.
- Harrison, W. D., C. F. Raymond, M. Sturm, K. A. Echelmeyer, and N. F. Humphrey. 1989. First results from automated motion and stream measurements from Fels and Black Rapids glaciers, Alaska, U.S.A. . *Annals of Glaciology* 12:1.
- Hauck, C., K. Isaksen, D. Vonder Mühl, and J. L. Sollid. 2004. Geophysical surveys designed to delineate the altitudinal limit of mountain permafrost: an example from Jotunheimen, Norway. *Permafrost and Periglacial Processes* 15 (3):191-205.
- Hodge, S. M. 1974. Variations in the sliding of a temperate glacier. *Journal of Glaciology* 16:349-369.
- Hoel, A., and W. Werenskiöld. 1962. Glaciers and Snowfields in Norway. In *Skrifter: Norsk Polarinstitut*.
- Hooke, R. L. 2005. *Principles of glacier mechanics*. Cambridge: Cambridge University Press.

- Hooke, R. L., J. Brzozowski, and C. Bronge. 1983. Seasonal Variations in Surface Velocity, Storglaciären, Sweden. *Geografiska Annaler. Series A, Physical Geography* 65 (3/4):263-277.
- Hooke, R. L., P. Calla, P. Holmlund, M. Nilsson, and A. Stroeven. 1989. A 3 year record of seasonal variations in surface velocity, Storglaciären, Sweden. *Journal of Glaciology* 35 (120):235-247.
- Hurrell, J. W. 1995. Decadal trends in the North Atlantic oscillation. *Science* 269:676-679.
- Hurrell, J. W. 2003. *The North Atlantic oscillation: climatic significance and environmental impact*: American Geophysical Union.
- Hurrell, J. W., and H. Van Loon. 1997. Decadal variations in climate associated with the North Atlantic Oscillation. In *Climatic Change at High Elevation Sites*, 69-94: Springer.
- Huss, M. 2013. Density assumptions for converting geodetic glacier volume change to mass change. *Cryosphere* 7 (3).
- Huss, M., M. Funk, and A. Ohmura. 2009. Strong Alpine glacier melt in the 1940s due to enhanced solar radiation. *Geophysical Research Letters* 36 (23):L23501.
- Iken, A. 1974. *Velocity fluctuations of an arctic valley glacier: a study of the White Glacier, Axel Heiberg Island, Canadian Arctic Archipelago*: McGill University.
- Iken, A., and R. A. Bindschadler. 1986. Combined measurements of subglacial water pressure and surface velocity of Findelengletscher, Switzerland: conclusions about drainage system and sliding mechanism. *Journal of Glaciology* 32 (110):101-119.
- Iken, A., H. Röthlisberger, A. Flotron, and W. Haeberli. 1983. The uplift of Unteraargletscher at the beginning of the melt season—A consequence of water storage at the bed. *Journal of Glaciology* 29 (101):28-47.
- Imhof, P., A. Nesje, and S. U. Nussbaumer. 2012. Climate and glacier fluctuations at Jostedalbreen and Folgefonna, southwestern Norway and in the western Alps from the 'Little Ice Age' until the present: The influence of the North Atlantic Oscillation. *The Holocene* 22 (2):235-247.
- Jacob, T., J. Wahr, W. T. Pfeffer, and S. Swenson. 2012. Recent contributions of glaciers and ice caps to sea level rise. *Nature* 482 (7386):514-518.
- Jóhannesson, T., C. Raymond, and E. Waddington. 1989. Time-scale for adjustment of glaciers to changes in mass balance. *Journal of Glaciology* 35 (121):355-369.
- Joughin, I., D. Winebrenner, M. Fahnestock, R. Kwok, and W. Krabill. 1996. Measurement of ice-sheet topography using satellite-radar interferometry. *Journal of Glaciology* 42 (140):10-22.
- Kamb, B., and H. Engelhardt. 1987. Waves of accelerated motion in a glacier approaching surge: the mini-surges of Variegated Glacier, Alaska, USA. *Journal of Glaciology* 33 (113):27-46.
- Kamb, B., C. Raymond, W. Harrison, H. Engelhardt, K. Echelmeyer, N. Humphrey, M. Brugman, and T. Pfeffer. 1985. Glacier surge mechanism: 1982–1983 surge of Variegated Glacier, Alaska. *Science* 227 (4686):469-479.
- Kjøllmoen, B. 1997. Volumendringer på Harbardsbreen 1966-96, 17: NVE.
- Kjøllmoen, B., L. M. Andreassen, H. Elvehøy, M. Jackson, and R. H. Giesen. 2011. Glaciological investigations in Norway in 2010, ed. B. Kjøllmoen. Oslo: Norwegian Water Resources and Energy Directorate.
- Koblet, T., I. Gärtner-Roer, M. Zemp, P. Jansson, P. Thee, W. Haeberli, and P. Homlund. 2010. Determination of length, area, and volume changes at Storglaciären, Sweden, from multi-temporal aerial images (1959–1999). *The Cryosphere Discussions* 4 (1):347-379.

- Krimmel, R. M., and L. A. Rasmussen. 1986. Using sequential photography to estimate ice velocity at the terminus of Columbia Glacier, Alaska. *Annals of Glaciology* 8:117-123.
- Krimmel, R. M., and B. H. Vaugh. 1987. Columbia Glacier, Alaska: changes in velocity 1977-1986. *Journal of Geophysical Research* 92:8961-8968.
- Larsen, C. F., R. J. Motyka, A. A. Arendt, K. A. Echelmeyer, and P. E. Geissler. 2007. Glacier changes in southeast Alaska and northwest British Columbia and contribution to sea level rise. *Journal of Geophysical Research: Earth Surface (2003–2012)* 112 (F1).
- Liestøl, O. 1962. Special Investigations on Hellstugubreen and Teverråbreen. In *Glaciers and snowfields in Norway*, eds. A. Hoel and W. Werenskiold, 175-218. Oslo: Norsk Polarinstitutt.
- Lillesand, T. M., R. W. Kiefer, and J. W. Chipman. 2004. *Remote sensing and image interpretation*: John Wiley & Sons Ltd.
- Luckman, A., T. Murray, H. Jiskoot, H. Pritchard, and T. Strozzi. 2003. ERS SAR feature-tracking measurement of outlet glacier velocities on a regional scale in East Greenland. *Annals of Glaciology* 36 (1):129-134.
- Luterbacher, J., E. Xoplaki, D. Dietrich, P. Jones, T. Davies, D. Portis, J. Gonzalez-Rouco, H. Von Storch, D. Gyalistras, and C. Casty. 2001. Extending North Atlantic oscillation reconstructions back to 1500. *Atmospheric Science Letters* 2 (1-4):114-124.
- Massonnet, D., and K. L. Feigl. 1998. Radar interferometry and its application to changes in the Earth's surface. *Reviews of Geophysics* 36 (4):441-500.
- Matthews, J. A. 2005. 'Little Ice Age' glacier variations in Jotunheimen, southern Norway: a study in regionally controlled lichenometric dating of recessional moraines with implications for climate and lichen growth rates. *The Holocene* 15 (1):1-19.
- McCabe, G. J., A. G. Fountain, and M. Dyrgerov. 2000. Variability in winter mass balance of Northern Hemisphere glaciers and relations with atmospheric circulation. *Arctic, Antarctic, and Alpine Research*:64-72.
- Meier, M. F. 1960. Mode of flow of Saskatchewan Glacier, Alberta, Canada. In *United States Geological Survey Professional Paper*. Washington: United States Geological Survey.
- Meier, M. F. 1984. Contribution of small glaciers to global sea level. *Science* 226 (4681):1418-1421.
- Nesje, A., Ø. Lie, and S. O. Dahl. 2000. Is the North Atlantic Oscillation reflected in Scandinavian glacier mass balance records? *Journal of Quaternary Science* 15 (6):587-601.
- Nesje, A., and J. A. Matthews. 2012. The Briksdalsbre Event: A winter precipitation-induced decadal-scale glacial advance in southern Norway in the ad 1990s and its implications. *The Holocene* 22 (2):249-261.
- NOAA. 2014. *Monthly Teleconnection Index: North Atlantic Oscillation* 2012 [cited 2014]. Available from <http://www.cpc.ncep.noaa.gov/data/teledoc/nao.shtml>.
- Nye, J. 1960. The response of glaciers and ice-sheets to seasonal and climatic changes. *Proceedings of the Royal Society of London. Series A. Mathematical and Physical Sciences* 256 (1287):559-584.
- Oerlemans, J. 1991. A model for the surface balance of ice masses: Part I: alpine glaciers. *Zeitschrift für Gletscherkunde und Glazialgeologie* 27:63-83.
- Oerlemans, J. 1994. Quantifying global warming from the retreat of glaciers. *Science-AAAS-Weekly Paper Edition-including Guide to Scientific Information* 264 (5156):243-244.
- Oerlemans, J. 2005. Extracting a Climate Signal from 169 Glacier Records. *Science* 308 (5722):675-677.

- Oerlemans, J., B. Anderson, A. Hubbard, P. Huybrechts, T. Johannesson, W. Knap, M. Schmeits, A. Stroeven, R. Van de Wal, and J. Wallinga. 1998. Modelling the response of glaciers to climate warming. *Climate Dynamics* 14 (4):267-274.
- Oerlemans, J., R. Giesen, and M. Van den Broeke. 2009. Retreating alpine glaciers: increased melt rates due to accumulation of dust (Vadret da Morteratsch, Switzerland). *Journal of Glaciology* 55 (192):729-736.
- Paul, F., and W. Haeberli. 2008. Spatial variability of glacier elevation changes in the Swiss Alps obtained from two digital elevation models. *Geophysical Research Letters* 35 (21).
- Pillewizer, W. 1949. Zur Frage jahreszeitlicher schwankungen in der geschwindigkeit der gletscherbewegung. *Zeitschrift für Gletscherkunde und Glazialgeologie* 1:29-38.
- Purdie, H., M. Brook, and I. Fuller. 2008. Seasonal variation in ablation and surface velocity on a temperate maritime glacier: Fox Glacier, New Zealand. *Arctic, Antarctic, and Alpine Research* 40 (1):140-147.
- Pytte, R. 1964. Hellstugubreen: en glasiologisk undersøkelse. Hovedoppgave, R. Pytte, Oslo.
- Rignot, E., A. Rivera, and G. Casassa. 2003. Contribution of the Patagonia Icefields of South America to sea level rise. *Science* 302 (5644):434-437.
- Rivera, A., and G. Casassa. 1999. Volume changes on Pio XI glacier, Patagonia: 1975–1995. *Global and Planetary Change* 22 (1):233-244.
- Sapiano, J. J., W. Harrison, and K. Echelmeyer. 1998. Elevation, volume and terminus changes of nine glaciers in North America. *Journal of Glaciology* 44 (146):119-135.
- Saraswat, P., T. H. Syed, J. S. Famiglietti, E. J. Fielding, R. Crippen, and N. Gupta. 2013. Recent changes in the snout position and surface velocity of Gangotri glacier observed from space. *International Journal of Remote Sensing* 34 (24):16.
- Schiefer, E., B. Menounos, and R. Wheate. 2007. Recent volume loss of British Columbian glaciers, Canada. *Geophysical Research Letters* 34 (16).
- Schimpp, O. 1958. Der Eishaushalt am Hintereisferner in den Jahren 1952-53 und 1953-54. *International Association of Scientific Hydrology* 4 (301-314).
- Scott, J. B., G. H. Gudmundsson, A. M. Smith, R. G. Bingham, H. D. Pritchard, and D. G. Vaughan. 2009. Increased rate of acceleration on Pine Island Glacier strongly coupled to changes in gravitational driving stress. *The Cryosphere Discussions* 3 (1):223-242.
- Støren, E. N., S. O. Dahl, and Ø. Lie. 2008. Separation of late-Holocene episodic paraglacial events and glacier fluctuations in eastern Jotunheimen, central southern Norway. *The Holocene* 18 (8):1179-1191.
- Surazakov, A. B., and V. B. Aizen. 2006. Estimating volume change of mountain glaciers using SRTM and map-based topographic data. *Geoscience and Remote Sensing, IEEE Transactions on* 44 (10):2991-2995.
- Van Loon, H., and J. Williams. 1976. The connection between trends of mean temperature and circulation at the surface: Part I. winter. *Monthly Weather Review* 104 (4):365-380.
- Walker, G. T., and E. W. Bliss. 1932. World Weather V. *Memoirs of the R. M. S.* (4):53-83
- Wallace, J. M., and D. S. Gutzler. 1981. Teleconnections in the geopotential height field during the northern hemisphere winter. *Monthly Weather Review* (109):784-812.
- Willis, I. C. 1991. The hydrological context and geomorphological significance of glacier motion: Midtdalsbreen, Norway, University of Cambridge.
- Willis, I. C. 1995. Intra-annual variations in glacier motion: a review. *Progress in Physical Geography* 19:46.
- Willis, J., D. Chambers, C. Kuo, and C. Chum. 2010. Global sea level rise. *Oceanography* 23 (4):26.

- Winkler, S., and J. A. Matthews. 2010. Holocene glacier chronologies: Are 'high-resolution' global and inter-hemispheric comparisons possible? *The Holocene* 20 (7):1137-1147.
- Zemp, M., E. Thibert, M. Huss, D. Stumm, C. Rolstad Denby, C. Nuth, S. Nussbaumer, G. Moholdt, A. Mercer, and C. Mayer. 2013. Uncertainties and re-analysis of glacier mass balance measurements. *The Cryosphere Discussions* 7 (2):789-839.
- Østrem, G., K. D. Selvig, and K. Tandberg. 1988. *Atlas over breer i Sør-Norge*. Oslo: Avdelingen.
- Østrem, G., and A. Tvede. 1986. Comparison of glacier maps—A source of climatological information? *Geografiska Annaler. Series A. Physical Geography* 38 (3):225-231.